



Norwegian University of
Science and Technology

The Applicability of Urban Streets as Temporary Open Floodways

A case study from Bergen, Norway

Thea Ingeborg Skrede

Civil and Environmental Engineering

Submission date: June 2018

Supervisor: Tone Merete Muthanna, IBM

Norwegian University of Science and Technology
Department of Civil and Environmental Engineering

Description of Master Thesis spring 2018

Candidate name: Thea Ingeborg Skrede

Subject: Stormwater

Title: Applicability of urban streets as temporary open floodways

Due date: 25.06.2018

Background

In Norway, future challenges in the water sector are mainly dominated by climate change and urbanization, in addition to an aging and degrading water infrastructure. These challenges are expected to cause more frequent flooding or combined sewer overflows (CSO), especially in urban areas. An increase in urban flooding events will cause a significant disturbance of daily life and high monetary damages to both public and private properties, in addition to damages to infrastructure and public safety. However, adapting and designing infrastructure for future extreme events are both challenging and expensive, moreover, the cost of such adaption might exceed the cost of damages they prevent. Therefore, there is a need to look for alternative solutions to prevent, handle and control urban floodwater. The aim of this master thesis is to investigate if urban streets can be used as a part of Norwegian stormwater management, and function as temporary safe open floodways during extreme events to transport and contain urban floodwater in addition to reduce combined sewer overflows. This study propose and evaluate the measure of routing floodwater in an urban street.

The present study is part of the BINGO project (www.projectbingo.eu), whose goal in the Bergen research site (Damsgård area) is to assess the impact of climate change, evaluate measures to reduce flash floods and reduce the frequency of CSO to the recipient.

Research questions

The master thesis aim to answer the following research questions:

- a. How should the performance and applicability of using urban streets as temporary floodways be evaluated?
- b. What are the most important hydraulic performance criteria and design criteria for an urban street used as a temporary floodway?
- c. What are the most important hazard criteria's for floodways in urban streets to be considered safe?

Collaboration partners: Bergen municipalities, BINGO project

Location: The Master thesis will be conducted at the Department of Civil and Environmental Engineering. The candidate should have regular meetings with advisors(s). The simulations and models will be used with licenses and software available at the Department of Civil and Environmental Engineering.

Advisors: Tone Merete Muthanna, Erle Kristvik

“To understand water is to understand the cosmos, the marvels of nature, and
life itself”

~ Masaru Emoto

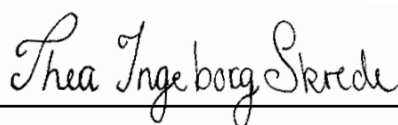
Preface

This report is the final product of the course “*TVM4905 Water and wastewater engineering, Master’s thesis*” at the Norwegian University of Science and Technology (NTNU), Department of Civil and Environmental Engineering. The topic investigated in this thesis began autumn 2017 as a preliminary studies part of the course specialization Project in the course “*TVM4510 - Water and Wastewater Engineering*”. The purpose of the thesis is to investigate the applicability of utilizing urban streets as temporary floodways during extreme events. Firstly, I would like to express my deepest gratitude to my supervisor Associate Professor Tone Merete Muthanna for her advice, support and guidance throughout this study and the process of researching and writing a scientific article. Thank you for all the interesting conversations and motivation during this study, and for allowing me to pick the research topic a truly enjoyed working with. In addition, I would like to express my gratefulness to PhD candidate Erle Kristvik and Postdoctoral Ashenafi Seifu for their support and guidance in addition to helping me with my questions during this process.

The present study was made possible by the BINGO project- *Bringing INnovation to onGOing water management* –a better future under climate change (projectbingo.eu). In addition, I would also like to thank:

- Professor Knut Alfredsen, for help and guidance on using hydraulic models.
- Marit Aase at Bergen Municipality for proving me with information of Bergen’s municipality’s stormwater management and climate change adaptations.
- Nazia Zia for providing me with Lidar data and drainage lines of the study area.
- My family and friends for supporting me through the new and different experience of writing a master thesis.

Trondheim, June 25, 2018



Thea Ingeborg Skrede

Thesis structure

Traditionally, a Master thesis at NTNU will result in an extensive report covering the studied topic. However, this master thesis is presented as a manuscript written according to the requirements and structure of a research article. As NTNU's vision is "knowledge for a better world", it is the author's wish that this thesis and the research within could be available to whomever might find it useful. Therefore, an article structure is chosen to promote the research work and to facilitate the study's availability for an international audience. The thesis's summary is written in Norwegian and is intended to be presented in the Norwegian building and construction industry magazine *Byggeindustrien* in the column: *Nytt fra NTNU*.

This thesis is written in English as a part of the international BINGO-project. In connection with the master thesis, the manuscript is submitted as a research article to the Hydrology Research Journal and is at this date accepted to be presented at the Nordic Water conference in Bergen, Norway. The format of this report is therefore based on an article format for the Hydrology Research Journal which can be found in Appendix A. The master thesis manuscript is intentionally more extensive than a traditional research article, to cover the work studied, its background, its limitations and its implications for Bergen municipality. In addition, illustrative figures of the results are presented in the manuscript, but can also be found as larger versions in Appendix N

Sammendrag

Urbane gaters egnethet som midlertidige flomveger

- En casestudie fra Bergen.

«**Våtere, villere og mildere**» I løpet av det kommende århundret vil klimaet i Norge bli villere, våtere og mildere. Vi kan forvente både flere og kraftigere regnskyll kombinert med en stadig økende urbanisering. Urbanisering fører til flere tette flater som reduserer infiltrasjon og dermed øker presset på det eksisterende overvanns- og avløpsnett. Allerede etablerte avløps- og overvannssystemer er dimensjonert for helt andre klimaforhold enn de vi kan forvente i fremtiden. Dette vil medføre store utfordringer med overvannshåndtering i urbane områder, og norske byer bør derfor forberede seg på å håndtere større vannmengder på overflaten, i rørsystemer eller på avveie. Der det ikke er mulig å transportere bort regnvannet i rør, må det lages plass til vannet på overflaten. Det må gjennomføres løsninger slik at vannet på overflaten ikke påfører samfunnet store kostnader eller ødeleggelser i byområder. Det vil ikke være tilstrekkelig å kun forebygge mot flom; det må også etableres løsninger som reduserer skadeomfanget så mye som mulig ved flom.

«**København under vann**» Den 2. juli 2011 falt det ca. 150 mm regn på bare to timer i København. Skadeomfanget beløp seg til nesten 7 milliarder kroner i forsikringsutbetalinger fordelt på 90.000 rapporterte vannskader. I tillegg førte flomvann til milliardskader på offentlige anlegg, veier og infrastruktur. I deler av København var det så mye vann i gatene at biltrafikken stanset helt og ambulanser ikke kom frem til sykehus. Etter denne hendelsen har København utarbeidet egne skybruddsplaner med tiltak for å redusere skadeomfanget ved kraftige regnskyll. Ett av disse er å utforme gater slik at de kan oversvømmes uten å føre til skade på bygninger eller mennesker. Når Norge står ovenfor lignende utfordringer, er det et behov for å teste ut om samme løsning kan fungere her også. Norske byer har ofte en helt annen topografisk utforming enn Københavns flate landskap, deriblant en del bratte gater, som dersom de benyttes som flomveger, vil gi større hastigheter og økt skadepotensiale enn i København.

«**Vann på ville veier**» Det er kostbart å dimensjonere og oppgradere avløpsnett til å håndtere klimaforandringer i tillegg til økt urbanisering. Derfor skal økninger i vannmengder fra klimaendringer helst håndteres på overflaten som lokale, åpne og fleksible overvannsløsninger.

En modell for helhetlig utforming og dimensjonering av overvannsanlegg for håndtering av overvann er tretrinnsstrategien utarbeidet av Lindholm m. fl (2008). Tretrinnsstrategien kategoriserer håndteringen av nedbør og overvann basert på regnvolum og ulikt samfunnsøkonomisk gjentaksintervall; (1) Infiltrer den lille nedbøren, (2) Fordrøy og forsink den middels store nedbøren og (3) Led store sjeldne nedbørshendelser trygt bort med åpne flomveger. I de tilfellene hvor de øvrige systemene ikke klarer å håndtere nedbørmengden, skal flomveger sikre trygg transport av vann til nærmeste resipient. Det har vært gjennomført lite forskning på design eller prestasjonskrav til flomveger, annet enn at de skal dimensjoneres for et gjentaksintervall på 100 år. Det mangler klare retningslinjer på hva en trygg flomveg er, og hvilke krav man skal sette til utformingen av en flomveg. I byområder er det ofte lite tilgjengelig areal som kan omformes til flomveger, slik at det et behov for å ta i bruk eksisterende areal, f.eks.: bygater.

«Vann i by – ingen veier å gå» Byområder består som oftest av store tette flater, og flomvann samles fort opp i gater og på veier. Byens unike topografi kan føre til at bygater blir til plutselige, ukontrollerte og uplanlagte flomveger under ekstremvær. Slike veiflommer har tidligere skapt problemer med fremkommelighet og ført til store skader på gater og veier i norske byer. Der det ikke er mulig å håndtere overvannet på andre flater, bør det vurderes løsninger for å redusere skader og fare for befolkningen når gaten er oversvømt. Målet med masteroppgaven er å ta i bruk hydrauliske modeller for å undersøke og evaluere egnetheten til gater som midlertidige flomveger og demonstrerer hvordan HEC-RAS 2D kan brukes til å kartlegge flomvegernes plassering i terrenget med tilhørende farepotensialer som: f. eks flomdybde, hastighet og fare for erosjon. I tillegg gir bruken av HEC-RAS 2D detaljert informasjon om vanninntrengsler i private hager, oppkjørsler og fare for vanninntrengsler gjennom kjellervinduer. Studien er gjennomført på en typisk bygate i Bergen med to kjørefelt, asfalterte fortau på begge sider og bilparkering. Gaten leder ut mot en egnet resipient og karakteriseres av bratt terreng. Resultatene fra denne masterstudien indikerer at selv om det er et stort behov å utrede trygge flomveger, er det ett enda større behov for å kartlegge de flomvegene som er eksisterende i terrenget, og som aktiviseres under ekstrem nedbør. Slike flomveger bør kartlegges med mer avanserte metoder enn dagens GIS-baserte aktsomhetskart. Studien viser at bruk av ulike sikkerhetskriterier har stor påvirkning på om flomvegen kan klassifiseres som trygg. Dette viser behovet for utarbeidelse av statlige sikkerhetskrav til flomveger i by, både for de eksisterende i terrenget og for nye planlagte.

«**Anbefaling**» Resultatene viser at gater er egnet som bruk til flomveger, fordi de største vannmengdene holdes i kjørefeltet, mens vannhastigheten og dybden er betydelig lavere på fortauet. Studien viser at utformingen av gatenettverket og gatetversnittet kan redusere skadepotensialet til gater som flomveger betraktelig, ved blant annet innføring av høyere kantsteiner eller ved å lede flomvannet i gater som ligger vinkelrett på terrenghelningen. I tillegg er det funnet en tydelig sammenheng mellom parkerte biler og høyere farepotensialer for fotgjengere grunnet høyere vannhastigheter. Dette betyr at det kan være stor effekt av å implementere parkingsforbud i gater med høy helning ved varsel om ekstremvær.

How beautiful is the rain!

After the dust and the heat,

In the broad and fiery street,

In the narrow lane,

How beautiful is the rain!

~ Henry W. Longfellow

Table of content

List of figures	I
Abbreviations	II
Abstract	1
1. Introduction	1
2. Study area and Materials	6
3. Method and Materials	8
4. Results and Discussion	18
5. Concluding Remarks	35
6. Acknowledgements	37
7. References	38
Appendix A – Framework for Article	42
Appendix B – Study area and Lidar data coverage	43
Appendix C – Study area and Drainage lines	44
Appendix D- Watersheds and sub basins	45
Appendix E- Slope distribution in watersheds	46
Appendix F– Time area diagram	47
Appendix G – Formulas for Time of Concentration.	48
Appendix H – Discharge hydrograph	49
Appendix I – Control point placement	50
Appendix J – Control point 3	51
Appendix K – Control point 4	52
Appendix L – Control point 5	53
Appendix M– Control point 6	54
Appendix N– Result from modelling	55

List of figures

Figure 1- Study Area And Study Site Characteristics.....	7
Figure 2 - Design Storm Hyetograph With 25 And 100 Years Return Period.....	10
Figure 3 – Design Storm Hydrograph With Overflow Capacity For Watershed A And B	12
Figure 4- Velocity Distribution In Cells With 2.0 M By 2.0m Grid For With Dw	14
Figure 5- Overview Of Computational Grid Mesh And Grid Cells.....	15
Figure 6 - Maximum Velocity Simulated In The Street Segment For Different Return Periods.....	18
Figure 7- Hazard Potential In The Street For Watershed B With A 100 Year Return Period.	21
Figure 8 – Flood Velocity And Hazard Potential Around Urban Obstacles.....	22
Figure 9- Simulated Velocity And Depth Over Time At Two Representative Control Points	27
Figure 10- Sign Of Instability At 0.2m Resolution With The Full Momentum Equation	29
Figure 11- Tin--Representation Of Street Cross-Section In Hec-Ras.....	30
Figure 12- Delay Between Peak Velocity And Peak Intensity With Different Return Periods (T).....	31
Figure 13- Velocity Profiles In Street Cross Section.....	34

Abbreviations

1D	One dimensional
2D	Two dimensional
CSO	Combined Sewer Overflow
DEM	Digital Elevation Model
DSM	Digital Surface Model
DTM	Digital Terrain Model
DW	Diffusive wave
FM	Full Momentum
GIS	Geographic information system
HEC	Hydrologic Engineering Center
IDF	Intensity Duration Frequency
LIDAR	LIght Detection And Ranging
SVE	Saint Venant equations
Coarse resolution	> 20 m
Extremely fine resolution	= 0.1 m
Fine resolution	< 2 m
High resolution	< 5 m
Very fine resolution	< 1 m

APPLICABILITY OF URBAN STREETS AS TEMPORARY OPEN FLOODWAYS

– a case study from Bergen, Norway

Thea Ingeborg Skrede

Department of Civil and Environmental Engineering.

The Norwegian University of Science and Technology (NTNU)

Abstract Climate change coupled with urbanization and its increasing impervious surfaces have caused major challenges for the water sector worldwide. In Norway, an ageing infrastructure with already insufficient drainage capacities results in large amounts of runoff during high intensity rainfall events causing frequent floods in urban areas. Due to limited available space to handle the future projected increase in stormwater, there is a need to utilize already occupied space for stormwater management, such as roads and streets, during extreme events. Limited research has been done on the design and applicability of urban streets as temporarily flood ways diverting stormwater to the nearest recipient. This paper will study the benefits and limitations of adapting urban streets as safe flood ways to route stormwater by modelling an urban street as a floodway. Streets as floodways will require additional hydraulic performance criteria and safety criteria. Performance criteria are identified and evaluated, and a method is proposed for evaluation of urban streets applicability as floodways. The method can be used to evaluate the applicability of multifunctional streets used as urban floodways and can be adapted by municipalities as a decision support tool for stormwater management.

Key words: Floodways, HEC-RAS, Hydraulic Modelling, Stormwater Management, Urban Drainage, Urban Flood Modelling

1. Introduction

Climate change coupled with urbanization and increasing impervious surfaces have caused major challenges for the water sector worldwide due to increasing magnitude and frequency of floods [1-3]. Climate change in Norway is expected to increase both the intensity and frequency of precipitation [4]. This coupled with urbanization will result in more frequent pluvial flooding and challenges with stormwater management in urban areas [5].

An expected increase in surface runoff from extreme events, both in total volume and peak runoff rates will result in; flooding due to insufficient drainage capacities; degradation of ecological and biological systems; and pollution from combined sewer overflows (CSOs) [6].

In Norway, the three-step strategic approach introduced by Lindholm et al (2008) is widely accepted as industry standard and applied by municipalities to adapt stormwater management to climate change and urbanization impacts [6]. The three-step strategy advise municipalities to: (1) Catch and handle the first millimeter of the storm as infiltration; (2) Collect and detain the next millimeters; and (3) Convey what cannot be handled in the previous steps in open safe floodways [7]. In the recent years, a considerable amount of studies have been conducted on the design and applicability of green roofs, infiltration and detention solutions [8]. In addition, the focus of Norwegian municipalities have primarily been on the two first steps; infiltration and detention solutions among others local measures [9]. The third step: convey stormwater in secure and safe open floodways has received less attention. In urban areas, unoccupied and available surface area are often scarce, hence there is a need to look for existing space which can be utilized for stormwater transport during extreme events.

This study concentrates on the third step of the three step-strategy and the use of urban streets to safely transport stormwater runoff exceeding sewer system capacity and thresholds of step 1 and 2. Limited research have been conducted on the design and applicability of using urban streets as temporarily floodways to divert stormwater to the nearest recipient. However, in Copenhagen, climate change and urbanization have led the city to develop a cloudburst plan, which introduces the possibility of adapting urban streets and roads to floodways as a measure to control and safely divert pluvial flooding [10]. In the area of Damsgård, located in the city Bergen, frequent flooding coupled with a reinvigoration of the area with the vision of “*clean water from the mountain to the fjord*” have caused Bergen municipality to consider new measures to avoid urban flooding and combined sewer overflows into the receiving water; Puddefjord. However, the central area of Copenhagen is known for its relatively low-lying flat topography, whereas Damsgård is characterized by steep hills and local conditions will therefore prompt differing requirements and considerations to the use of urban streets floodways.

In the recent years, several authors have developed and tested different methodologies to simulate urban flooding (see, for instance [11-13]). However, urban flooding is difficult to simulate due to different complex flood generation mechanisms, such as diverse climatic, topographic, hydrologic, hydraulic conditions and processes on the surface and in the drainage network [12, 14-16]. A dual-drainage concept is often introduced to describe urban flooding and the two systems interactions; (1) Major drainage systems (i.e. surface flood) ; and (2) minor systems comprise (i.e. drainage sewer network) [17]. However, during many urban flooding events the sewer system may operate at capacity or the surface drainage system is insufficient [18], and the major system (the surface flow) operates without interaction from the minor system [19].

Mark et al (2004) note that urban surfaces often are characterized by obstacles such as building, sidewalks, road camber and drains, hence, lack of accurate representation of these drastically alter surface water flow paths [13, 20]. In addition, head losses due from flows over or around such features are particularly difficult to represent and simulate [21]. Hence, models for urban flood analysis require a high resolution (<5m) to simulate complex flow paths and blockage effects, and the lack of accurate representation of such obstacles and fine scale topographic features can drastically alter the accuracy of the model results [20-22]. Mark et al. 2004 recommend a grid resolution of 1–5 m [23]. Since surface flow is strongly influenced by topography and urban obstacles, Digital Elevation Models (DEM) at appropriate resolutions are central to simulate urban water surface flow [24]. Hunter et al. 2008 found that terrain data available from modern airborne laser scanning, also referred to as "Light Detection And Ranging" (LIDAR) systems are sufficiently accurate for simulating urban flows and LIDAR data have been successfully used by multiple researches in flood inundation models [20, 22]. However, result accuracy is not always increased by higher grid resolution, as limitations and uncertainties always will affect flood modelling [25]. In literature, these uncertainties are the most widely studied [26]; (1) choice of model structures [11, 13, 27, 28]; (2) model parameters, [12, 28-31]; and (3) model inputs (channel geometry and DEM, initial and boundary conditions(i.e. flood hydrographs))[12, 20, 26, 32]. A common problem with modelling of sub-urban and urban flooding is that they often are ungauged, with little calibration and validation data available [12, 33] and model reliability increases with the amount of measurement data that can be used for their instantiation and calibration [21].

Urban flooding has been analyzed by several authors using one dimensional (1D) [23, 34] and two-dimensional (2D) models [13, 22, 35] or coupled 1D/2D models considering dual drainage [21, 24, 36]. Several authors have investigated the phenomena of flooding on urban streets [23, 35, 37], street flooding at very fine resolutions [38, 39], different resolutions ability to accurately represent street cross-sections and street networks [35, 38] or flow at street junctions [35, 40]. Guillén et al. 2017 used HEC-RAS 1D and large-scale particle image velocimetry to study the velocity distribution in a street cross-section and calibrated the results with amateur videos of an urban flash flood. De Almeida et al. 2018 notes that the road network can be particularly efficient in transporting water across the urban area and therefore plays an important role in the ultimate distribution of surface flow [39], and uses an extremely fine resolution (i.e. 10cm) with shallow water equations to analyze the road networks effect on urban flooding.

However, to the author's knowledge, no studies yet have been performed on the use of urban streets as temporary floodways in the context of urban stormwater management. In addition, no authors have studied the impact and challenges of using an urban street as a temporary floodway. With the aim of practically, a model with good user support and low learning threshold is preferred. In this study, only a 2D dimensional approach is considered. However, a number of works pointed out that flow at street junctions and intersections require 3D modeling to be well represented, but 2D is considered sufficient at high flows [35].

The HEC-RAS model was developed by the Hydrologic Engineering Center (HEC) of United States Army Corps of Engineers and has been applied in many studies for flood inundation modelling [12, 41, 42]. Since HEC-RAS 5.0.4 2D is freely available and open source, it shows a large potential for flood planning in urban areas. For users with little experience in flood modelling, HEC-RAS is easily operated and could therefore be a beneficial tool for Norwegian municipalities. In comparison, the MIKE FLOOD series from Denmark [26], InfoWorks ICM (UK) [17], TUFLOW (Australia) [43] or LISFLOOD-FP (UK) [30, 38, 39] could have been used to simulate the urban street as a floodway. For a dual drainage approach; SWMM (US) or MIKE URBAN/MIKE FLOOD could have been employed [44].

Numerical flood models are important tools for understanding flood events, flood hazard assessment and flood management planning [41]. Typically, models flow parameters (i.e. flow depth, flow velocity, flood duration) [45], are used to evaluate flood risk and danger. Danger to people, vehicles, buildings and infrastructure is often assessed using the concept of flood hazard. In literature, there is a conventional agreement that there is a relationship between the hazard level for people exposed to a flood, and the depth and velocity in flood water [46-49]. Most authors have suggested a relationship between the depth-velocity product (yv_c) and human stability in water [46-49]. For pedestrians a safety threshold of $(v \times y) = 0.22 [m^2s^{-1}]$ is suggested [50]. However, Russo et al. 2013 propose that for flooded streets with shallow water (6-20 cm) a velocity threshold should be used as hazard criteria, as presented in Table 1. For a comprehensive review, see [50]. In addition, in literature velocity thresholds have been used to describe the negative effect of floodwater on vehicles and incipient velocity to predict when a vehicle is moved by flood water [51].

Hazard level for pedestrians	Velocity [m/s]
Low hazard	1.51
Medium hazard	1.56
High hazard	1.88

Table 1 - Hazard level for pedestrians exposed to flood in an urban streets

For floodways not to cause significant damage to the urban environment, the relationship between urban flooding and damage to buildings and structures needs to be defined. Flood damage to buildings is considered either monetary or structural [52]. Structural damages are related to the velocity of the floodwater [53], whereas monetary damages to the maximum depth and flood duration [54]. Monetary damages are often derived from insurance claims as depth-damage function, related to the specific parameters of the flood [55]. In Copenhagen such a relationship is defined by a maximum 10 centimeter depth threshold, where exceeding depths is expected to cause monetary losses based on insurance claims [10].

In Norway, depth-damage profiles derived from previous urban pluvial floods could be used to determine damage potential for buildings. This highlights the need for specific safety and hazard criteria for the use of open floodways in Norwegian cities. Hence for Norwegian municipalities to use urban streets as floodway, a suitable methodology and performance criteria must be defined.

In this study, such a methodology is introduced as a case study in Bergen, Norway and the applicability of using urban streets as temporary floodways will be addressed according to the following research objectives:

- * Define how the performance and applicability of using urban streets as temporary floodways should be evaluated
- * Investigate the most important hydraulic performance criteria for an urban street used as a temporary floodway
- * Investigate the hazard criteria for safe floodways in urban streets

2. Study area and Materials

The Damsgård area is located along the Puddefjord in Bergen, a city on the west coast of Norway. Bergen is a coastal city with a cold and wet climate. Bergen is renowned as “The rainiest city in Europe” [56] with an annual mean precipitation of 2,550 mm [57]. The study area is characterized by steep slopes, ranging from sea level to 468m above mean sea level. The slopes are mostly vegetated and disconnected from the fjord by a strip of urban area. Large amounts of runoff from the vegetated steep hillside, in addition to impervious surface in the urban area below cause extensive flash floods and frequent (CSO) to the Puddefjord. A detailed description and map of the area can be presented in Figure 1 and Table 2 describe the areas characteristics. Bergen municipality is investigating different adaptation measures to reduce the amount of flash floods and CSO to the fjord. One measure is to divert runoff from the forested mountain before it reaches the urban area, and route the runoff to the fjord as an open floodway in the existing street network.

The street of Damsgårdsallmenningen is suggested as an applicable street segment for this study. From a research point of view, the street of Damsgårdsallmenningen is ideal to be modelled as a floodway for multiple reasons; (1) It leads directly to a recipient; (2) The stormwater run-off from a large watershed could easily be routed to the street without passing through an urban area and subsequently becoming polluted; (3) The street is straight without turns or lane widenings, and therefore has a nearly continuous cross-section over the entire street segment; (4) The street segment also includes intersections and is widely used for parking, which allows for flow evaluations of situations commonly occurring in urban areas in Norway;

(5) The street has sidewalks on both sides of the two driving lanes, which makes the street segment a good representation of a quite typical urban street in Norwegian cities; (6) the street is quite steep with different slopes along the segment, which allows this study to evaluate if steep urban street can be used as floodways; and (7) is located in an area with significant flooding problems and it exists a political will to reduce the stormwater pollution.

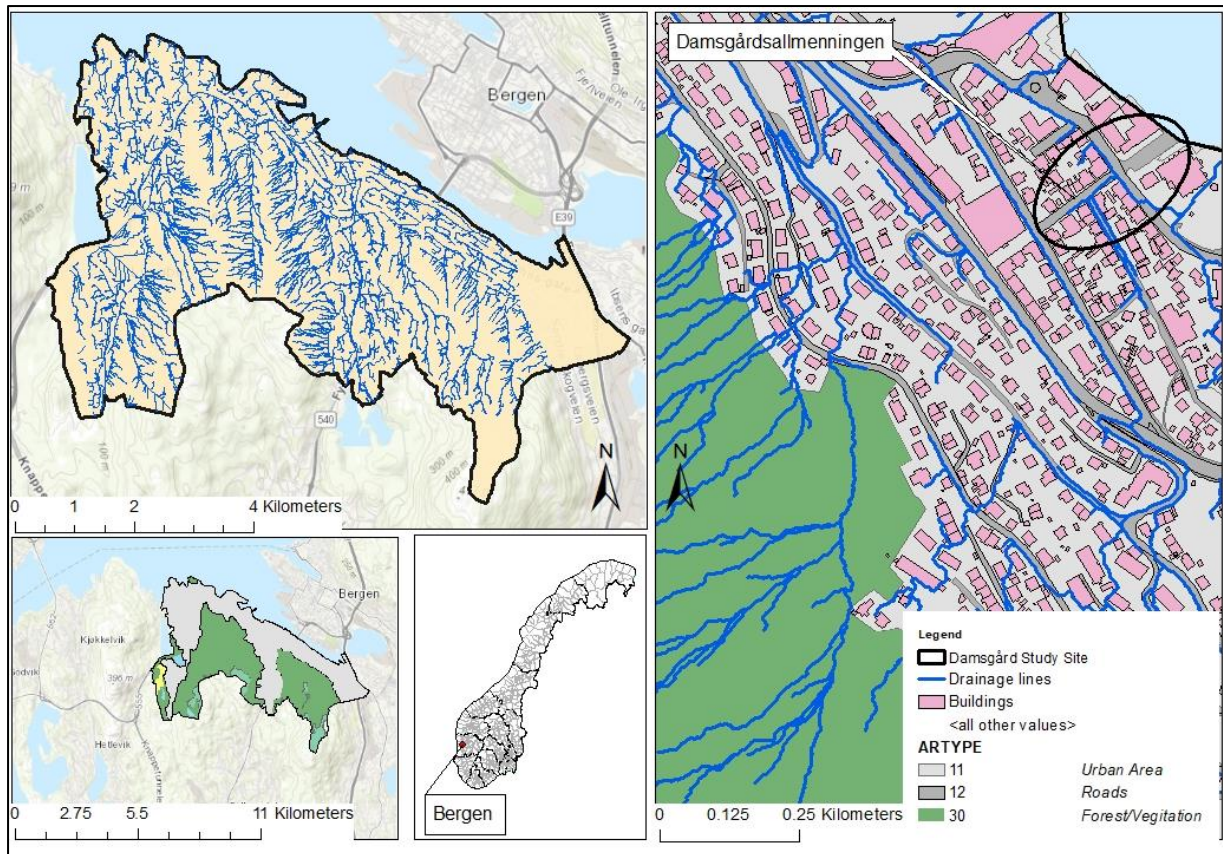


Figure 1- Study area and study site characteristics.

Watershed A and B (appendix D) is considered suitable areas for which a stormwater runoff could be routed to Damsgårdsallmenningen. For the purpose of this study, it is assumed that the drainage system is operating at full capacity, and that stormwater on the surface does not interact with the sewage network or the sewer drain grills. Travel time or transport from the watershed to the street is not considered, in addition to the design of the transportation-solution from the watershed outlet to the Damsgårdsallmenningen. It assumed to be no moving vehicles or pedestrians in the street during the flood event.

Area	Size	Land use	Slope (Degrees)	Runoff travel distance	Response time (min)
Damsgård	34.389 194 km^2	Built-up 48.3%, Forest 44.2% Open Land 4.8%	-	-	-
Watershed A	276 319 m^2	Forest 100%	Min = 0.14, Max =86.22 Average = 52.29	L=785 m	$T_c = 27.8$
Watershed B	481 036 m^2	Forest 100%	Min = 0.010, Max = 86.22 Average = 48.05	L=1132 m	$T_c = 33.5$

Table 2- Study site characteristics

Bergen municipality has high resolution Lidar-data available for Damsgård and GIS-derived drainage lines for the catchment. For this study, a specific Digital surface model (DSM) of the area in the resolution 0.1m*0.1m is rasterized from LIDAR data in ArcMap 10.6. A Digital Terrain Model (DTM) and a DSM in the resolution of 1.0m*1.0m downloaded from <https://hoydedata.no/LaserInnsyn/>. Precipitation intensity and return periods are obtained for Florida gauge station in Bergen and downloaded from www.eklima.no. The programs used in this case study are HEC-RAS 5.0.4 and ArcMap 10.6. All maps are projected in WGS_1984_UTM_Zone_32N

3. Method and Materials

The following method is developed to assess necessary performance indicators for using urban streets as temporary open floodways. A case study approach was used to test the proposed method, which consist of three interdependent parts; (1) Development of an inflow hydrograph; (2) Hydraulic performance testing; and (3) Hazard identification and analysis. Part 1 and 2 derives flow characteristics to be evaluated in part 3 by proposed safety criteria. In part 1 the main objective is to derive a synthetic inflow hydrograph. This can be achieved by a variety of methods. Calculation of runoff may be done as hydrograph or peak discharge. In this study, hydrographs are chosen to find peak depths and depth distribution over time. Peak flow is used to evaluate the worst conditions the public may be exposed to if the street should be used as an open floodway. Hence, peak discharge of the hydrographs should be precisely calculated if the

first objective is to establish the map of the peak water depths in the area [35]. In Norway, most municipalities have computational methods or models to derive peak discharge or use observed storm. In addition, the rational method, as first described by Mulvaney in 1851 and later by Kuichling in 1889, is commonly used in urban areas as a well-established method by Norwegian municipalities. Since there is little evidence of flows in the study area beyond drainage lines and because the area is ungauged, this case study input is restricted to synthetic hydrographs and runoff calculations and the hydrograph response must be estimated: The watershed is smaller than 50 hectare and the rational method is therefore an acceptable method [58]. Combining the rational method with mathematical convolution into what is commonly called time-area-method [59] allows for the generation of flow hydrographs.

In this case study, the aim is to evaluate if it is feasible to convey stormwater-runoff through an urban street to the recipient, instead of the flooding in the whole urban area, thus reducing the total flooded surface area subsequently the pollution in the stormwater. The watersheds size and response are assumed since run-off does not originally flow to the urban street. The watersheds are based on drainage lines and topography of the area that is considered to connect to a possible street. Due to the lack of historical runoff time series of the area, there is a need to calculate synthetic event hyetographs based on of precipitation data from Bergen. Open floodways in Norway should be designed for precipitation events with a 100 year return period, and to manage the runoff volume not captured in stage 1 and 2 of the three-stage strategies from the *Norwegian Water Guideline for handling surface stormwater* [6].

Practically, the open floodway would be activated for precipitation events not handled by the sewage system in Bergen (20 year) [58] or by the previous stages of the three-steps methodology [7]. Therefore, a design storm of 25 year return period is included to model the effect of a small storm not exceeding the overflow ($O_{watershed}$) capacity. A climate factor of 1.4 is applied to precipitation data from Florida to account for potential development in precipitation due to climate change, which is the recommended climate factor for durations less than three hours for Hordaland county [60]. Design storms hyetographs are constructed for a 25 and a 100-year return period with and without climate factor and can be found in Figure 2.

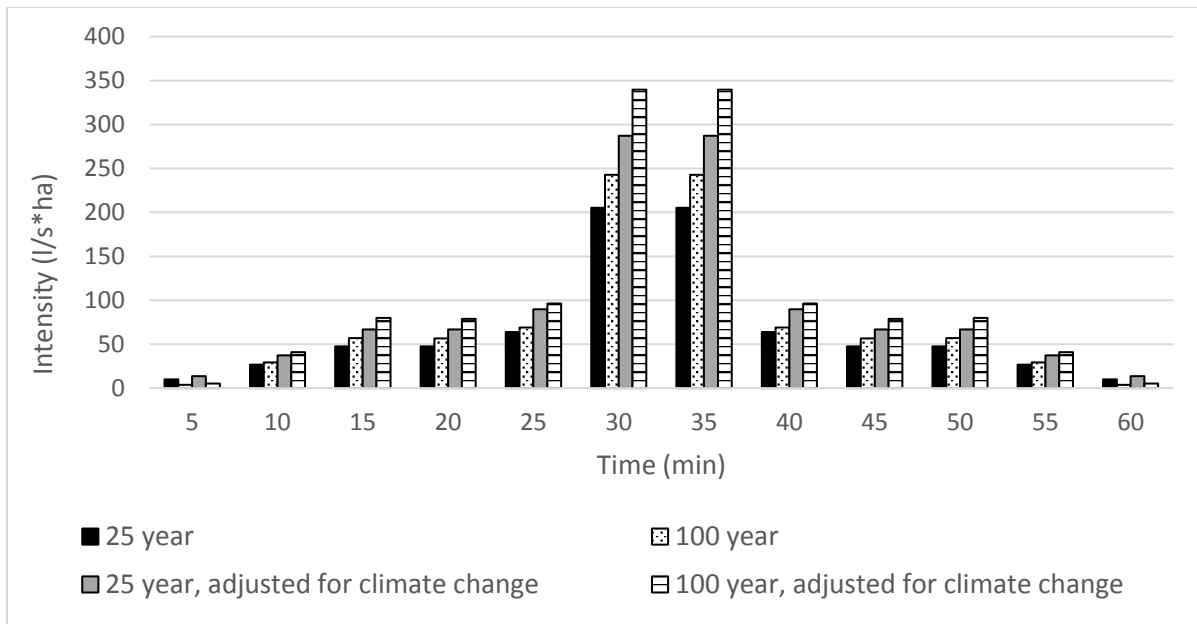


Figure 2 - Design storm hyetograph with 25 and 100 years return period.

Duration of the storm is often set as the time of concentration to find the peak flow with the rational method. Precipitation events with longer durations have statistically lower intensities, and maximum flow is reached at the time of concentrations. [61]. Two possible approaches for deciding design duration were considered: (1) Using a duration equal to concentration time; and (2) using one-hour events, which often are used for urban drainage network design [60, 62]. In this study, precipitation events for modelling were calculated using hyetographs as input, to ensure that the high-intensity minutes of a storm with variable intensity were represented in a hyetograph for 1 hour rainfall event derived from IDF- curves [60]. Other design storms and designs flows could be used based on availability of data, since different design hyetographs produce flood peak estimates that are consistently biased in most of the climatic and hydrologic conditions. [63].

The two watersheds were split into sub basins based on isochrones and drainage lines. Isochrones of equal travel time were constructed based the watersheds topography and response time, where concentration is used as an appropriate representation of response time [64]. Travel time is assumed to be independent of intensity. In order to find time of concentration, travel time from the most remote point on the hydrologic boundary of each sub basin is found using the method introduced by Kirpich in 1940 for channel flow and Kerby in

1959 for overland flow¹. Based on the drainage lines derived from the study areas topography, run-off is assumed to flow as overland flow until the lower boundary of the watersheds, where it is routed to the outlet of the watershed in an open channel, where water is transported to the urban street. Watershed A is divided into four sub basins, and Watershed B is divided into 6. Watershed B is considered an extension of Watershed A, which can be viewed in appendix D. Length of overland flow and length of channel was found for each sub basin of the watersheds using a Digital Terrain Model (DTM) with a resolution of 1.0 m x 1.0 m and the measure tool in ArcMap. The slope of the channel and the sub basins were found using 3D analyst with the profile graph from the point furthest from the outlet of each sub basin to the outlet using drainage lines. Times of concentrations are 33.5 min and 27.8 min, for watershed B and A respectively. Time of concentrations of the sub basins were then used to develop a time-area diagram that indicates the distribution of travel time of different parts of the watershed drains to the outlet [65]

A synthetic hydrograph was created for each watershed according to the Time–Area Method and time-area diagram based on the six sub basins physical characteristics (size, slope, length, land use) and times-of-concentration. Abstractions from the storage and infiltration were included in the runoff-coefficient in order to represent that the first few millimeters of precipitation do not contribute to stormwater runoff [66]. A conservative run-off coefficient for the vegetated area was used, due to steep slopes, high intensity precipitation resulting in low infiltration. The soil is assumed not saturated from previous precipitation events. Bergen municipality's guidelines for run-off calculations advises a run-off coefficient for forested areas in the range of 0.30-0.50. Since the watershed is characterized by step hills the higher range of 0.5 is used in the run-off calculations [58]. The existing sewer system is assumed to have an overflow, with a capacity designed for a 20 year event, ensuring that smaller storms are handled by the sewage system network, and the urban street is only activated as a flood way during extreme events. The pipe that drains the watershed is a 0.40 m smooth concrete pipe with a slope of 100 mm/m, and is assumed to have a capacity of 650 l/s. The capacity of the overflow is extracted from the hydrograph, as demonstrated in Figure 3. Runoff exceeding 650 l/s is handled by Damsgårdsallmenningen.

¹ Equation set for calculating time of concentrations can be found in appendix G

With implementation of infiltration and retention measures from step 1 and 2, abstractions should be subtracted from the stormwater hydrograph. The synthetic input hydrographs represent the direct run-off that is considered routed to the street segment included abstractions from overflow and stormwater management measures.

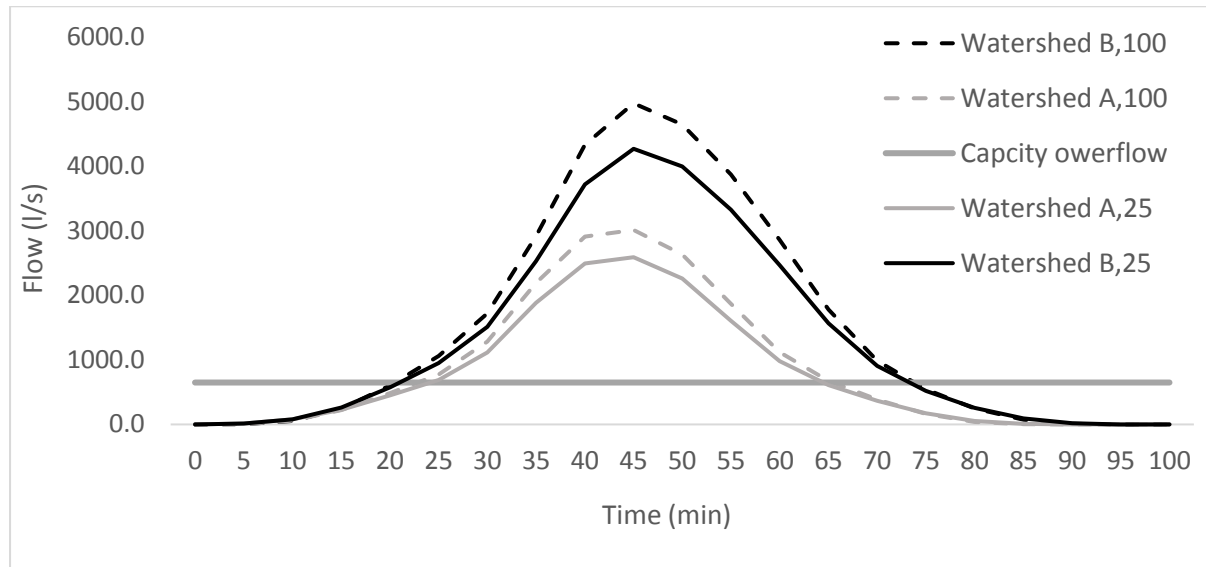


Figure 3 – Design storm hydrograph with overflow capacity for watershed A and B

3.1 Modelling

HEC-RAS 5.0.4 2D numerical models solve either the Saint Venant equations (SVE) , or the 2D Diffusive Wave equations over a computational mesh [42]:

$$\frac{\partial \xi}{\partial t} + \frac{\partial p}{\partial x} + \frac{\partial q}{\partial y} = 0 \quad (1)$$

$$\frac{\partial p}{\partial t} + \frac{\partial}{\partial x} \left(\frac{p^2}{h} \right) + \frac{\partial}{\partial y} \left(\frac{pq}{h} \right) = - \frac{n^2 p q \sqrt{p^2 + q^2}}{h^2} - g h \frac{\partial \xi}{\partial x} + p f + \frac{\partial}{\rho \partial x} (h \tau_{xx}) + \frac{\partial}{\rho \partial y} (h \tau_{xy}) \quad (2)$$

$$\frac{\partial q}{\partial t} + \frac{\partial}{\partial y} \left(\frac{q^2}{h} \right) + \frac{\partial}{\partial x} \left(\frac{pq}{h} \right) = - \frac{n^2 q p \sqrt{p^2 + q^2}}{h^2} - g h \frac{\partial \xi}{\partial y} + q f + \frac{\partial}{\rho \partial y} (h \tau_{yy}) + \frac{\partial}{\rho \partial x} (h \tau_{xy}) \quad (3)$$

Where h is the water depth [m], p and q are the specific flow in the x and y direction [$m^2 s^{-1}$], ξ is the water surface elevation [m], g is gravity acceleration [$m s^{-2}$], n is Manning's resistance, ρ is the water density [$kg m^{-3}$], τ_{xy} , τ_{xx} and τ_{yy} are the components of the effective shear stress and f is the Coriolis [s^{-1}] [42]. SVE is also known as the shallow water equations or in HEC-RAS: full momentum (FM) [67]. The full momentum includes Coriolis effects and representation of horizontal turbulent dispersion of momentum [67].

With the Diffusive Wave (DW), inertial terms of the momentum equation (Eq. (2), (3)) are neglected leading to a simplified equation not accounting for local or convective acceleration [67] [42]. Initially, the present study considered both the full Saint Venant equations and the diffusive wave, however there can be significant differences in flood extent between the diffusive models and full momentum in steep catchments where the flow is inertia dominated [13]. The methods provided different results, but simulation solving the 2D diffusive wave equations was about 2 times faster. Fewtrell al. 2008 note that the diffusion wave approximation will become less appropriate as slope and subsequently velocity increase [30] and if a refined topographic representation is available the complete shallow water equations should be used [18]. Due to low roughness on urban asphalt, steep slopes, confined wetted perimeter and known cases of flash flooding in the area, the full momentum was used for the analysis to more accurately simulate rapid changes in velocity. Then, the full momentum equations are solved with an iteration scheme with maximum 40 iterations. The stability of the numerical computations is strongly dependent on the relationship between the time step, grid size and maximum iterations. In order to ensure the stability of the 2D model, the grid size and time step was optimized according to the Courant–Friedrichs–Lewy condition for shallow water flows [67]:

$$Cr = \frac{v \Delta t}{\Delta x} \leq 1 \quad (4)$$

or

$$\Delta x \leq \frac{v \Delta t}{Cr} \quad (\text{With } Cr = 1.0) \quad (5)$$

Where Cr is the courant number, v is the flood wave velocity [$m s^{-1}$], Δt is the computational time step [s] and Δx is the grid resolution [m]. The 2D model was set up using a computational domain defined by a closed polygon, with a computational mesh generated from grid cells within the domain boundary. The computational cells may be arranged in a staggered or a non-staggered grid composed by polygons between 3 sides and 8 sides [42]. The computational mesh is drawn on an underlying terrain model with a resolution of 0.10 m by 0.10 m. The Terrain is extracted from LIDAR data and rasterized using the ArcMap 10.6 toolbox. This study uses a Digital Surface Model (DSM), and the extremely fine resolution is chosen to capture velocity around urban features such as vehicles, curb design and pedestrians. The computational domain (2D mesh) was constructed of a total 29810 cells, from a staggered grid composed of rectangular cells 1 m by 1 m, which generated a grid mesh with the maximum cell size of 1.85 [m^2], a minimum cell size of 0.3 [m^2] and an average cell size of 0.98 [m^2].

Finer grid cell sizes were considered and tested, but with HEC-RAS limitation of minimum time step of 0.1 seconds the model was not stable for cell size smaller than 1 m by 1m, as demonstrated by high courant numbers in Table 3. In addition, coarser grid size were also tested to evaluate grid size effect on computational cost and accuracy. HEC-RAS is a “high resolution subgrid model” where the computational cell is based on the underlying terrain and uses the underlying terrain to develop geometric hydraulic property tables to represent the computational cell [67]. Hence, the model accuracy of HEC-RAS 2D is dependent on the resolution of the terrain model, not the computational mesh cell size. This is also evident from Figure 4, which shows that HEC-RAS is able to simulate flow distribution inside a grid cell of 2 by 2 meter.

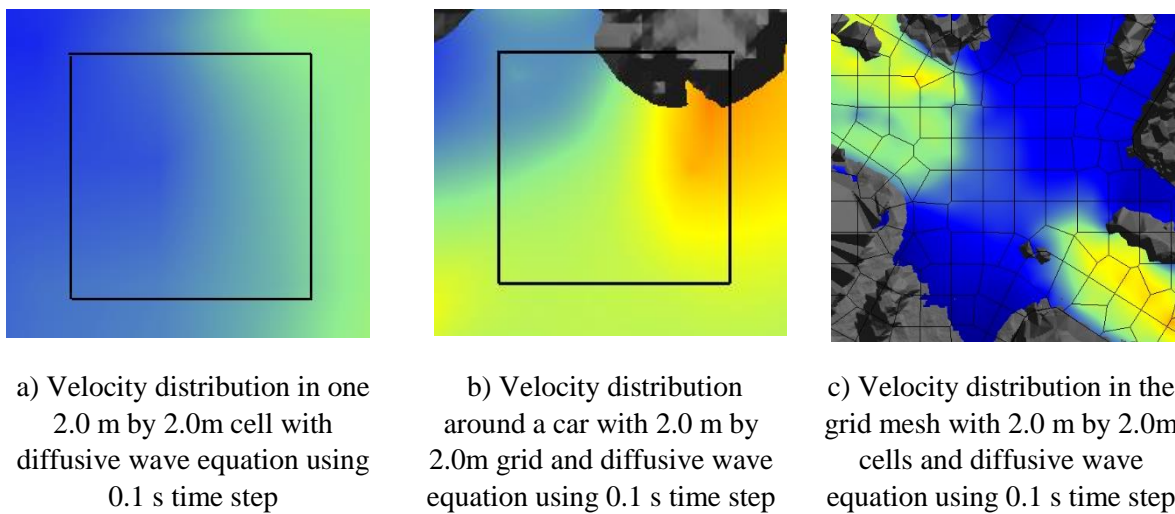
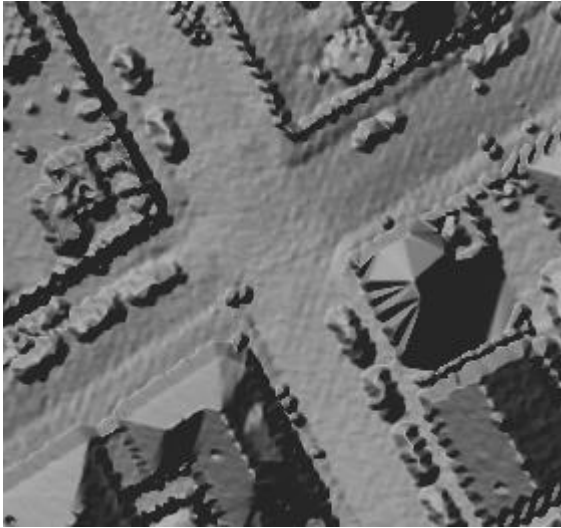
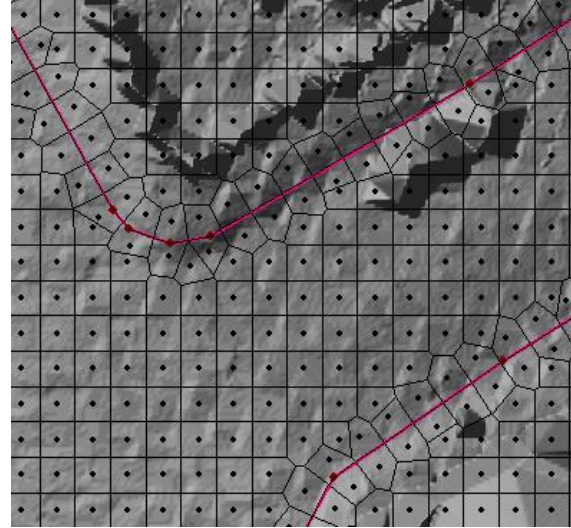


Figure 4- Velocity distribution in cells with 2.0 m by 2.0m grid for with DW using a time step of 0.1 s

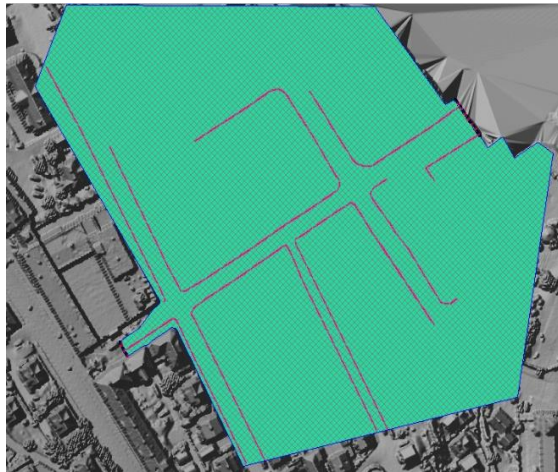
In previous studies conducted with 2D HEC-RAS [41, 42], the grid size was selected with the same resolution as the terrain model with applications to rural rivers [41, 42]. However, it is evident from Figure 4 that for urban modeling HEC-RAS is able to distribute velocity within the grid cell using the underlying terrain, and that the grid size could be coarser than the terrain resolution, thus reducing computational time and resulting in a stable courant number (< 1). Previous studies that have been conducted on urban flood modeling have mostly used a Digital Elevation Model (DEM) where obstacles such as vehicles, buildings and vegetation were removed from the DEM [68]. An accurate simulation of the effects of urban objects is better represented with a topography representing a lot of details and urban features that can be taken into account by a two-dimensional (2D) flow analysis [35, 68]. This study is therefore conducted with high resolution Lidar digital elevation data from Bergen, which then were converted into a 0.1x0.1 m Digital Surface Model (DSM) in ArcMap by using “LAS to raster”-tool without removing first return and surface features.



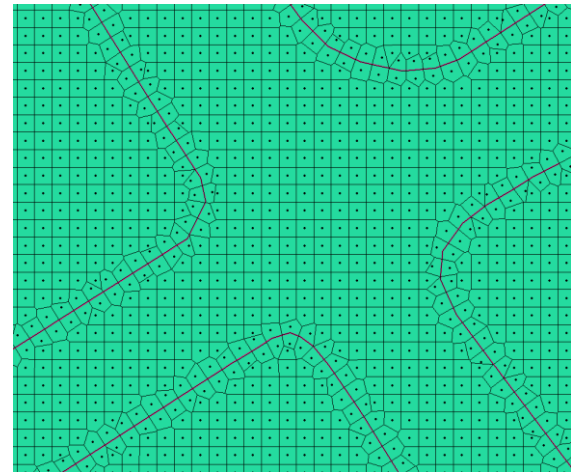
a) Terrain resolution with the presence of urban obstacles represented by parked vehicles



b) Grid coverage over urban obstacles with break lines with a resolution of 1 m by 1 m



c) Break lines placement within the computational grid of resolution of 1 m by 1 m



d) Break lines with cell face allignment the computational grid of resolution of 1 m by 1 m

Figure 5- Overview of computational grid mesh and grid cells.

Placement of the computational grid should ensure that polygon borders at the inlet boundary capture the planed design of the inlet structure. In this study, a channel with walls is assumed. The present study used two types of boundary conditions for 2D simulation: one hydrograph boundary condition upstream and one normal depth boundary condition downstream. The hydrograph boundary condition was located at the upstream start of the street segment, where the stormwater from Watershed A and B is assumed routed. The flow hydrograph is the synthetic discharge hydrographs from watershed A and B. In HEC-RAS, the energy slope is used to distribute the discharge over the cells that integrate the boundary; the distribution is based on the specified slope and the pre-processed hydraulic properties of each cell [42].

Considering the slope of the street segment, the energy slope was set to the average slope of the first segment of the street where the upstream boundary is located with a slope of 0.078125 m/m.

Cell size [m*m]	Number of cells	Equation set	Time step [s]	Run time [h]	Maximum velocity [m/s]	Courant number
0.2*0.2	732 953	Full momentum	0.1	58:25:23	13.5	6.75
0.5*0.5	117 038	Full momentum	0.1	05:23:14	6.7	1.34
1.0*1.0	29 810	Full momentum	0.1	01:25:28	6.5	0.65
1.5*1.5	13574	Full momentum	0.1	00:49:53	6.5	0.43
2.0*2.0	7657	Full momentum	0.1	00:29:09	6.4	0.32
0.2*0.2	732 953	Diffusive wave	0.1	25:06:34	10.5	5.25
0.5*0.5	117 038	Diffusive wave	0.1	03:02:58	10.1	2.02
1.0*1.0	29 810	Diffusive wave	0.1	00:40:36	7.48	0.75
1.5*1.5	13574	Diffusive wave	0.1	00:20:20	7.81	0.52
2.0*2.0	7657	Diffusive wave	0.1	00:06:55	7.87	0.39

Table 3- Model parameters from grid-sensitivity analysis for watershed B with a 100 year return period

It was assumed disconnected gutters and no runoff from private properties or from roofs on to the street. The volume from precipitation on the street is also assumed negligible, due to the small area compared to runoff from the watershed. Therefore, if the precipitation volume falling on the studied area are small compared to the input hydrographs volumes, their effects will be very small and it is not worth representing them [35]. Therefore, only the synthetic hydrograph is used as boundary condition, Though, HEC-RAS 5.0.4 has the ability to use precipitation over the grid, in addition to a hydrograph boundary input. The downstream boundary is located at the end of the street segment. Other solutions would be to extend the downstream boundary to include all segments of the domain boundary where water is expected to flow out of the computational domain [42]. Water at the border will either accumulate or change direction and will not flow out of the computational domain, hence in urban modeling, it is important to have a large enough grid to ensure that flow is not disrupted by the computational borders. Different placements and shapes of the mesh were evaluated quickly to test the sensitivity of grid placement to ensure that water was allowed to flow freely not disrupted by the border of the computational grid. Output boundary was placed where water was seen ponding on the boundary of the grid to ensure that water was allowed flow freely.

To avoid this issue, output boundary could be placed on the boundary of the grid where ponding of water were observed to allow water to flow out of the model boundaries. To avoid this issue, the output boundary could be placed on the boundary of the grid where ponding of water was observed to allow water to flow out of the model boundaries. For the model to accurately simulate velocity changes in the boundary between the driving lane and the sidewalk, the cells face should be parallel to the edge of the sidewalk (curb), to induce overflow only when the water depth exceeded the curb height. Therefore, Break Lines were added along the curb of the sidewalk for grid sizes higher than 1.0m. The area is started out dry, and is represented by a completely dry channel being exposed to a flood wave. Hence, the time steps need to be small for HEC-RAS to represent the wetting of the cells more accurately and avoid instability due to large time steps in the input hydrograph. If instability occurs, the time values in the hydrograph could be interpolated to avoid rapid changes [67]. All simulations with a higher time step than 0.1 s were unstable and resulted in a Courant number in the range of 6.75-15.

The roughness coefficient of the entire area is set to 0.016, as suggested for rough asphalt surfaces by Chow in 1959 [69]. The surface roughness is the only calibration parameter required by the HEC-RAS 2D (not considering the placement of the grid polygon/alignment of grid cells). Consequently, the roughness coefficient is the most common parameter to calibrate against observed flow in urban flood modelling with a high resolution 2D approach [35]. However, often in flood forecasting and urban flood modeling, one would not have calibration data, unless a flood of similar magnitude had occurred before [70]. The conventional solution to lack of calibration data is therefore to conduct a sensitivity analysis using an appropriate range of roughness to increase the confidence in the model [70]. Therefore, the model was tested with different manning's roughness values to test the model sensitivity for manning's parameter and the corresponding uncertainty in the results. Higher manning's values resulted in lower velocities but did not affect the results significantly and the value of 0.016 chosen.

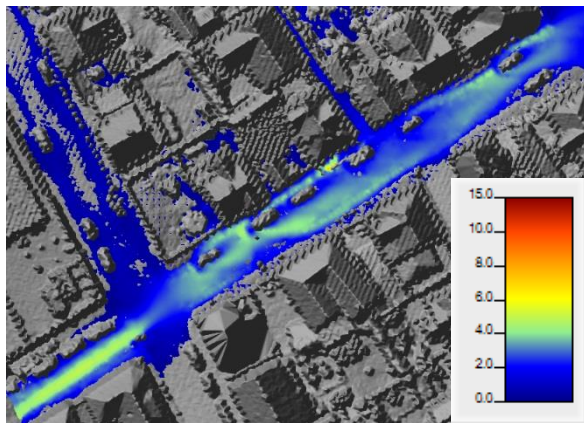
Watershed	Return period [Year]	Cell size [m*m]	Equation set	Terrain resolution [m*m]	Manning	Time step [s]
B	25	1*1	Full momentum	0.1*0.1	0.016	0.1
B	100	1*1	Full momentum	0.1*0.1	0.016	0.1
A	25	1*1	Full momentum	0.1*0.1	0.016	0.1
A	100	1*1	Full momentum	0.1*0.1	0.016	0.1

Table 4- Design scenarios used to evaluate the hazard potential

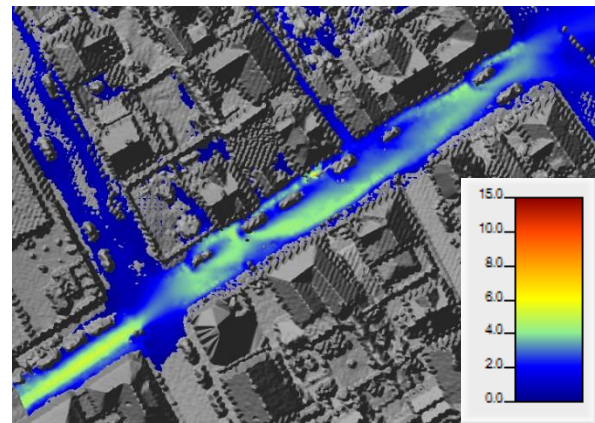
Then the model was run with different flooding scenarios as presented in Table 4. Finally, the product of the resulting water velocities (v) and water depths (h) in addition to maximum velocities were analysed for each watershed and return period in order to evaluate the impact of using the street as an open floodway.

4. Results and Discussion

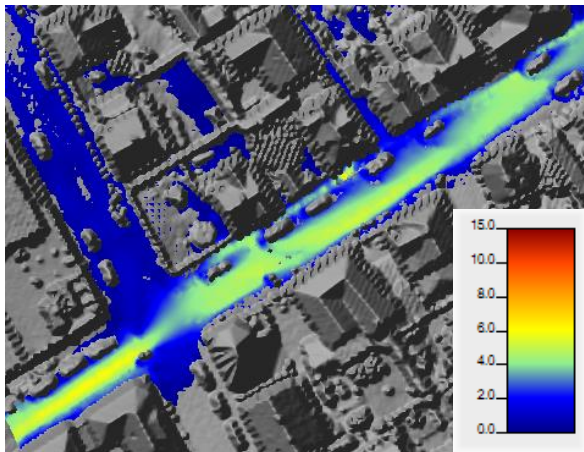
The first figure presents maximum velocity conditions during storms with a 60 minute duration with 25 and 100-years return periods for both watershed A and B.



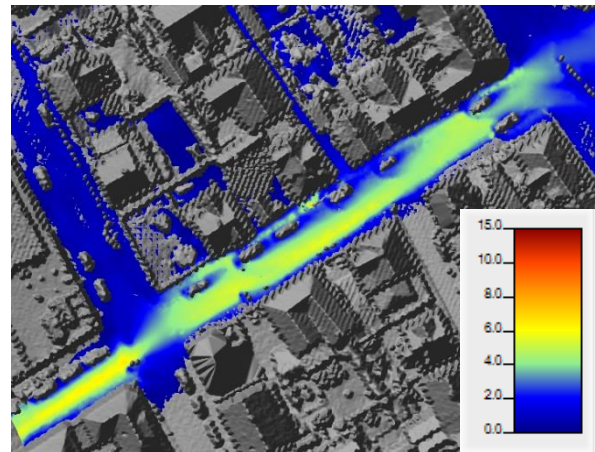
Maximum velocity distribution [m/s] in the street with runoff from watershed A for a 60 minutes storm with $T= 25$ year



Maximum velocity distribution [m/s] in the street with runoff from watershed A for a 60 minutes storm with $T= 100$ year



Maximum velocity distribution [m/s] in the street with runoff from watershed B for a 60 minutes storm with $T= 25$ year



Maximum velocity distribution [m/s] in the street with runoff from watershed B for a 60 minutes storm with $T= 100$ year

Figure 6 - Maximum velocity simulated in the street segment for different return periods.

Velocities are used to represent the hazard potential in the street for evaluation of pedestrian safety for an urban street as a floodway in Figure 6 and to represent flow around vehicles.

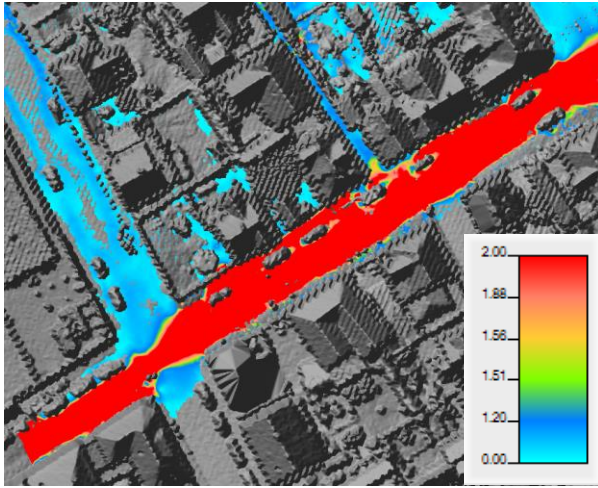
In addition, depth-velocity maps are shown against velocity in Figure 7. During the initial stages of the flood, the maximum hazard conditions were found at the upper boundary of the street, where the transportation-outlet (from watershed e.g. culvert, channel, and swales) and the inlet where stormwater would reach the floodway is located. This indicates that the design and placement of the inlet is important, and safety measures such as walls and levees should be considered. The first event (T=100 year), was used to evaluate if the street could be considered a *Safe* floodway during the design storm for open floodways in the three-step strategy (i.e. 100 year). From Figure 6 it is evident that high velocities (in the range of 6-7 m/s) are present, however, these are mainly in the driving lane and significantly lower at the sidewalk. This indicates that the hazard potential is lower if the public is not exposed to the driving lane while the floodway is active, by e.g. implementation of higher curbstones. However, this might impact the street performance as a part of the city and traffic system.

The second event (T=25 year) was applied to demonstrate flow conditions during a relatively small precipitation event, which is large enough to activate the street while exceeding the capacity of the sewage system. The event results in velocities in the range of 4-5 m/s, which indicates that even for a small storm (i.e. T= 25), hazardous velocities are expected, in addition, these happens at relatively low depths. However, the results indicates that the size of the upstream watershed is an important consideration for the implementation of urban streets as floodways as Watershed B result in significantly higher velocities, both in the driving lane and at the sidewalk. Hence, watershed B is less suitable than watershed A if hazard potential is the constricting design criteria rather than transport capacity. This implicates that the use of multiple streets as floodways might be beneficial instead of using one major floodway, to reduce maximum flow and velocity. A major floodway would require more measures to reduce hazard potential e.g. higher curbs, wider driving lanes, reversed road crown (v-profile) or other solutions which increase the wetted perimeter of the street, but that would require extensive alteration of the street cross-section and might affect the functionality of the street as a part of the traffic system and universal design, and the street would no longer fulfill design criteria by the National Road Authority (Statens Vegvesen). A multiple floodway system would results in a larger total flooded area, but with lower risk to the public. A larger wetted area results in larger damage potential to adjoining properties, which implementation might cause a need for combination of public and private flood proofing measures up to a certain depth criteria.

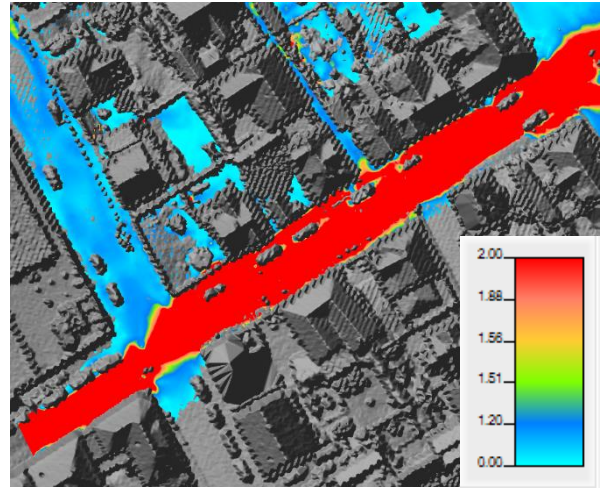
For damage to the environment and adjoining properties, flow depth in addition to water intrusion are significant parameters to evaluate the damage potential of the floodway. It is therefore a technological, legislative, and financial challenge if Bergen municipalities were to adapt the existing street design and street cross-sections in such a way that flood damage and hazard conditions would be reduced to a minimal level. Moreover, these challenges call for defined interfaces between maintenance responsibility and division of responsibility between the public, municipalities and insurance agencies.

Activation frequency is also a major performance indicator for the floodway. A frequency analysis should therefore be conducted to assess how often the watershed overflow is exceeded and activate the urban street as a floodway, in addition to the distribution of velocities during different magnitudes and durations of activation. Such an analysis should include precipitation forecast and precipitation data, to see which events would exceed the capacity of the overflow, resulting in the activation of the flood street. A key factor of the implementation of an urban street as a floodway is that the floodway should be temporary, and the development of a floodway should not hinder the use of the street during dry conditions. Therefore, the activation time, duration, and frequency are important design criteria for the floodway as it should function as a street most of the time, and not disrupt its main function: urban street.

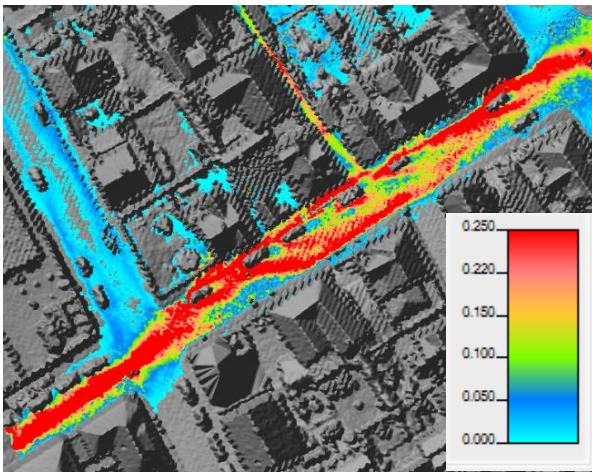
High velocity low depth flows are considered more dangerous in urban areas than high depth low velocity, due to sliding instability [50]. The depth-velocity product threshold in the street is less affected by depth due to the magnitude of the peak velocity. Thus, demonstrating that velocity is the dominating parameter in hazard potential, this is also evident in Figure 7, where hazard potential from velocity is greater than the depth-velocity safety threshold, proving the importance of using the right safety criteria. In this study, a velocity based threshold is considered the most suitable (in agreement with recent literature[50]). This is demonstrated in Figure 7, where hazard level in the water flow around the two parked cars indicates safe levels with depth-velocity compared to high hazard with velocity threshold. This is due to the low depth (4 cm-12 cm) lowering the depth-velocity product to safe levels, while a high velocity indicates hazardous conditions. This is also clear at the south sidewalk by the inlet, where depth-velocity product indicates safe conditions, while velocity indicates dangerously high hazard levels.



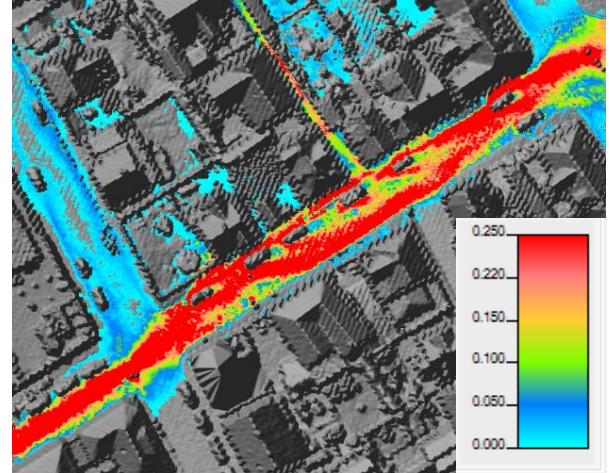
Maximum hazard potential from velocity [m/s] in the street from Watershed A, T= 100



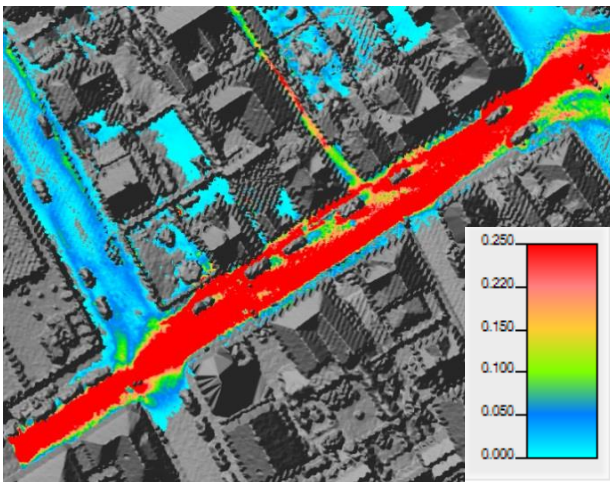
Maximum hazard potential from velocity [m/s] in the street from Watershed B, T= 100 year



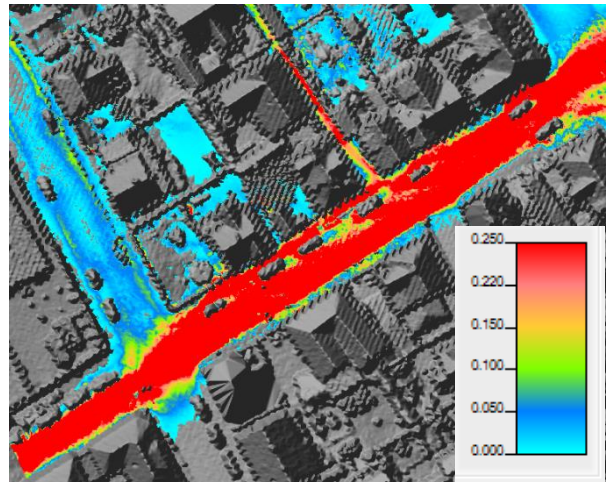
Maximum depth-velocity [m^2/s] product in the street from Watershed A, T= 25 year



Maximum depth-velocity product [m^2/s] in the street from Watershed A , T= 100 year



Maximum depth-velocity product [m^2/s] in the street from Watershed B, T= 25 year



Maximum depth-velocity product [m^2/s] in the street from Watershed B, T= 100 year

Figure 7- Hazard potential in the street for watershed B with a 100 year return period.

With the use of hazard criteria in Table 1, low hazard ($v = 1.51$ m/s) corresponds to a maximum depth of 0.146 m (y_m) if depth-velocity should not exceed $0.22 \text{ m}^2 \text{ s}^{-1}$, which is 4.6 cm higher than maximum depths recommended in Copenhagen cloudburstplan[10]. A maximum depth of 0.1 m results in an allowable velocity of 2.2 m/s which is significantly larger than the 1.51 m/s defined for low hazard. In Norway, curb height vary from 4 cm to 10 cm, and in this case y_m would result in a water surface of 4.6-10.6 cm above sidewalk, and thus might basement windows or windows well next to the floodway be particularly exposed to flood damage. To avoid this issue, municipalities should aim to design floodways where maximum depth do not affect private properties ($y_m = \text{curb height} + \text{height from cross fall}$).

Note that at the street intersections and subsequently, pedestrians crossing, the velocity profiles are lower, due to an increase in available flow area and a larger wetted perimeter. This indicates that if an urban street should be used as a floodway, the safest place to cross is at the street intersections. And from a practical point of view, placement of pedestrians crossing during a flood should be placed where the flow area is increased (e.g. intersections). Such a reduction of velocity could also be due to higher roughness, but in this study the roughness is constant over the entire grid area, even though one would expect higher roughness in backyards and the boundary between surfaces.

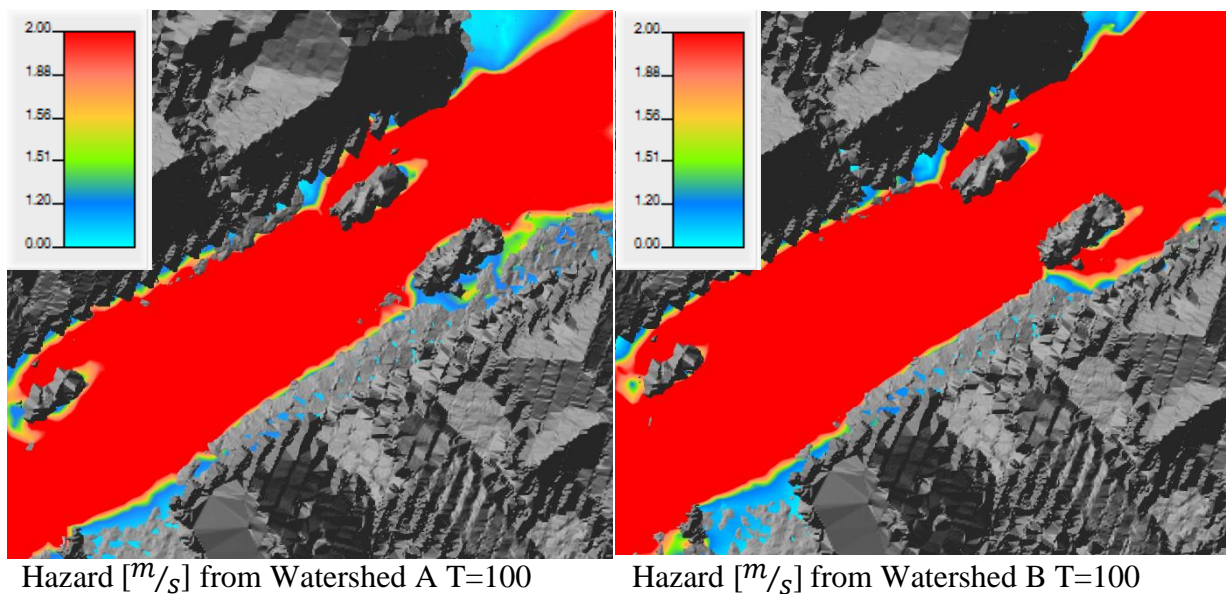


Figure 8 – Flood velocity as hazard potential around urban obstacles

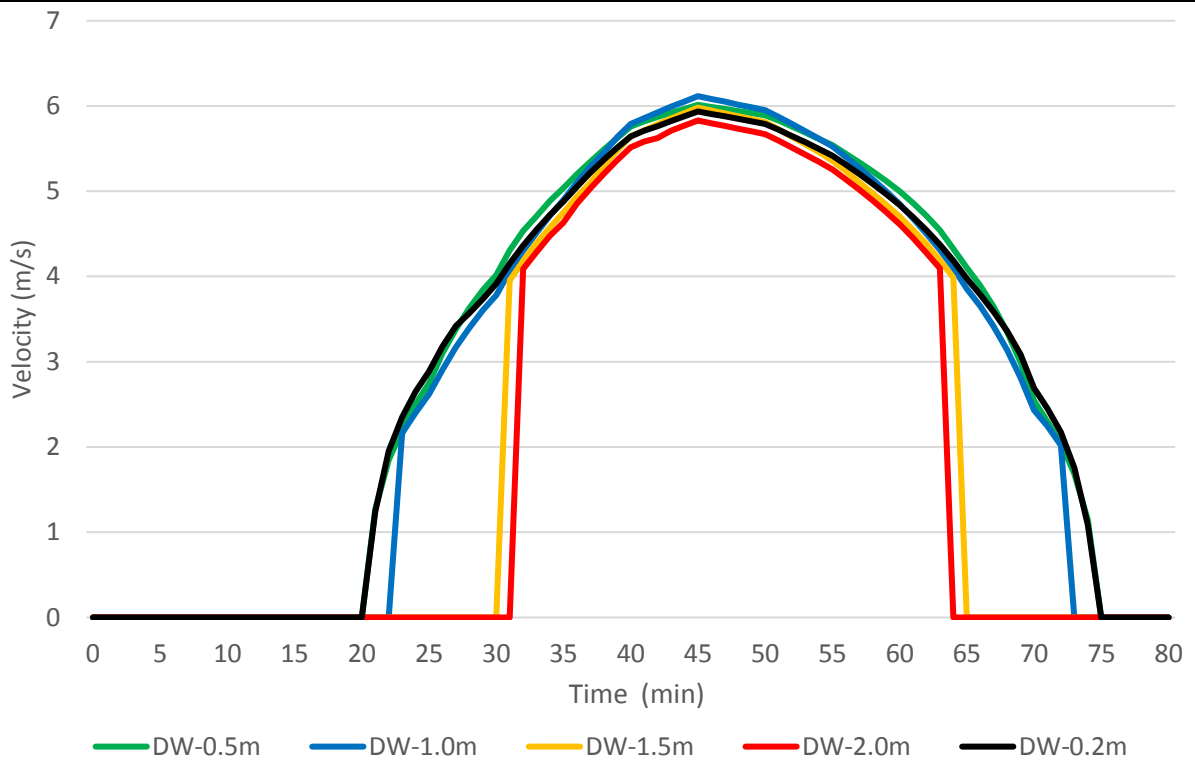
There is a significant correlation between the presence of urban obstacles (i.e. parked vehicles) and the magnitude of the hazard conditions: high depth-velocity products and a substantial increase in velocity. Note that velocity profiles are higher around the vehicles, and the water flow is visually disrupted by the presence of urban obstacles. From Figure 7 and Figure 8 it is evident that flow conditions around vehicles induce an elevated hazard potential as opposed to a cleared street. It is also evident that the presence of parked vehicles on both sides of the street causes increased velocities and subsequently increased hazard potential due to the constriction.

Figure 8 demonstrates that vehicles on both side of the street results in higher depths velocity and high hazard at the sidewalk with the use of velocity as hazard potential from Table 1, where red indicates high hazard and green low. Arguably, this indicates that it would be beneficial with a parking ban on days when high intensity precipitation is expected. The results show that to avoid unsafe conditions along the southern sidewalk (i.e. $<0.22m^2s^{-1}$) that when using a depth-velocity product as hazard criteria, the street segment can only serve as a floodway for watershed A at approximately 27 hectare with parking on both sides of the street.

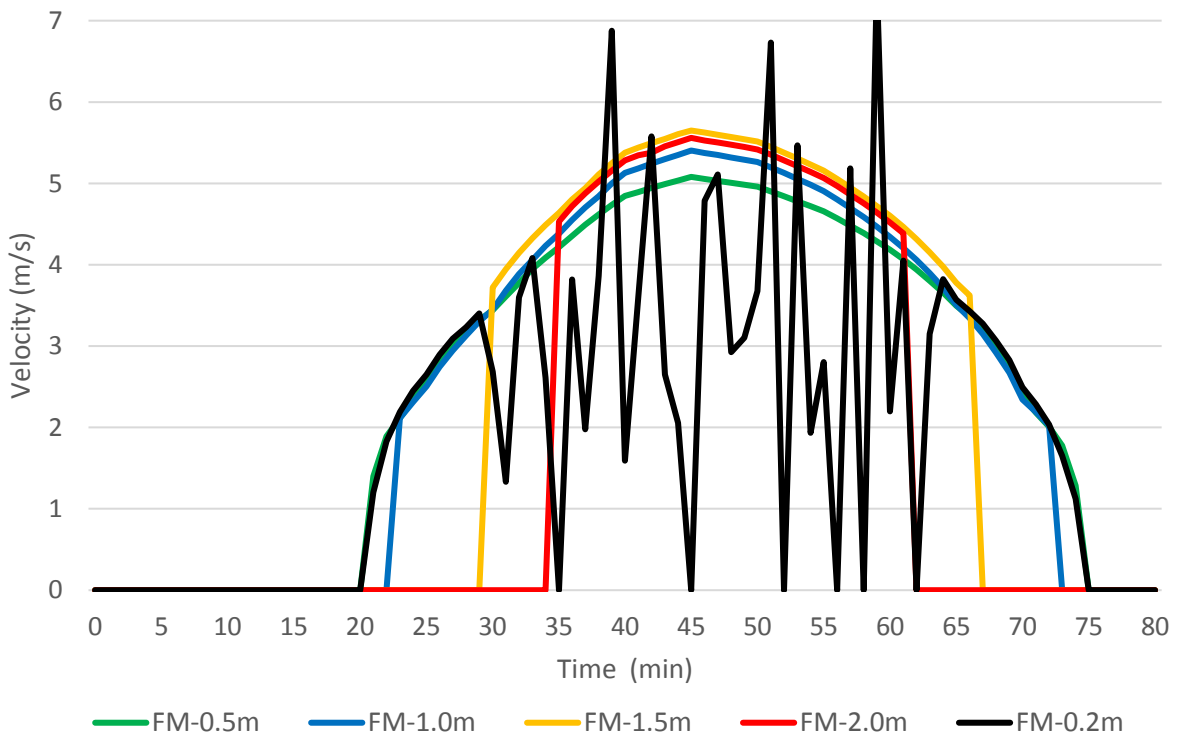
4.1 Limitation and uncertainties

As a significant correlation was observed between the presence of urban obstacles and hazard potential, it is important to note that in this study, such obstacles were represented as continuous “walls” where in reality, the water would flow around the tires and under the body of the vehicle. Which could result in significant lift and pressure conditions under and around the vehicles. Whereas in the model, water can only flow around or over the vehicle However, this is a widely researched topic in flood hazard mapping [71] and out of scope of this study. A comparison between the DSM and a clean DTM was not conducted in this study, but may be done to study the effect of a forecast-based parking ban and to examine how much the urban objects affect the results but this is out of scope of this study.

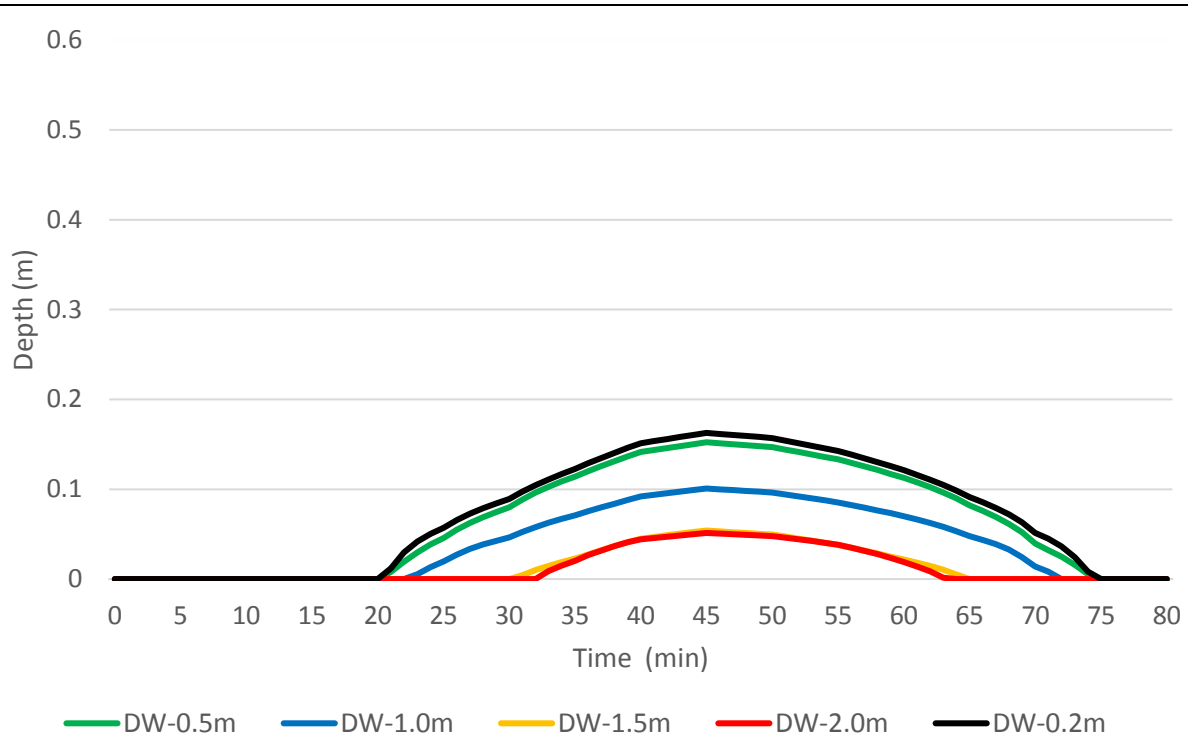
This study evaluated the effect of different computational grid sizes, as presented in Figure 9, but did not test the effect of different terrain model resolutions. In order to analyze the global effect of terrain model resolution on simulation results, different terrain models should be benchmarked, but this considered is out of scope of this study.



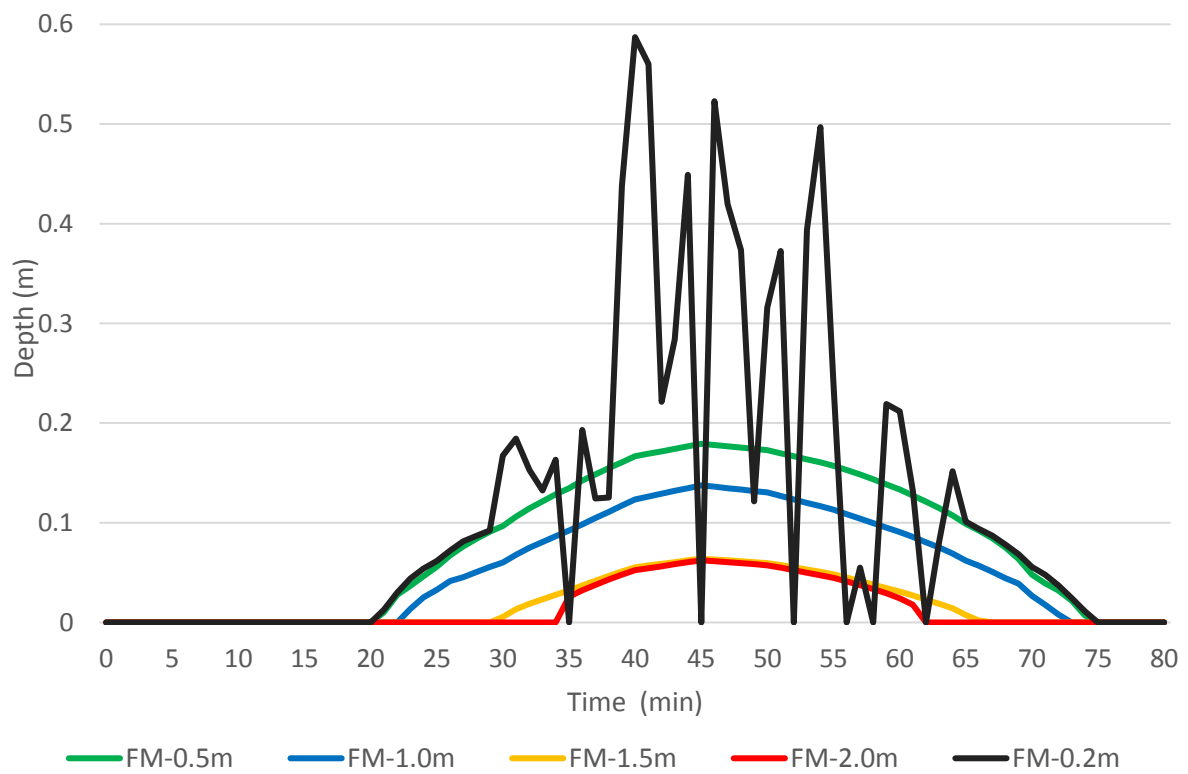
a) Distribution of model velocity at control point 1 for different grid resolutions with the diffusive wave equation for watershed B with 100 year storm.



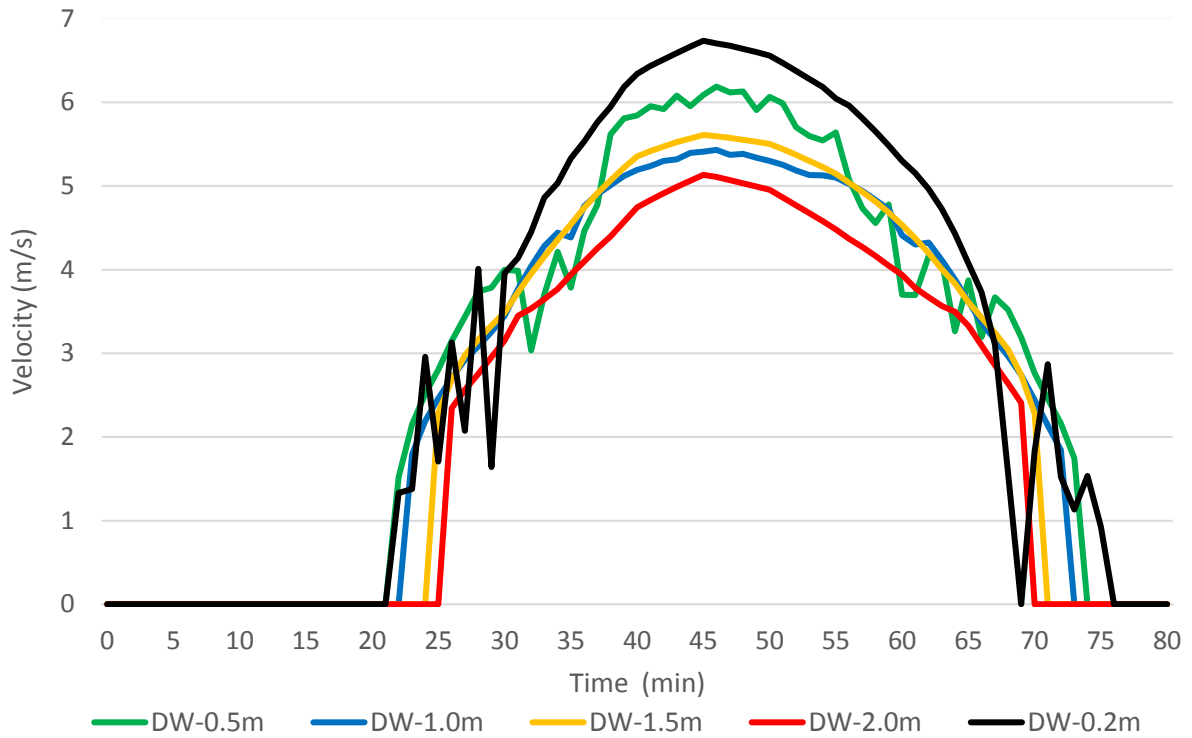
b) Distribution of model velocity at control point 1 for different grid resolutions with the full momentum equation or watershed B with 100 year storm.



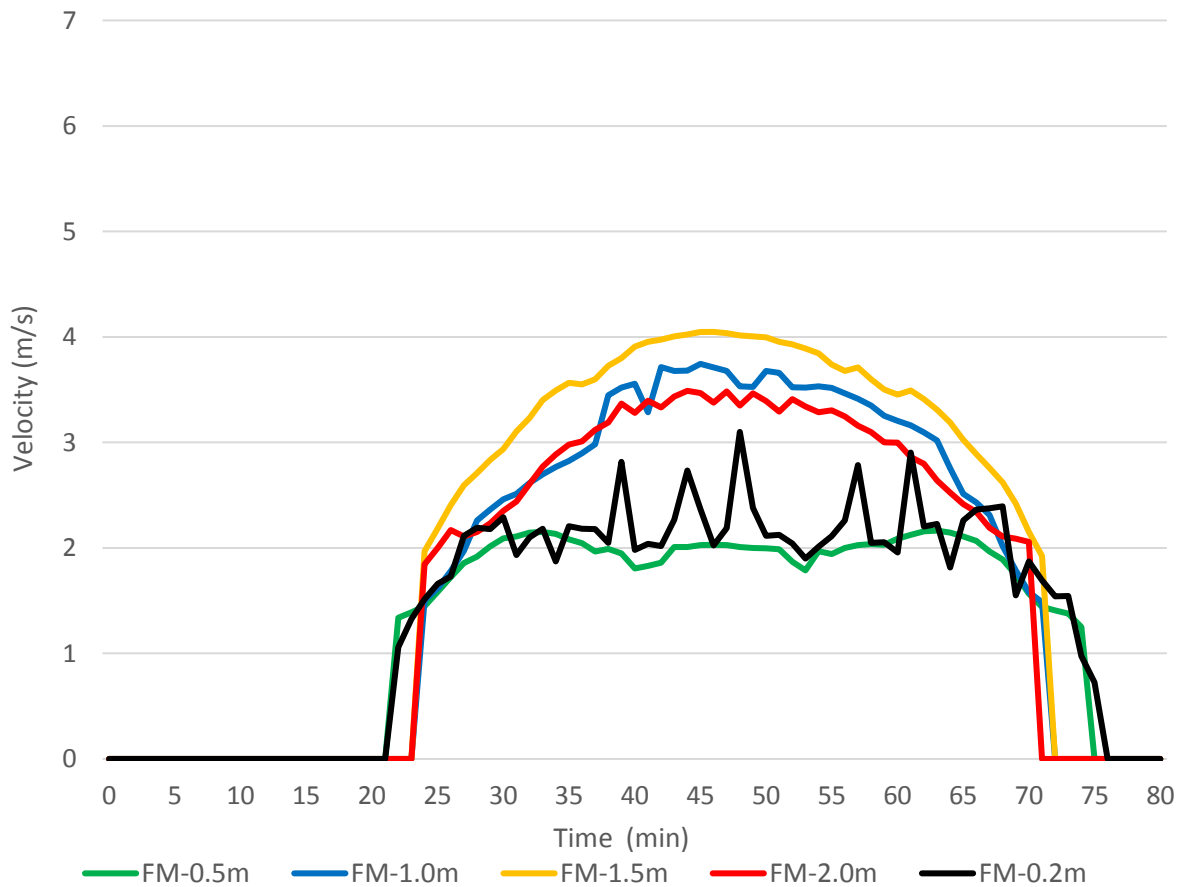
c) Distribution of model depth at control point 1 for different grid resolutions with the diffusive wave equation for watershed B with 100 year storm.



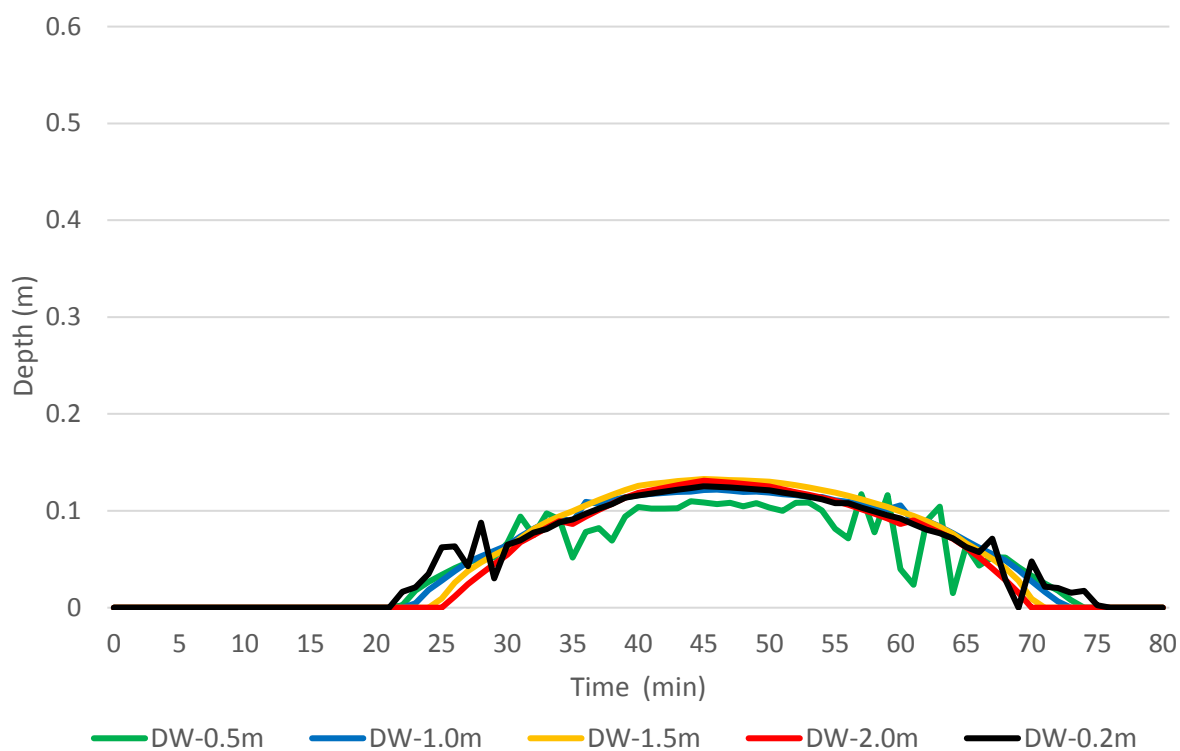
d) Distribution of model depth at control point 1 for different grid resolutions with the full momentum equation or watershed B with 100 year storm.



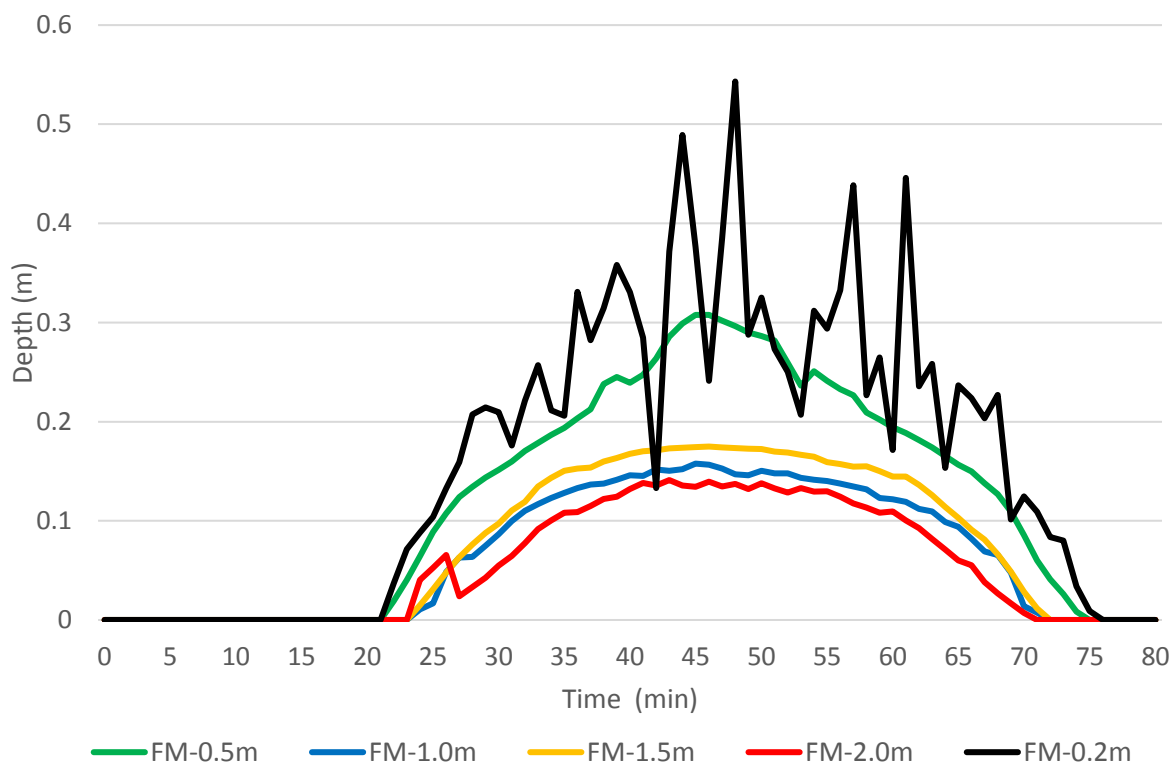
e) Distribution of model velocity at control point 2 for different grid resolutions with the diffusive wave equation for watershed B with 100 year storm.



f) Distribution of model velocity at control point 2 for different grid resolutions with the full momentum equation or watershed B with 100 year storm.



g) Distribution of model depth at control point 2 for different grid resolutions with the diffusive wave equation for watershed B with 100 year storm.



h) Distribution of model depth at control point 2 for different grid resolutions with the full momentum equation or watershed B with 100 year storm.

Figure 9- Simulated velocity and depth over time at two representative control points (two of six) at the five grid resolutions where the a, c, e, g is the diffusive approximation and b,d,f,h is full momentum.

Figure 9 shows the evolution of water depths and velocity at two representative control points (point locations are presented in appendix I) throughout the simulation using the diffusive wave approximation and the full momentum equation at grid resolutions of 0.2 m, 0.5 m, 1 m, 1.5 m and 2 m. Discrepancies between the two equations sets are visually evident and Figure 9 illustrate the differences in depth and velocity profiles over time. The diffusive wave is more stable at higher Courant number than the full momentum [67]. However, it is interesting to note that difference in velocities is greater than the difference in depths for both equation set (not considering FM-0.2). The variation in results is likely due to the instability in the numerical model and relationship between time step/cell sizes resulting in high Courant numbers. In addition, the diffusive wave yields higher velocities and lower depth than the full momentum, but seems more consistent at different resolutions. From Figure 9 it is evident that the relative difference in depths from the diffusive wave is of a lesser magnitude than with the full momentum at different grid sizes. As noted in previous studies on urban flooding, there is noticeable reduction in model performance at very fine grid resolutions up to 1 m over the entire domain in this case. In addition, results from grid resolutions of 0.5 and 0.2 in Figure 9 b², e, f and h is visually not consistent with the other resolutions.

Resolution 2.0 m and 1.5 m does not properly represent the wetting front for both equations, thus a rapid increase in velocity at 30-35 min compared to the slow build up at 20 min with the other resolutions (Figure 9 a, b, c). Figure 9 illustrates the importance of a grid size sensitivity test and how the grid size affects the accuracy of the results. In addition, coarser resolutions might yield correct peak velocity do not seem to be able to represent the increase in velocity over time. This study was conducted on a steep street, where the local or convective acceleration are expected to affect the results. From Figure 9e and f, diffusive wave predicts peak velocity at 5.1-6.7 m/s compared to 4.01-2.0 with the full momentum (3.0 is 0.2 and 0.5 is disregarded). The trends in Figure 9 is in agreement with a benchmarking performed by Pender and Néelz (2010) where it is noted that most diffusive wave 2D models were not initially designed to deliver velocity estimates and do not produce consistent estimates of velocities when compared to models based on the full momentum [72]. Fewtrell et al. 2011 note that although water depth estimates at grid scales coarser than 1 m appear robust, velocity estimates at these scales seem to be inconsistent. Though are not directly comparable due to different numerical approaches.

² Only 0.2 in Figure 9b.

The results from the different model runs verifies that there is a correlation between grid size and instability in the resulting simulated velocities. This is likely due to HEC-RAS limitation of minimum 0.1 s time step. This indicates that grid sizes bellow 1 m unsuitable for urban modeling in HEC-RAS, and the terrain is resolution more essential.

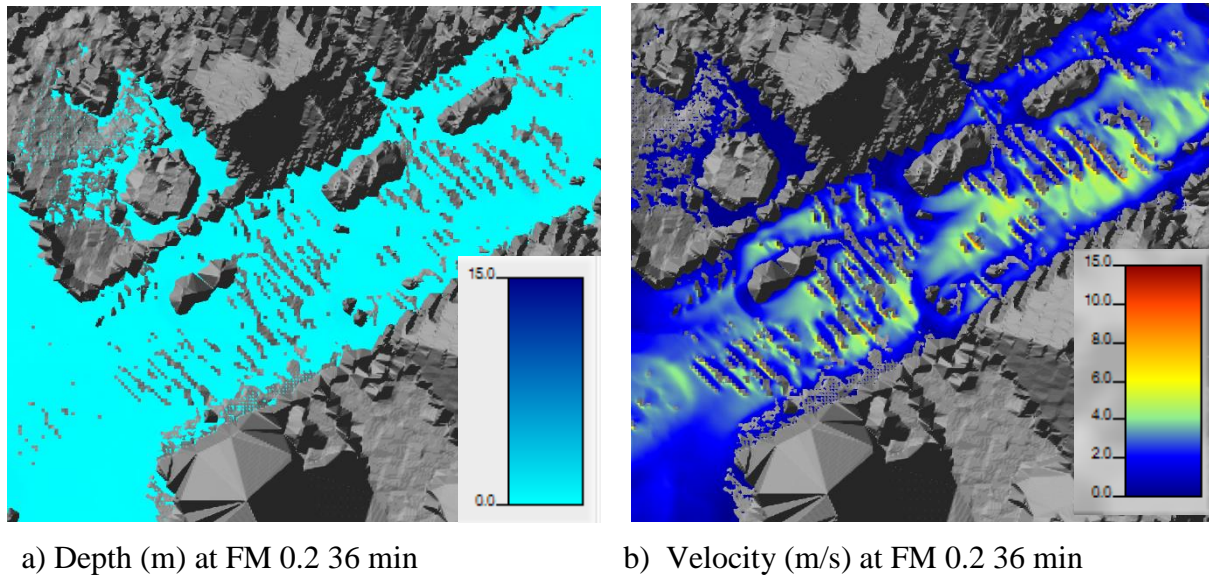


Figure 10- Sign of instability at 0.2m resolution with the full momentum equation for watershed B with a 100 year return period

Figure 9b illustrates that the Full momentum at 0.2 m grid size is clearly instable (FM-0.2). As evident when velocity rapidly fluctuates from 6-7 m/s to zero in some points. For a flood of such magnitude, velocities going from 6-7 m/s to zero is considered unreasonable and a sign of instability. This is also evident in Figure 10, where some cells are dry, indicating that the model does not converge with 40 iterations. For urban areas, the limiting factor in modelling is HEC-RAS computational step, which is limited to 0.1 s. For the model to be able to utilize a finer grid mesh than 1.0 m, a smaller time step must be used but is not available in HEC-RAS 5.0.4.

Figure 11 illustrates how the TIN-model represent the street cross-section in HEC-RAS with the terrain profile in red plotted with station (meters) on the x-axis and elevation (meter) on the y-axis. Fewtrell et al (2008) note that urban environments often are characterized by high spatial height variability and the method of grid interpolation and elevation model is of great importance, and at coarser scale greatly affects the building representation [30]. However, HEC-RAS RAS-mapper utilizes a TIN-model to describe the terrain, and the triangular representation of the street cross-section does not represent the street as a continuous line.

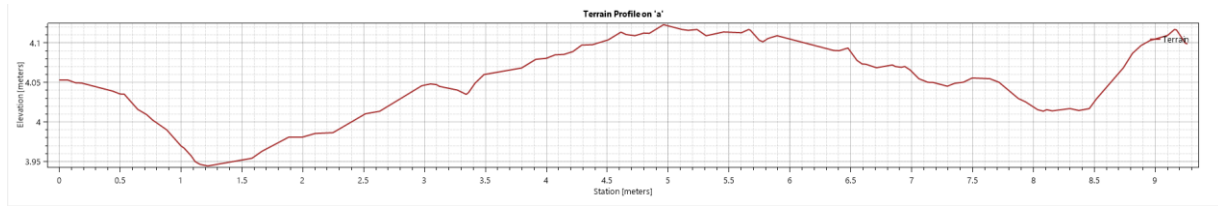


Figure 11- TIN--representation of street cross-section in HEC-RAS

Therefore the model might overestimate the storing and depression during the wetting front due to the terrain resolution. This could be the reason for the slow build up of velocity evident in Figure 9a-b.

Low velocities and low depth values at the sidewalk indicates that the use of roads as urban floodways could be a suitable measure for stormwater management in urban areas, however, it does require some alteration to the design of the street (e.g. higher curbs, reversed road cambers). The flood risk criteria used in this case study takes the higher risk of shallow depth and high velocity into account, but is not adjusted for debris. An open floodway directly from a vegetated and forested area could be expected to have a larger amount of debris which could affect the damage potential to pedestrians and properties, in addition the use of urban streets as floodway would require different maintenance than a standard urban street due to the risk of erosion and scouring. Other factors such as temperature and icing could also affect the total hazard potential for pedestrians. In addition, it is important to note that this study was conducted in a quite steep street, which affects the results, particularly velocity.

Precipitation over the street was assumed negligible, hence the results from this study should be validated with precipitation intensity at the point of maximum depth, velocity and flow. In addition, the delay caused by transportation of runoff to the street should be considered. As seen in Figure 12, the maximum velocity occurs 13-15 minutes after the peak intensity without considering the delay due to transportation of stormwater to the floodway. However, it is still reasonable to expect some uncertainty due to the absence of precipitation over the street, in addition to disruption in flow at the sidewalk due to flow from rooftops and gutters. The floodway should in addition be tested with storm events of lower duration than the lag time, to simulate a flood from a storm where the rain would have stopped before the floodway is activated – thus, a situation where a pedestrian might not expect flash flood since it is no longer raining.

The duration of the flood is not as significant in regards to hazard as the delay and lag time, since it is reasonable to expect that pedestrians might be more cautious to use the street during flood, but not have an expectation of when or how fast the floodway might become active. This indicates that implementation of a warning system is an important requirement for the use of urban streets as floodways, altering the public of the time to and extent of flooding on the street. HEC-RAS does show flood duration if the simulation time window is large enough. However, only if the water naturally drains away from the study area, since it does not account for evaporation, infiltration or drainage to the sewage network. It does, however, provide information of how long high velocities are expected, and where ponding will occur until the sewage network can drain the area.

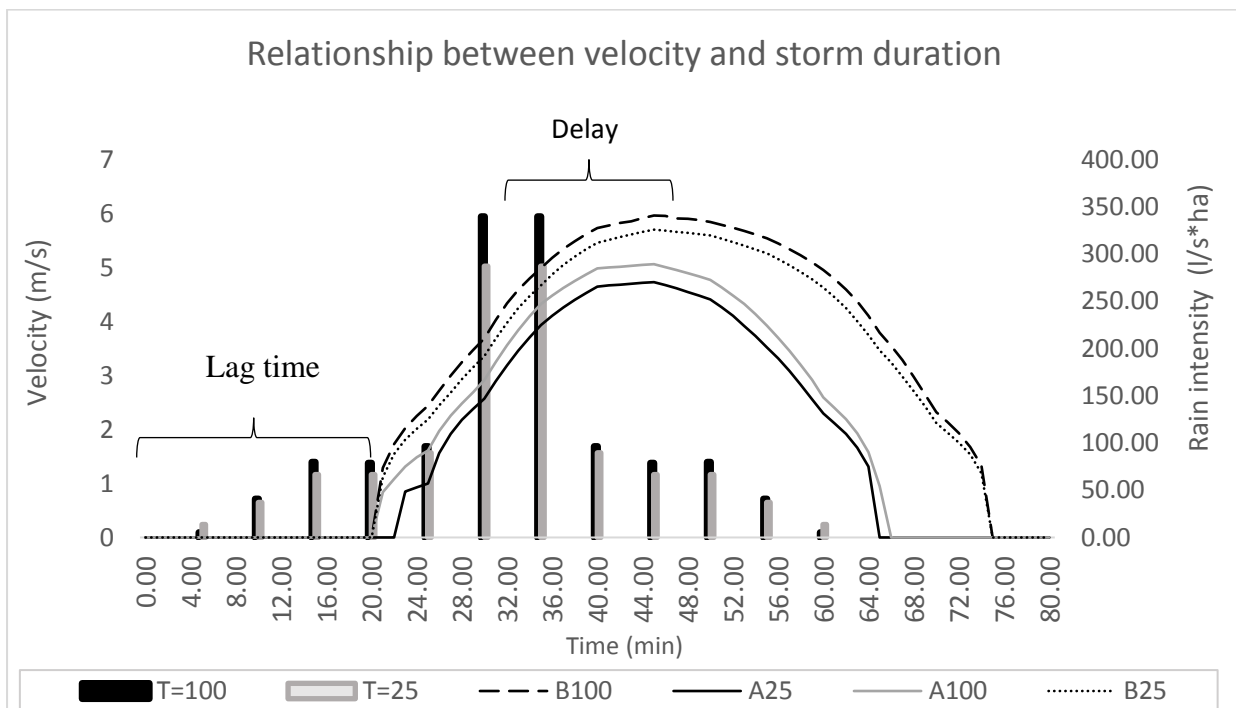


Figure 12- Delay between peak velocity and peak intensity with different return periods (T)

4.2 Implications of the results

The study demonstrated that for urban areas with rapid water movement, coarser resolution of the computational grid than the terrain is preferred, in contradiction to previous studies where grid size is selected at the same resolution as the underlying terrain [41, 42]. HEC-RAS 2D seems to offer a lot of potential in the evolution of the applicability of using an urban street as a floodway. However, the model is highly sensitive to the grid placement, size and time step, still it is the underlying terrain that is the significant parameter affecting accuracy.

At high volume and velocity of run-off, the leaking from the street in the intersections into adjoining streets is evident. This does indicate that the design and layout of intersections is an area of floodways which requires more research, and different design for confinement of water and safe crossing could be considered (i.e. use of elevated pedestrian crossing as water levees). The results offer much potential for using urban streets as floodways, as a routing in street perpendicular to the slope will reduce peak velocity. The findings indicate that even at high slopes, streets could be suitable as floodways due to safe conditions at the sidewalk. Moreover, floodways might be even more suitable for streets with a lower slope, however, then flood duration and flood intrusion be important performance criteria.

The methodology proposed is also suitable for mapping existing floodways in urban areas, especially when using distributed uniform precipitation over the area, thus reducing uncertainty from hydrograph and run-off estimation. HEC-RAS 2D “rain on grid” capabilities do not allow for calculation of infiltration losses, hence, net runoff hyetographs need to be calculated outside of HEC-RAS for use as input data. HEC-RAS 2D could be an important tool to assess a city or urban areas vulnerability to flood and to locate existing paths in the terrain which might become active floodways during extreme precipitation events. This could replace GIS-based drainage lines used to develop susceptibility maps used by Norwegian municipalities, and result in flood hazard-maps with information such as velocity, depth, and depth-velocity product, in addition to which area the water pond. This could be a fast, simple and easy method for municipalities to assess flood risk, in addition to find vulnerable and exposed areas where there is a need to develop safer floodways during extreme events. This study demonstrates, that due to the urban environments complex topography, shallow water and high velocity pose a significant hazard to pedestrians, especially in areas with high slopes. This indicates that there is a need for municipalities to expand flood mapping to include velocity distribution and specific hazard criteria.

Municipalities should include maximum flow depths and velocities in political regulations and design criteria in urban areas, both in open floodways and for surface flow for when only the major system is operational (e.g. sewer at capacity or blockage). The study have demonstrated that there are several suitable hazard criteria for urban environments in literature[50], and that HEC-RAS is a suitable and efficient tool for depth and velocity mapping in urban areas.

4.3 Further work

Calibration of the friction parameter is the conventional method to reduce uncertainty in flood modelling and fitting model predictions to observed values. (Fewtrell et al 2008). Hunter et al. 2008 note such a lack of observational data induces the need for sensitivity analysis with a range of suitable friction values. No calibration technique was used in this study. However, in literature there are examples techniques based on floodwater marks [35, 73] and use of private amateur recordings of floods [34] to calibrate results. This study used different grid resolutions and equations to evaluate the accuracy of the results. In literature, HEC-RAS have yet to be used to model urban flooding and studies employing calibration and validation techniques could be conducted to confirm the suitability of HEC-RAS as a tool for urban modeling. As HEC-RAS 2D does not require a georeferenced geometry representation of the street, only a digital terrain model, the quality of the terrain model is an important factor for result accuracy. Subsequently, since the availability of high resolution data is high in Norway, it makes HEC-RAS 2D a suitable tool for mapping and evaluation of urban floodways. Although, the confidence in the results should be verified using sensitivity studies of both roughness factor, energy slope, placement of upper and lower boundary, in addition the placement and layout of the computational grid. HEC-RAS does not have the capability to model infiltration, flow over drains, evaporation, groundwater flow, or snow melt. Thus, is limited to modelling surface runoff. Hence, the design storm and the design hydrograph should be representative of the watershed characteristics, the slope and travel time of the watershed. Therefore, future studies should include different hydrological conditions, which might significantly affect the results [12]. This study have noted that urban floodways should be perpendicular to the slope of the terrain, and further studies could evaluate the effect of such measure in regards to reduction of hazard potential or total flooded area.

Further work should include more detailed research on optimal design and alternative cross-sections of an urban street as a flood way, to evaluate solutions to detain the water in the street or to reduce velocity in the cross-section. Further work is required to find the optimal cross-sections for both transport capacity, hazard, safety and traffic function before urban streets could be designed as floodways. Guillén et al. 2017 studied velocity profiles in a street cross-section represented as a river with HEC-RAS 1D, but a 2D approach would yield more accurate results.

HEC-RAS 5.0.4 performance in this study, in addition the newly added ability to georeference new cross-sections in RAS-mapper (instead of using HEC-geoRAS) or edit river-geometry, thus subsequently edit the terrain, makes HEC-RAS 5.04 edible for further studies on velocity profiles and flow in different cross-sections.

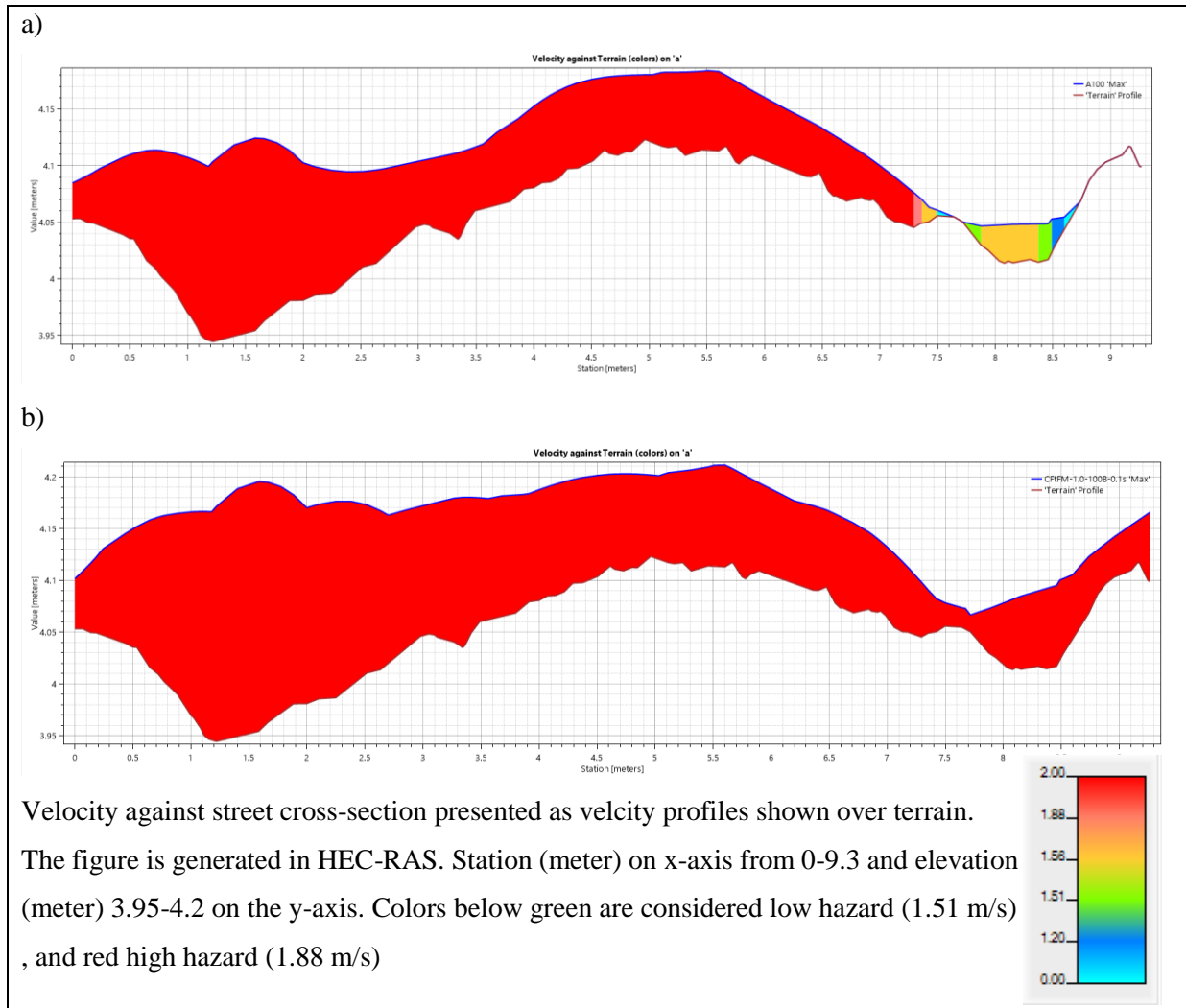


Figure 13- Velocity profiles in street cross-section for a) Watershed A and b) Watershed B, with hazard criteria from Table 1.

Such studies can evaluate the various street cross-section for best performance of an urban street as floodway, in addition to measures for reducing flooding and divert floodwater in urban areas. Figure 13 demonstrate how velocity profiles may be assessed in HEC-RAS 5.04, where the terrain profile represents the street cross-section plotted with velocity, and the sidewalks are represented by station 0-1.2 and 8.4-9.3. Other cross-sections such as reversed crown (v-profiles), and various curb heights could have a large impact on urban streets performance as a floodway.

In this study, the rational method combined with the time—area was employed due to its strong standing in Norwegian municipalities and since it is Bergen municipalities preferred method for watershed under 50 ha [58]. However, many researchers have discussed the accuracy and applicability of the rational formula, and have proposed more suitable methods [74]. Such methods could account for infiltration dependent on precipitation intensity, and be more applicable for hydrograph estimations at small and ungauged site [75]. In addition, studies have shown the need for sensitivity analysis in flood modelling in urban areas due to uncertainty from variation in hydrologic conditions or the use of different design storms [12]. Future studies on the development of urban streets as floodway should chose a suitable method for the design hydrograph, based on the available data and hydrologic conditions.

5. Concluding Remarks

A Digital Surface Model with a resolution of 10 cm was used with HEC-RAS 2D to evaluate the impact of using an urban street as a floodway, and to assess the corresponding hazard level. The study shows that HEC-RAS with a grid size of 1 by 1 meter over a street segment of 146 meter is a suitable tool to simulate the use of urban streets as a floodway however with some limitations. The accuracy of the results depends on the grid sizes. Result sensitivity due to mesh construction should thus be investigated in all projects. The study has also shown that grid size does not require the same resolution as the terrain, which can save computational cost but also highlight the need for good terrain models.

The computational time of 01:25:26 hours for a 1 meter by 1 meter grid resolution with the use of a normal computer is considered acceptable for municipality use. A limitation of this study, is that it evaluates a scenario with little data to calibrate and validate the results, hence the findings in this study must therefore be treated with caution.

This study identified several performance criteria for which the applicability of urban streets as floodway should be evaluated. The most important hydraulic performance are flood velocity, flood depth, transportation capacity, total flooding extent, flood duration and activation frequency. It was found that either transportation capacity or hazard potential were the restricting design criteria for an urban streets as a temporary floodway.

To decide if a floodway can be considered safe, the concept of hazard potential for pedestrian and the public is utilized. For the urban street not to cause significant damage to the environment, flood duration, depth and total flood extent is considered. The study identified the importance of using appropriate hazard criteria for the evaluation of hazard potential. This study identified velocity as the dominating factor in hazard potential for pedestrian as urban streets used as a floodway. Other factors affecting the hazard and damage potential of the floodway were: flood depth, depth-velocity product, total flooding extent and debris.

Other findings from the study:

- * A significant correlation between hazard on the street and the presence of urban obstacles (represented as vehicles). Urban obstacles affected flow distribution and increased velocity. The results from this study, may be used by municipalities to consider the removal of such obstacles by an implementation of a parking ban.
- * High hazard potential is found in the street, but due to the curb height a significantly lower velocity is present at the sidewalk. Thus, indicating that urban streets can still be suitable for floodways even if high velocities are present by implementation of higher curbstones.
- * Different placement floodways of on the street significantly affects the hazard potential and floodways would be safer if they are on streets which are perpendicular to the slope of the terrain, thus resulting in lower hazard potential.
- * HEC-RAS is an efficient tool for mapping floodways, additionally identifying existing floodways in the terrain. Subsequently, the method proposed could also be used to assess hazard potential due to extreme events, existing damage potential and identify vulnerable and flood exposed parts of the city in need of flood proofing.

As an overall conclusion, the use of steep urban streets would therefore not be recommended without substantial implementation of flood safety measures, such as levees or elevated pedestrian crossing, and elevated curbs. However, this would in addition to confinement of the flood also induce greater depth and velocities values in the street. Further research efforts in this area should therefore include design and placement of open floodways in urban areas and floodwater transport.

6. Acknowledgements

The present study was made possible by the BINGO project - *Bringing INnovation to onGOing water management – a better future under climate change* (projectbingo.eu) and by Klima 2050, Centre for Research-based Innovation (klima2050.no).

7. References

1. Hirabayashi, Y., et al., *Global flood risk under climate change*. Nature Climate Change, 2013. **3**(9): p. 816.
2. Palmer, M.A., et al., *Climate change and the world's river basins: anticipating management options*. Frontiers in Ecology and the Environment, 2008. **6**(2): p. 81-89.
3. Ryberg, K.R., W. Lin, and A.V. Vecchia, *Impact of climate variability on runoff in the North-Central United States*. Journal of Hydrologic Engineering, 2012. **19**(1): p. 148-158.
4. Hanssen-Bauer E.J., et al., *Climate in Norway 2100 – a knowledge base for climate adaptation*, in *NCCS report*, N.E. Agency, Editor. 2017, The Norwegian Centre for Climate Services. p. 204.
5. Nilsen, V., et al., *Analysing urban floods and combined sewer overflows in a changing climate*. Journal of Water and Climate Change, 2011. **2**(4): p. 260-271.
6. Nie, L., *Enhancing urban flood resilience – a case study for policy implementation*. Proceedings of the Institution of Civil Engineers - Water Management, 2016. **169**(2): p. 85-93.
7. Lindholm, O., et al., *Veiledning i klimatilpasset overvannshåndtering*, in *Norsk Vann*. 2008: Hamar.
8. Andenæs, E., et al., *Performance of Blue-Green Roofs in Cold Climates: A Scoping Review*. Buildings, 2018. **8**(4): p. 55.
9. Johannessen, B., T. Muthanna, and B. Braskerud, *Detention and Retention Behavior of Four Extensive Green Roofs in Three Nordic Climate Zones*. Water, 2018. **10**(6): p. 671.
10. The City of Copenhagen, *Cloudburst Management Plan 2012*. 2012, Technical and Environmental Administration.
11. Teng, J., et al., *Flood inundation modelling: A review of methods, recent advances and uncertainty analysis*. Environmental Modelling & Software, 2017. **90**: p. 201-216.
12. Papaioannou, G., et al., *An Operational Method for Flood Directive Implementation in Ungauged Urban Areas*. Hydrology, 2018. **5**(2): p. 24.
13. Hunter, N.M., et al., *Benchmarking 2D hydraulic models for urban flooding*. Proceedings of the Institution of Civil Engineers - Water Management, 2008. **161**(1): p. 13-30.
14. Djordjević, S., et al., *SIPSON–Simulation of Interaction between Pipe flow and Surface Overland flow in Networks*. Water Science and Technology, 2005. **52**(5): p. 275-283.
15. Leandro, J., A.S. Chen, and A. Schumann, *A 2D parallel diffusive wave model for floodplain inundation with variable time step (P-DWave)*. Journal of Hydrology, 2014. **517**: p. 250-259.
16. Fraga, I., L. Cea, and J. Puertas, *Validation of a 1D-2D dual drainage model under unsteady part-full and surcharged sewer conditions*. Urban Water Journal, 2017. **14**(1): p. 74-84.
17. Russo, B., et al., *Analysis of extreme flooding events through a calibrated 1D/2D coupled model: the case of Barcelona (Spain)*. Journal of Hydroinformatics, 2015. **17**(3): p. 473-491.
18. Gómez, M., F. Macchione, and B. Russo, *Methodologies to study the surface hydraulic behaviour of urban catchments during storm events*. Water Science and Technology, 2011. **63**(11): p. 2666-2673.
19. Diaz-Nieto, J., et al., *GIS Water-Balance Approach to Support Surface Water Flood-Risk Management*. Journal of Hydrologic Engineering, 2012. **17**(1): p. 55-67.

20. Turner, A., et al., *Flood Modeling Using a Synthesis of Multi-Platform LiDAR Data*. Water, 2013. **5**(4): p. 1533.
21. Vojinovic, Z. and D. Tutulic, *On the use of 1D and coupled 1D-2D modelling approaches for assessment of flood damage in urban areas*. Urban Water Journal, 2009. **6**(3): p. 183-199.
22. Fewtrell, T.J., et al., *Benchmarking urban flood models of varying complexity and scale using high resolution terrestrial LiDAR data*. Physics and Chemistry of the Earth, Parts A/B/C, 2011. **36**(7): p. 281-291.
23. Mark, O., et al., *Potential and limitations of 1D modelling of urban flooding*. Journal of Hydrology, 2004. **299**(3): p. 284-299.
24. Noh, S.J., et al., *Hyper-resolution 1D-2D urban flood modelling using LiDAR data and hybrid parallelization*. Environmental Modelling & Software, 2018. **103**: p. 131-145.
25. Dottori, F., G.D. Baldassarre, and E. Todini, *Detailed data is welcome, but with a pinch of salt: Accuracy, precision, and uncertainty in flood inundation modeling*. Water Resources Research, 2013. **49**(9): p. 6079-6085.
26. Papaioannou, G., et al., *Flood inundation mapping sensitivity to riverine spatial resolution and modelling approach*. Natural Hazards, 2016. **83**(1): p. 117-132.
27. Apel, H., et al., *Flood risk analyses—how detailed do we need to be?* Natural Hazards, 2009. **49**(1): p. 79-98.
28. Werner, M., S. Blazkova, and J. Petr, *Spatially distributed observations in constraining inundation modelling uncertainties*. Hydrological Processes, 2005. **19**(16): p. 3081-3096.
29. Bates, P.D., et al., *Bayesian updating of flood inundation likelihoods conditioned on flood extent data*. Hydrological Processes, 2004. **18**(17): p. 3347-3370.
30. Fewtrell, T.J., et al., *Evaluating the effect of scale in flood inundation modelling in urban environments*. Hydrological Processes, 2008. **22**(26): p. 5107-5118.
31. Pappenberger, F., et al., *Uncertainty in the calibration of effective roughness parameters in HEC-RAS using inundation and downstream level observations*. Journal of Hydrology, 2005. **302**(1): p. 46-69.
32. Pappenberger, F., et al., *Influence of uncertain boundary conditions and model structure on flood inundation predictions*. Advances in Water Resources, 2006. **29**(10): p. 1430-1449.
33. Kim, U. and J.J. Kaluarachchi, *Application of parameter estimation and regionalization methodologies to ungauged basins of the Upper Blue Nile River Basin, Ethiopia*. Journal of Hydrology, 2008. **362**(1): p. 39-56.
34. Guillén, N.F., et al., *Use of LSPIV in assessing urban flash flood vulnerability*. Natural Hazards, 2017. **87**(1): p. 383-394.
35. Mignot, E., A. Paquier, and S. Haider, *Modeling floods in a dense urban area using 2D shallow water equations*. Journal of Hydrology, 2006. **327**(1): p. 186-199.
36. Russo, B., et al. *Flood hazard assessment in the Raval District of Barcelona using a 1D/2D coupled model*. in *Proceedings of 9th International Conference on Urban Drainage Modelling, Belgrade, Serbia: Faculty of Civil Engineering, University of Belgrade*. 2012.
37. Gomez-Valentin, M., F. Macchione, and B. Russo, *Hydraulic behavior of urban streets during storm events*. Ingenieria Hidraulica en Mexico, 2009. **24**(3): p. 51-62.
38. Ozdemir, H., et al., *Evaluating scale and roughness effects in urban flood modelling using terrestrial LIDAR data*. Hydrology and Earth System Sciences, 2013. **10**: p. 5903-5942.

39. G.A.M., d.A., B. P., and O. H., *Modelling urban floods at submetre resolution: challenges or opportunities for flood risk management?* Journal of Flood Risk Management, 2018. **11**(S2): p. S855-S865.
40. Mignot, E., A. Paquier, and N. Rivière, *Experimental and numerical modeling of symmetrical four-branch supercritical*. Journal of Hydraulic Research, 2008. **46**(6): p. 723-738.
41. Patel, D.P., et al., *Assessment of flood inundation mapping of Surat city by coupled 1D/2D hydrodynamic modeling: a case application of the new HEC-RAS 5*. Natural Hazards, 2017. **89**(1): p. 93-130.
42. Moya Quiroga, V., et al., *Application of 2D numerical simulation for the analysis of the February 2014 Bolivian Amazonia flood: Application of the new HEC-RAS version 5*. RIBAGUA - Revista Iberoamericana del Agua, 2016. **3**(1): p. 25-33.
43. J., F.T., et al., *Geometric and structural river channel complexity and the prediction of urban inundation*. Hydrological Processes, 2011. **25**(20): p. 3173-3186.
44. Kourtis, I., V. Bellos, and V. Tsihrintzis. *Comparison of 1D-1D and 1D-2D urban flood models*. in *Proceedings of the 15th International Conference on Environmental Science and Technology (CEST 2017), Rhodes, Greece*. 2017.
45. Merz, B., et al., *Review article" Assessment of economic flood damage"*. Natural Hazards and Earth System Sciences, 2010. **10**(8): p. 1697.
46. Abt, S., et al., *Human stability in a high flood hazard zone*. JAWRA Journal of the American Water Resources Association, 1989. **25**(4): p. 881-890.
47. Lind, N., D. Hartford, and H. Assaf, *HYDRODYNAMIC MODELS OF HUMAN STABILITY IN A FLOOD1*. JAWRA Journal of the American Water Resources Association, 2004. **40**(1): p. 89-96.
48. Russo, B., M. Gómez, and F. Macchione, *Pedestrian hazard criteria for flooded urban areas*. Natural Hazards, 2013. **69**(1): p. 251-265.
49. Luca, M., P. Marco, and R. Roberto, *A conceptual model of people's vulnerability to floods*. Water Resources Research, 2015. **51**(1): p. 182-197.
50. Martínez-Gomariz, E., M. Gómez, and B. Russo, *Experimental study of the stability of pedestrians exposed to urban pluvial flooding*. Natural hazards, 2016. **82**(2): p. 1259-1278.
51. Xia, J., et al., *Formula of incipient velocity for flooded vehicles*. Natural Hazards, 2011. **58**(1): p. 1-14.
52. Merz, B., et al., *Estimation uncertainty of direct monetary flood damage to buildings*. Natural Hazards and Earth System Science, 2004. **4**(1): p. 153-163.
53. Kreibich, H., et al., *Is flow velocity a significant parameter in flood damage modelling?* Natural Hazards and Earth System Sciences, 2009. **9**(5): p. 1679.
54. Smith, D.I., *Flood damage estimation- A review of urban stage-damage curves and loss functions*. Water S. A., 1994. **20**(3): p. 231-238.
55. Kelman, I. and R. Spence, *An overview of flood actions on buildings*. Engineering Geology, 2004. **73**(3-4): p. 297-309.
56. Meze-Hausken, E., *Seasons in the sun - weather and climate front-page news stories in Europe's rainiest city, Bergen, Norway*. International Journal of Biometeorology, 2007. **52**(1): p. 17-31.
57. Jonassen, M.O., et al., *Simulations of the Bergen orographic wind shelter*. Tellus A: Dynamic Meteorology and Oceanography, 2013. **65**(1): p. 19206.
58. Bergen kommune, (The Municipality of Bergen), *Retningslinjer for overvannshåndtering i Bergen (Guidelines for stormwater handling in the Municipality of Bergen)*. 2005, Byrådsavdeling for byutvikling og Vann- og avløpsetaten (City

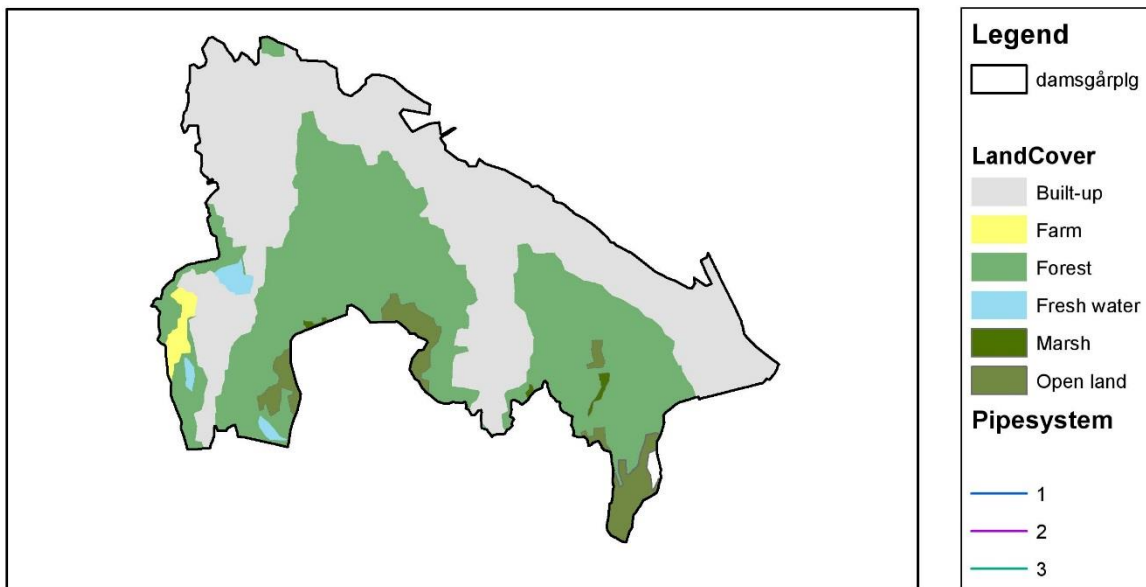
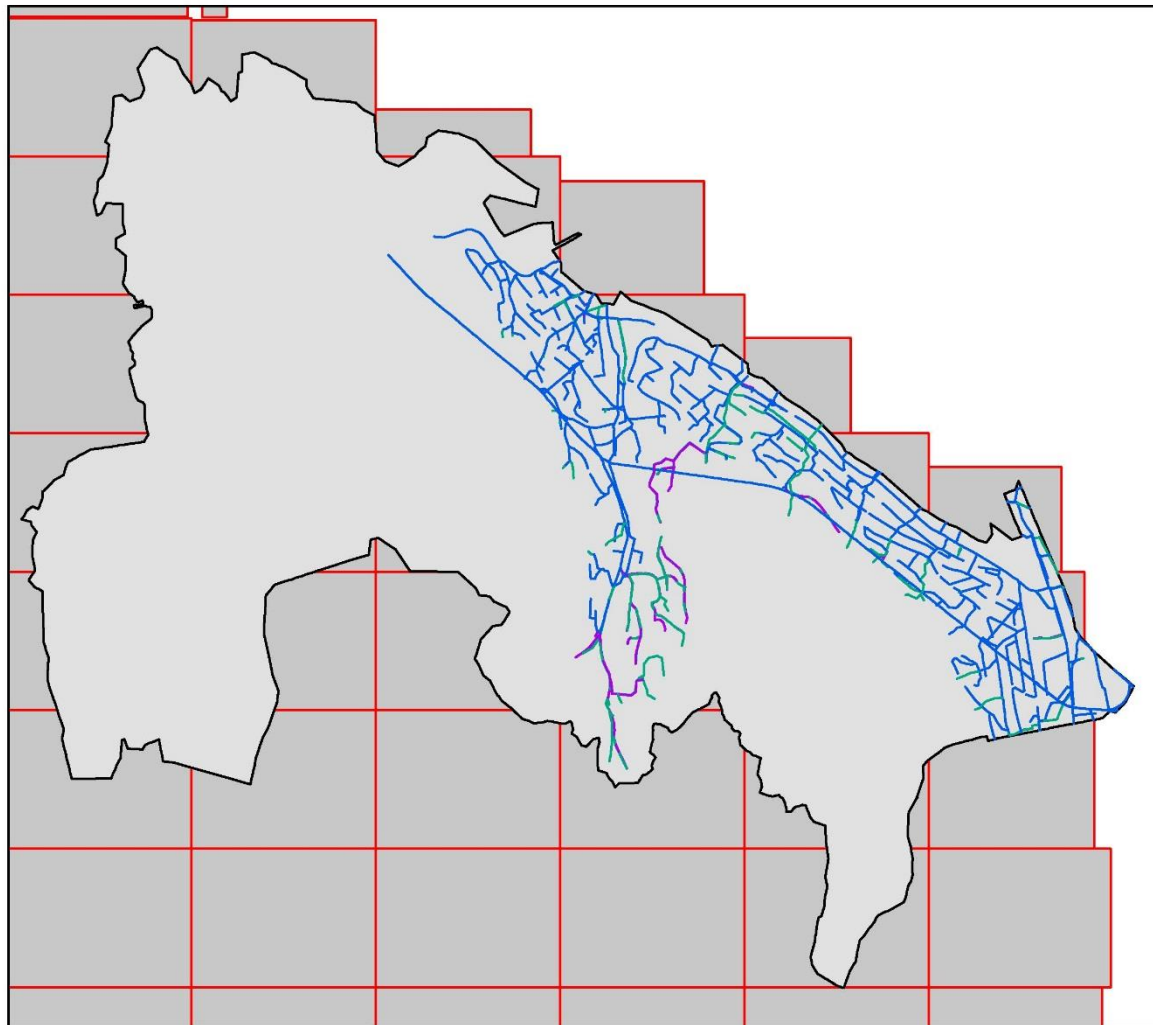
- Council for City Development and the Water and Wastewater Agency): Bergen, Norway.
59. Butler, D. and J. Davies, *Urban drainage*. 2003: Crc Press.
 60. Kristvik, E., et al., *Assessing the robustness of raingardens under climate change using SDSM and temporal downscaling*. Water Science and Technology, 2018. **77**(6): p. 1640-1650.
 61. Ven Chow , D.M., Larry Mays *Applied Hydrology*. McGraw Hill Series in Water Resources and Environmental Engineering. 1988, New York: McGraw-Hill.
 62. Herath, S.M., P.R. Sarukkalige, and V.T.V. Nguyen, *A spatial temporal downscaling approach to development of IDF relations for Perth airport region in the context of climate change*. Hydrological Sciences Journal, 2016. **61**(11): p. 2061-2070.
 63. Alfieri, L., F. Laio, and P. Claps, *A simulation experiment for optimal design hyetograph selection*. Hydrological Processes, 2008. **22**(6): p. 813-820.
 64. Singh, S.K., *Clark's and Espey's unit hydrographs vs the gamma unit hydrograph / Les hydrogrammes unitaires de Clark et de Espey vs l'hydrogramme unitaire de forme loi gamma*. Hydrological Sciences Journal, 2005. **50**(6): p. null-1067.
 65. Sadeghi, S.H.R., R. Mostafazadeh, and A. Sadoddin, *Changeability of simulated hydrograph from a steep watershed resulted from applying Clark's IUH and different time-area histograms*. Environmental Earth Sciences, 2015. **74**(4): p. 3629-3643.
 66. Villarreal, E.L., A. Semadeni-Davies, and L. Bengtsson, *Inner city stormwater control using a combination of best management practices*. Ecological Engineering, 2004. **22**(4): p. 279-298.
 67. Brunner G.W, *2D modeling user's manual*. 2016, Institute for Water Resources, Hydrologic Engineering Center.
 68. Haider, S., et al., *Urban flood modelling using computational fluid dynamics*. Proceedings of the Institution of Civil Engineers - Water and Maritime Engineering, 2003. **156**(2): p. 129-135.
 69. Chow, V.T., *Open-channel hydraulics*. 1959, New York, McGraw Hill.
 70. Hicks, F.E. and T. Peacock, *Suitability of HEC-RAS for Flood Forecasting*. Canadian Water Resources Journal / Revue canadienne des ressources hydriques, 2005. **30**(2): p. 159-174.
 71. Xia, J., et al., *Numerical assessment of flood hazard risk to people and vehicles in flash floods*. Environmental Modelling & Software, 2011. **26**(8): p. 987-998.
 72. Néelz, S., Pender, G., *Benchmarking of 2D Dydraulic Modelling Packages*. 2010.
 73. Parkes, B.L., et al., *Reducing Inconsistencies in Point Observations of Maximum Flood Inundation Level*. Earth Interactions, 2013. **17**(6): p. 1-27.
 74. Grimaldi, S. and A. Petroselli, *Do we still need the Rational Formula? An alternative empirical procedure for peak discharge estimation in small and ungauged basins*. Hydrological Sciences Journal, 2015. **60**(1): p. 67-77.
 75. Grimaldi, S., A. Petroselli, and N. Romano, *Curve-Number/Green-Ampt mixed procedure for net rainfall estimation: a case study of the Mignone watershed, IT*. Procedia Environmental Sciences, 2013. **19**: p. 113-121.
 76. Kirpich, Z.P., *Time of concentration of small agricultural watersheds*. Civil Engineering, 1940. **10**(6).
 77. Kerby, W., *Time of concentration for overland flow*. Civil Engineering, 1959. **29**: p. 60.

Appendix A – Framework for Article

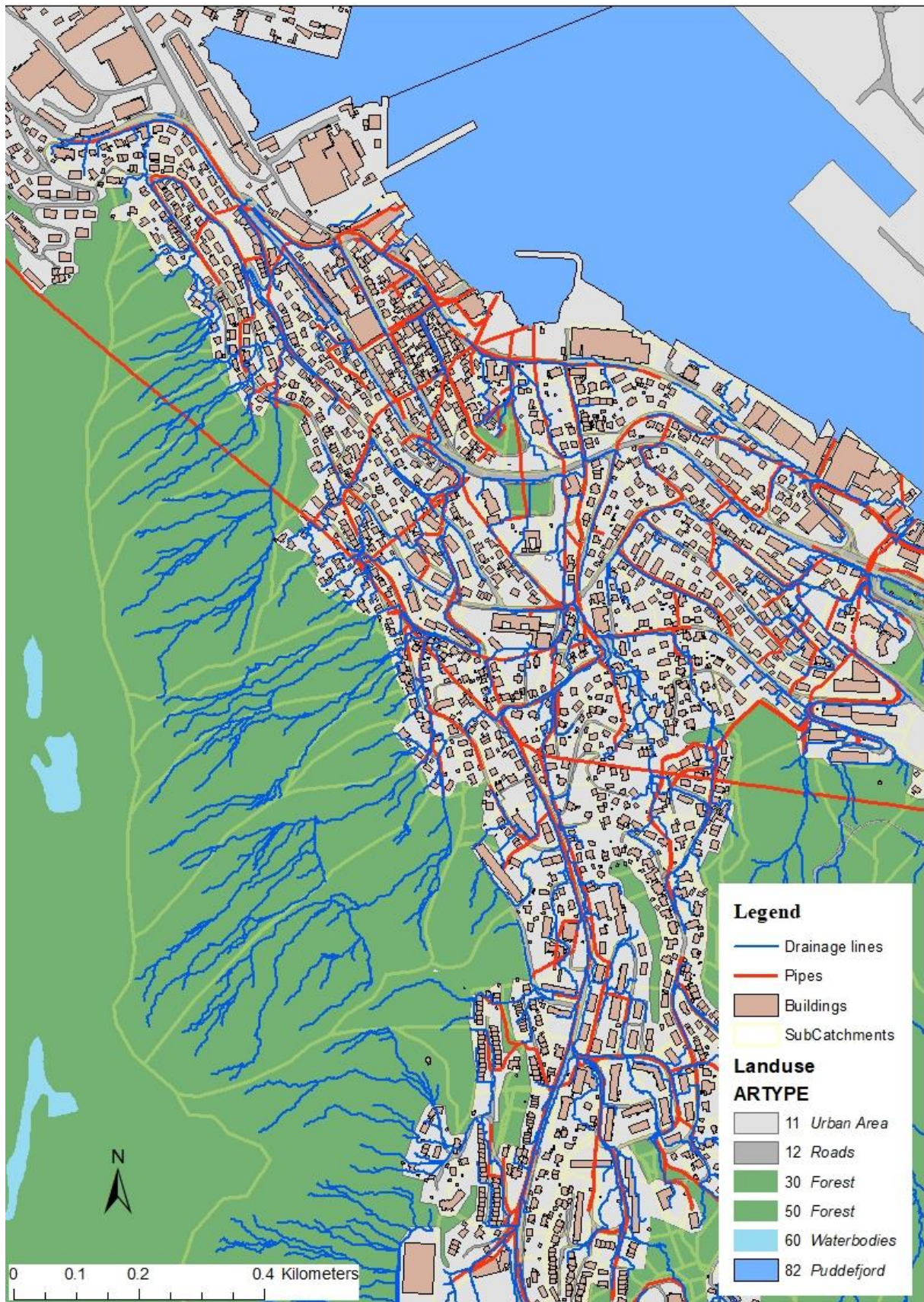
Article structure: The maximum acceptable length of a Research Paper is 10 000 words, minus 350 words for each normal-sized figure or table you include. Papers should contain:

- **Title**
- **Short title** of no more than 80 characters (including spaces)
- **Author name(s)**, full postal addresses for each author. Include the e-mail address for the corresponding author only.
- **Abstract:** no more than 200 words briefly specifying the aims of the work, the main results obtained, and the conclusions drawn.
- **Keywords:** up to 6 keywords (in alphabetical order)
- **Main text:** for clarity this should be subdivided into:
 - **Introduction:**
 - **Study area and data:** should describe the location, size, geographical and relevant climatic and other conditions of the region. It should clearly describe all the data used and their sources, including data periods, temporal resolution, limitations, quality, etc. Use of tables is encouraged where appropriate.
 - **Methods:** a brief description of the methods/techniques used
 - **Results and Discussion:** a clear presentation of experimental results obtained, highlighting any trends or points of interest and a brief explanation of the significance and implications of the work reported
 - **Conclusions:** a brief statement of what was undertaken in the study (one or two sentences) followed by what was established relative to the stated aims and objectives.
- **References:** Note that a paper is at risk of rejection if there are too few (<10) or too many references, or if a disproportionate share of the references cited are your own.
- **Supplementary Material:** Appendices and other Supplementary Material are permitted, and will be published online only.

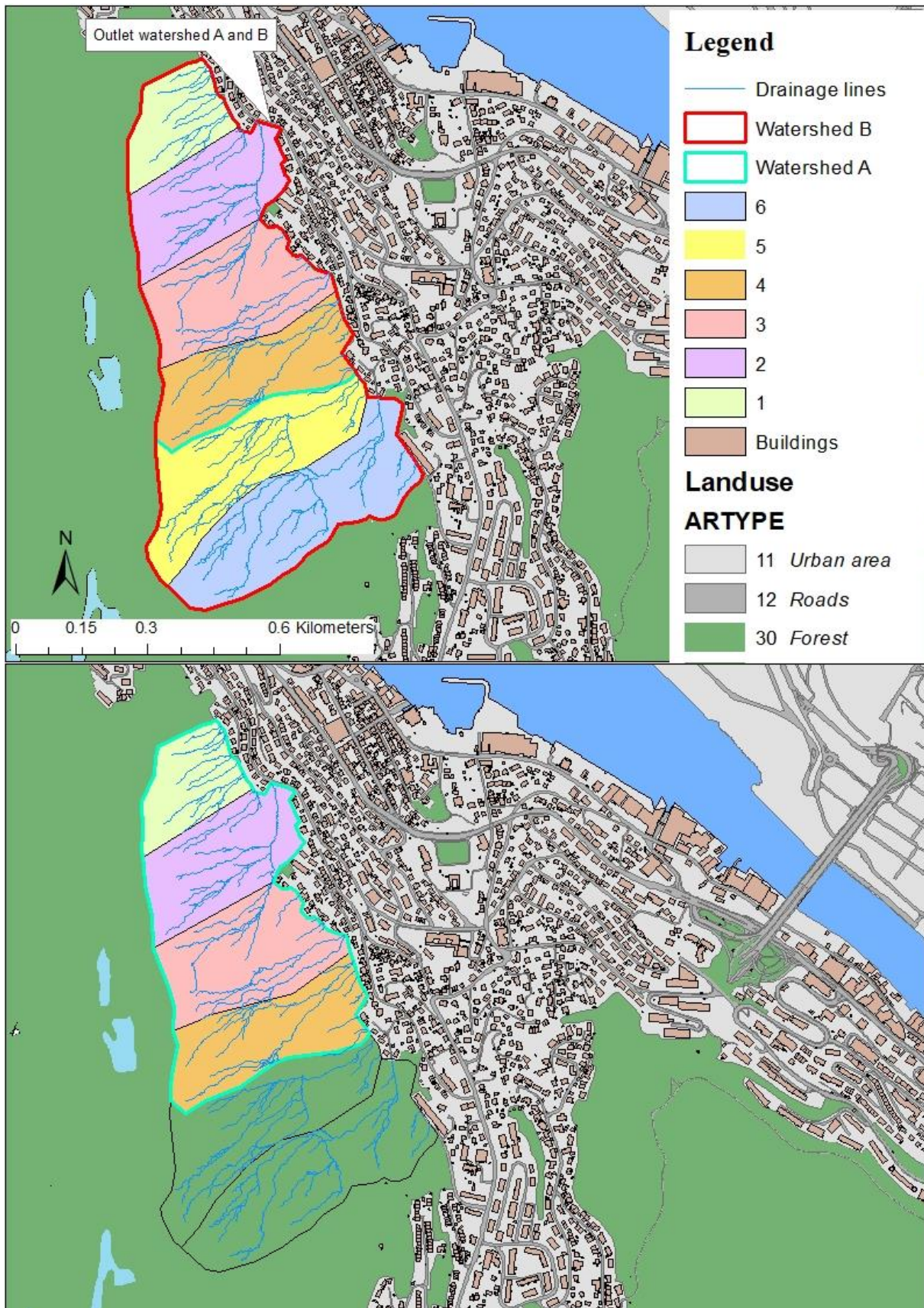
Appendix B – Study area and Lidar data coverage



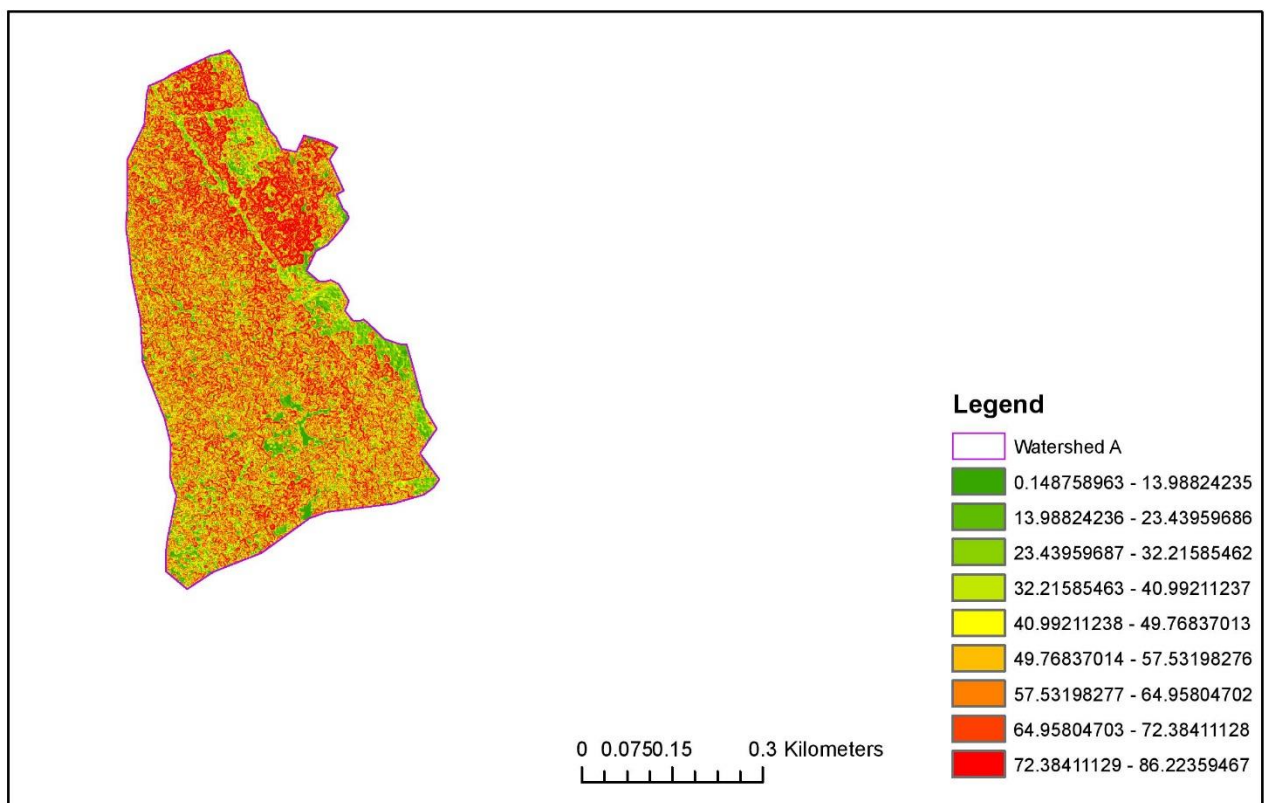
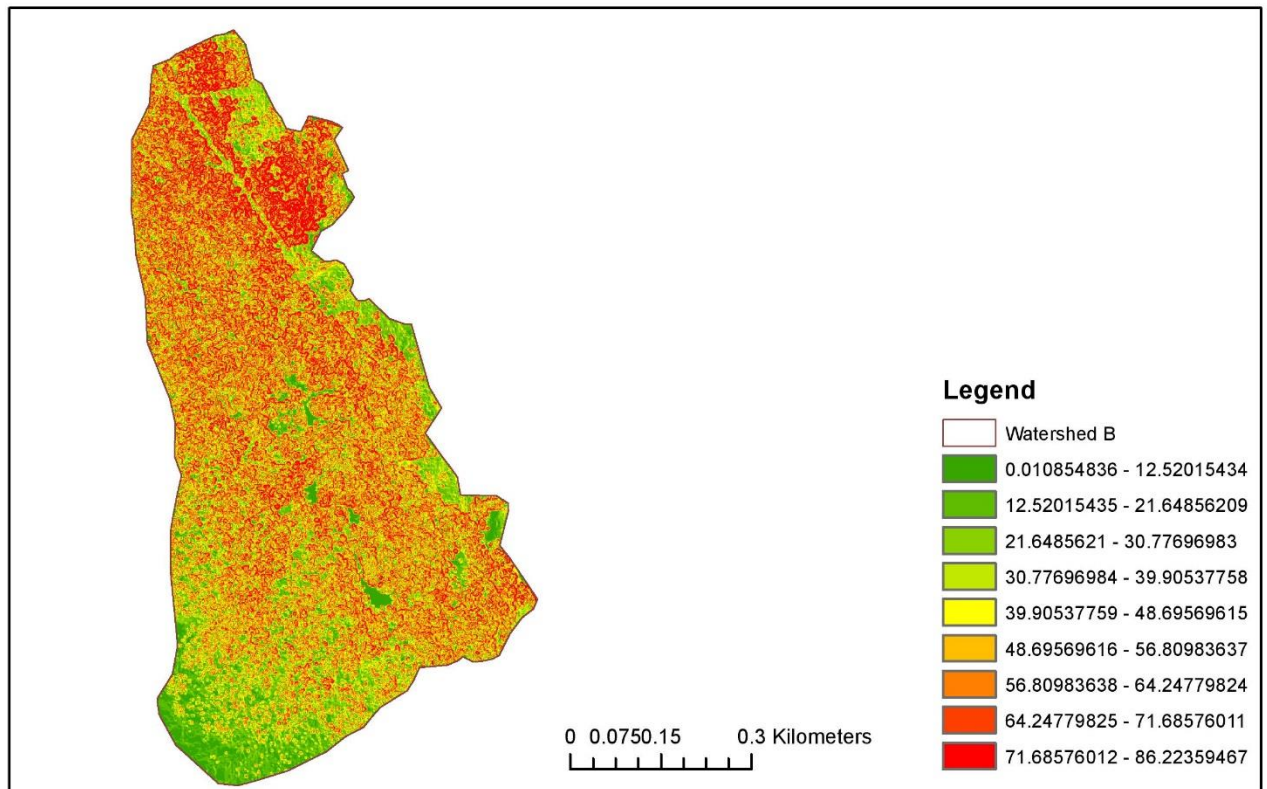
Appendix C – Study area and Drainage lines



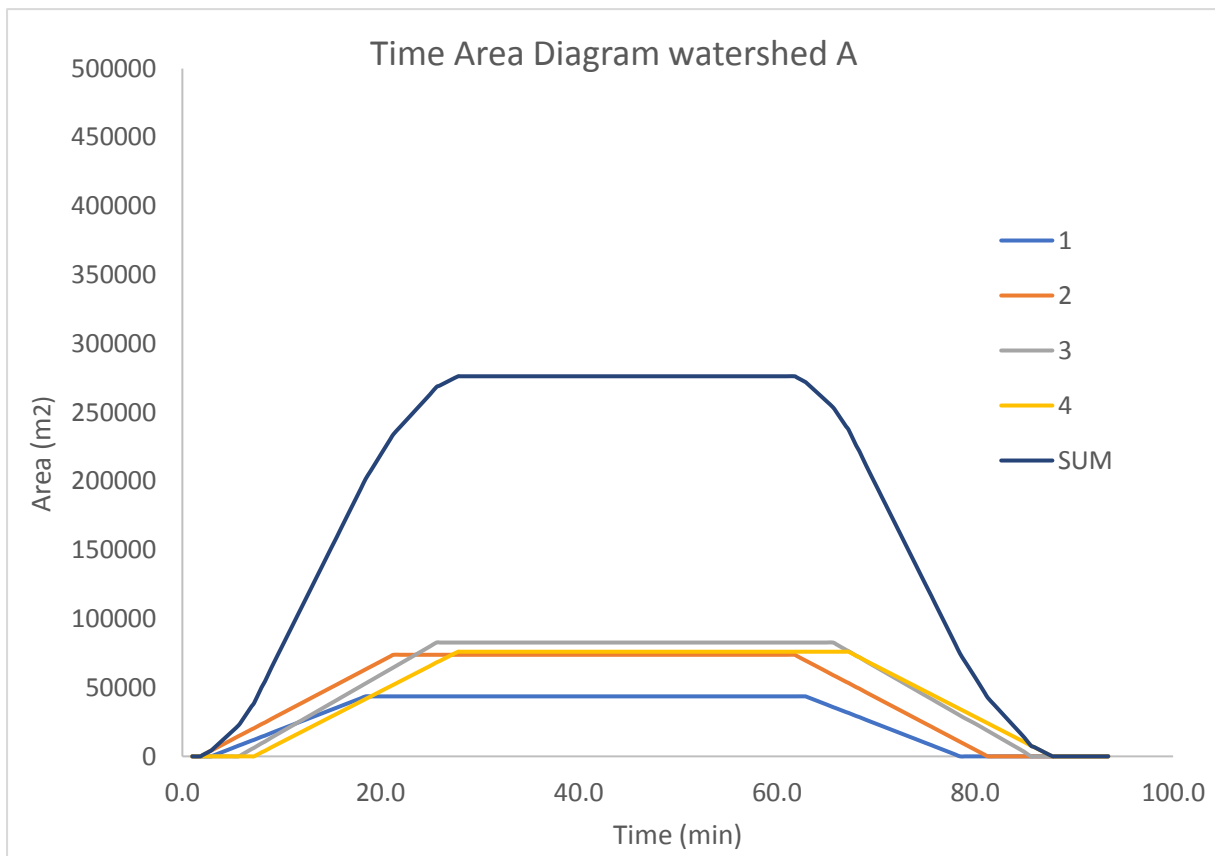
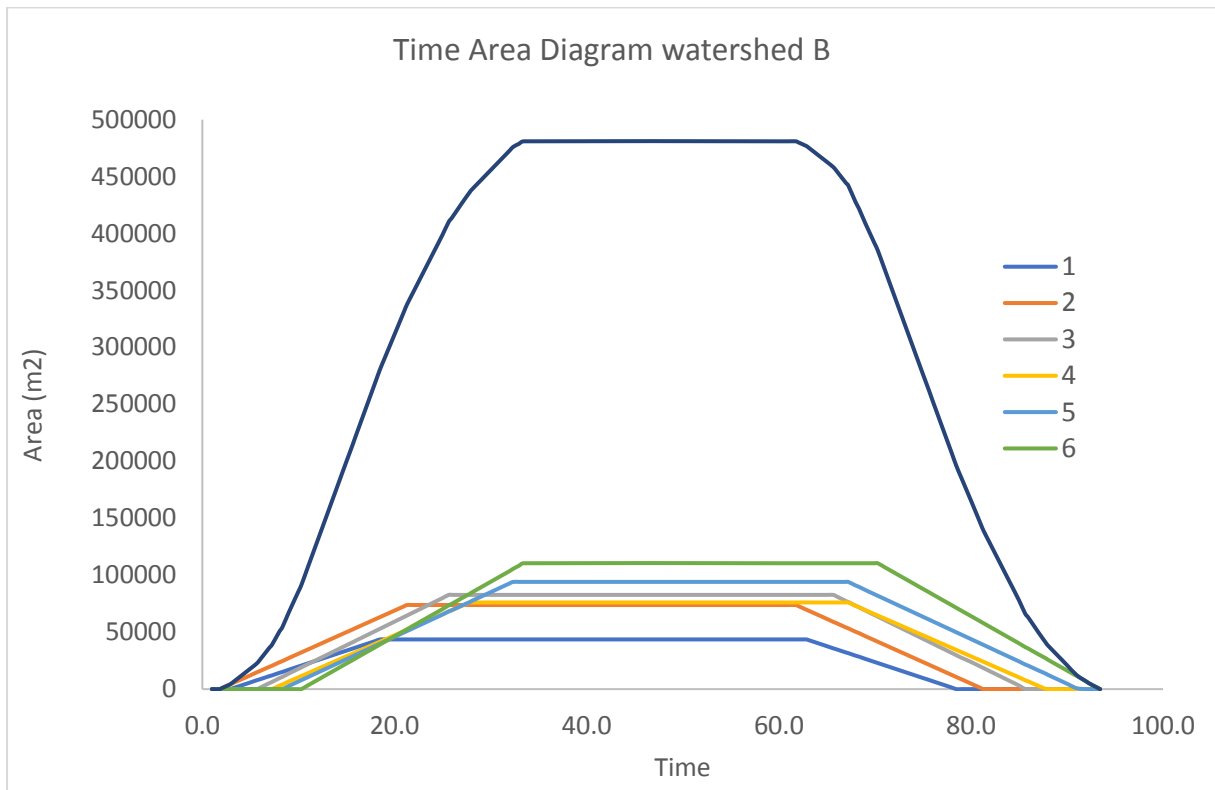
Appendix D- Watersheds and sub basins



Appendix E- Slope distribution in watersheds



Appendix F– Time area diagram



Appendix G – Formulas for Time of Concentration.

Based on the longest travel path of each watershed, Time of concentrations (t_c) are found using equation (1), (2) and (3). For channel flow, t_{ch} is time in channel in minutes, L the channel flow length (m) and S is the main channel slope. For overland flow, t_{ov} is time of overland flow in minutes, L overland flow length (m), N retardance coefficient, and S is the slope of terrain.

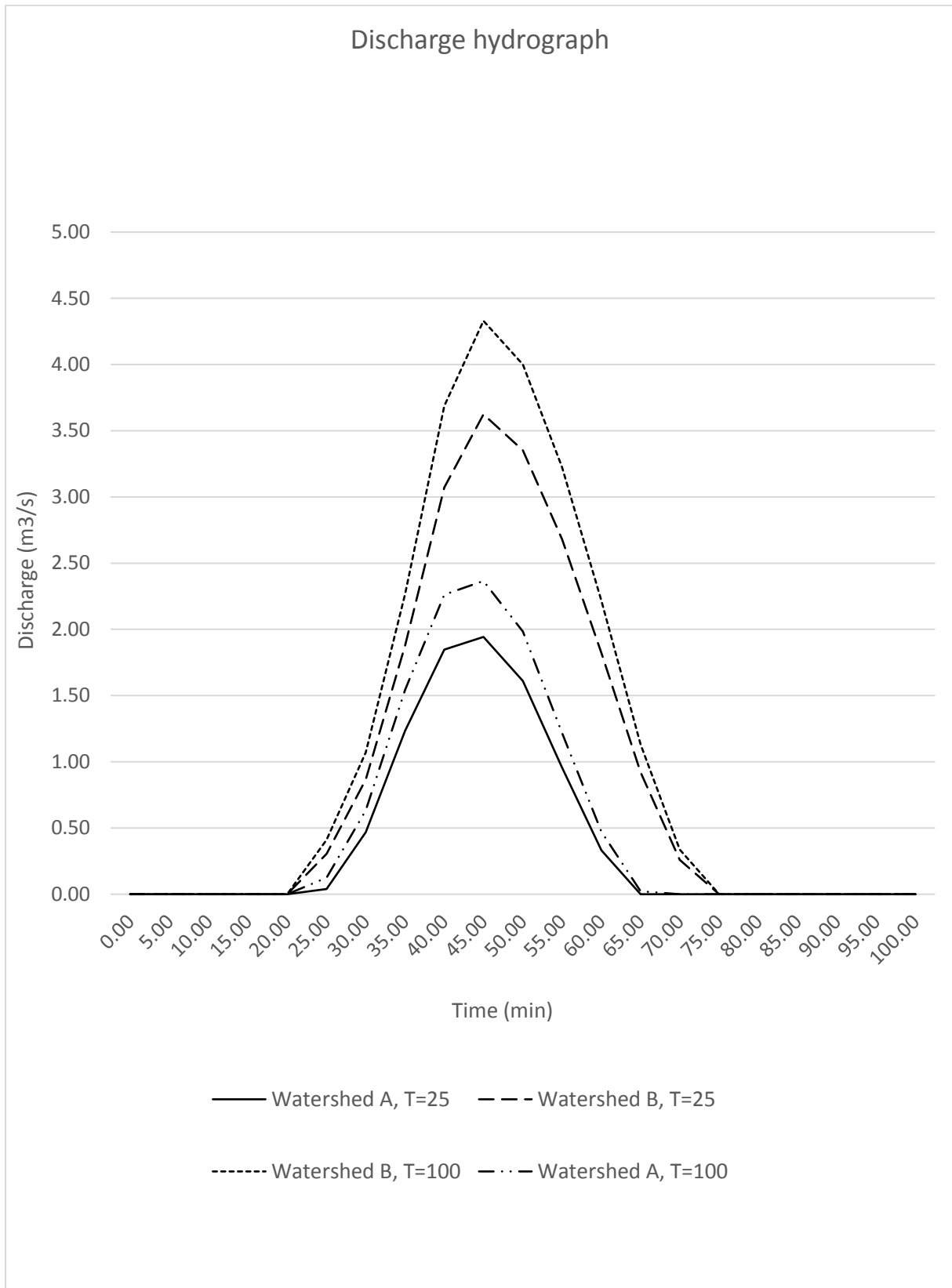
$$t_c = t_{ov} + t_{ch} \quad (6)$$

$$t_{ch} = \frac{0.06629L^{0.77}}{S^{0.385}} \quad [76] \quad (7)$$

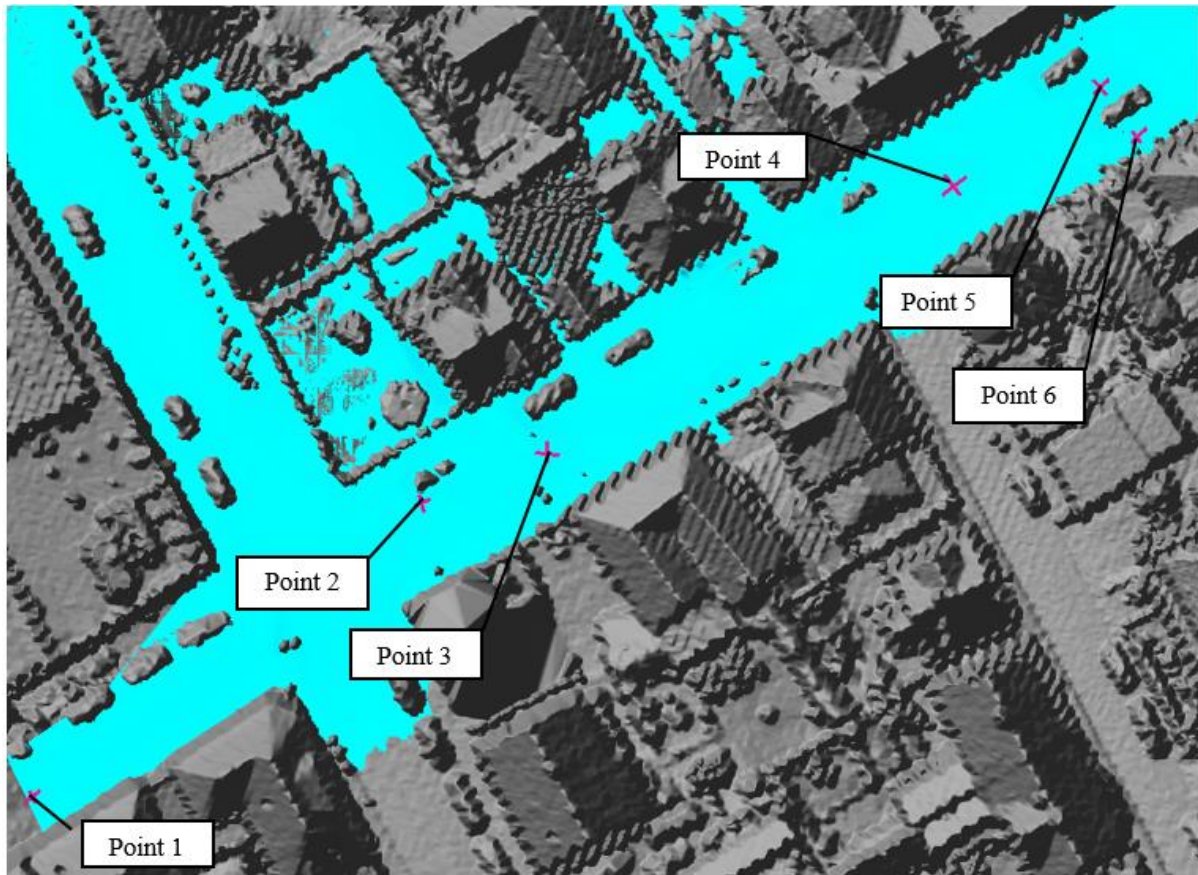
$$t_{ov} = \frac{1.44(L*N)^{0.467}}{S^{0.235}} \quad [77] \quad (8)$$

N=0.8 for deciduous forest

Appendix H – Discharge hydrograph

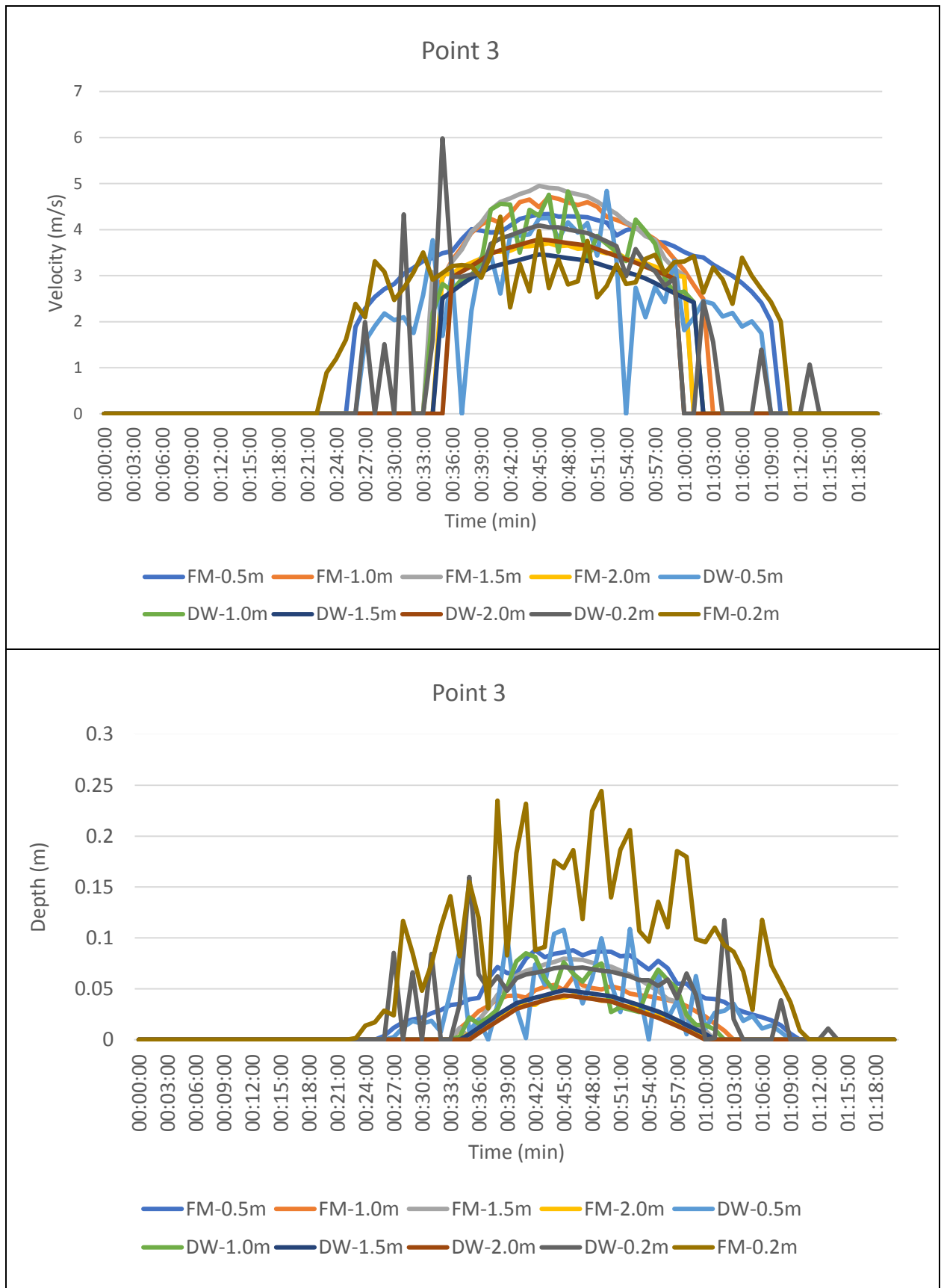


Appendix I – Control point placement

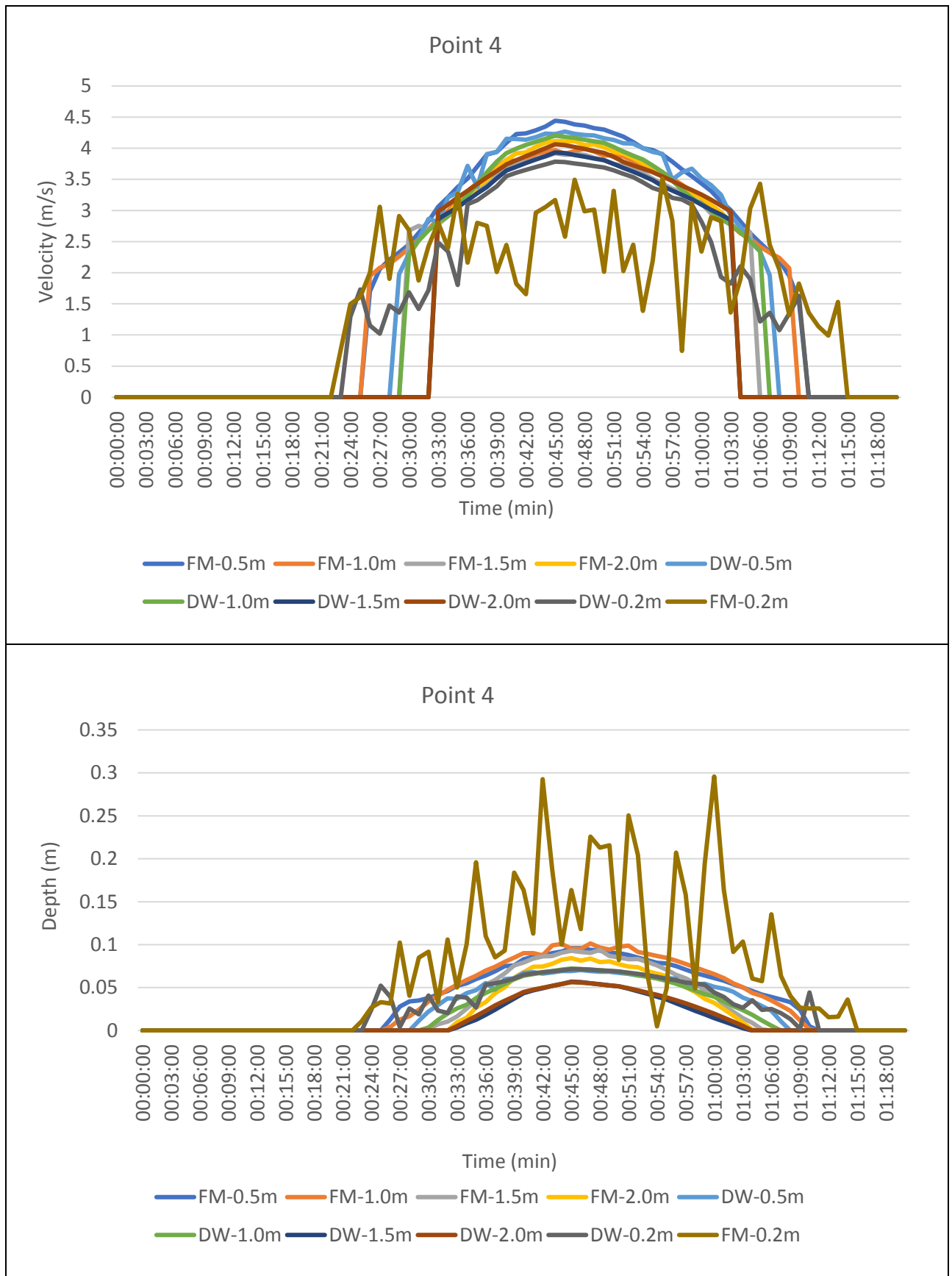


Control point	Description
Point 1	Inlet, upper boundary
Point 2	Flow around car
Point 3	Flow in street cross-section
Point 4	Flow in street cross-section
Point 5	Flow in contraction
Point 6	Flow around car, sidewalk

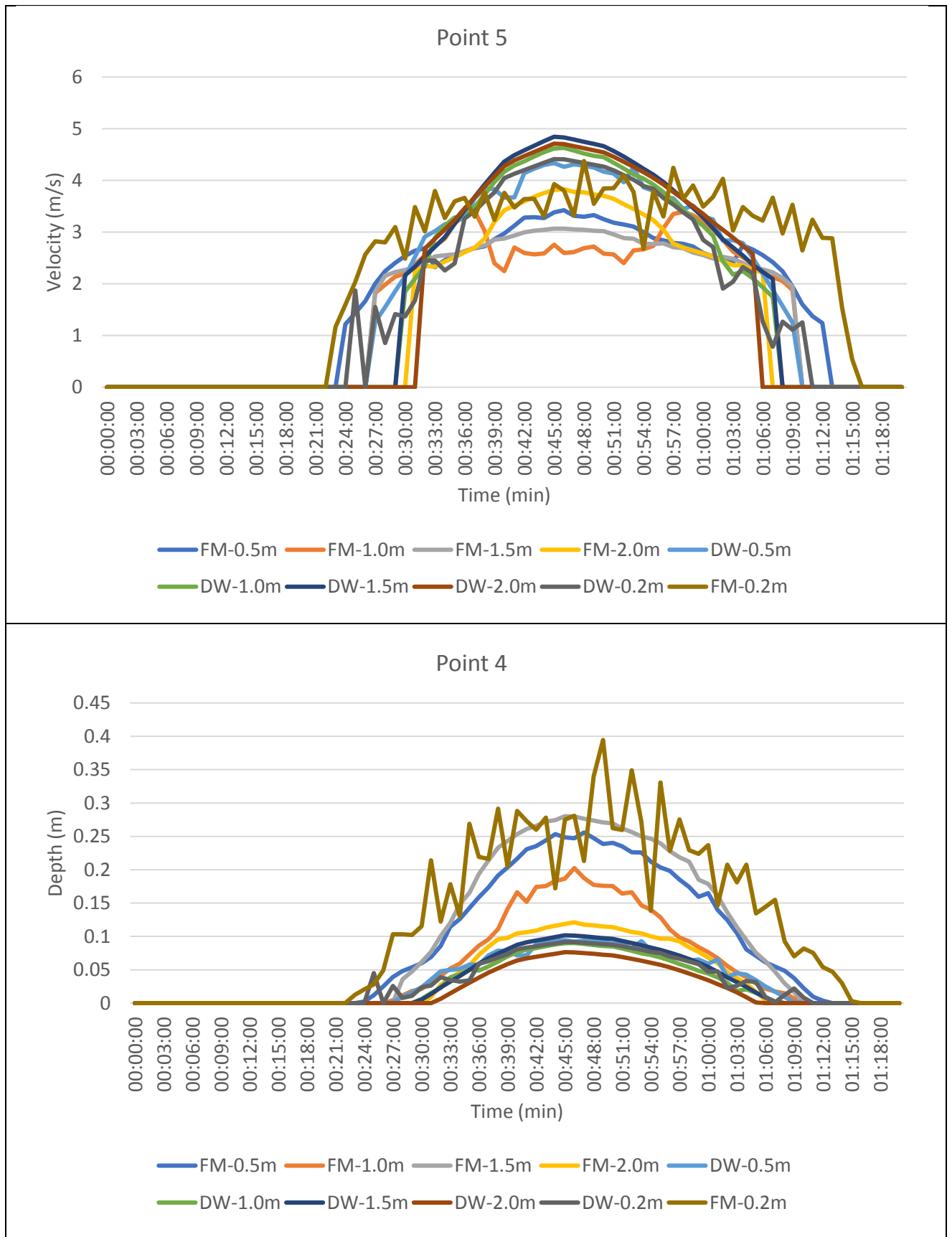
Appendix J – Control point 3



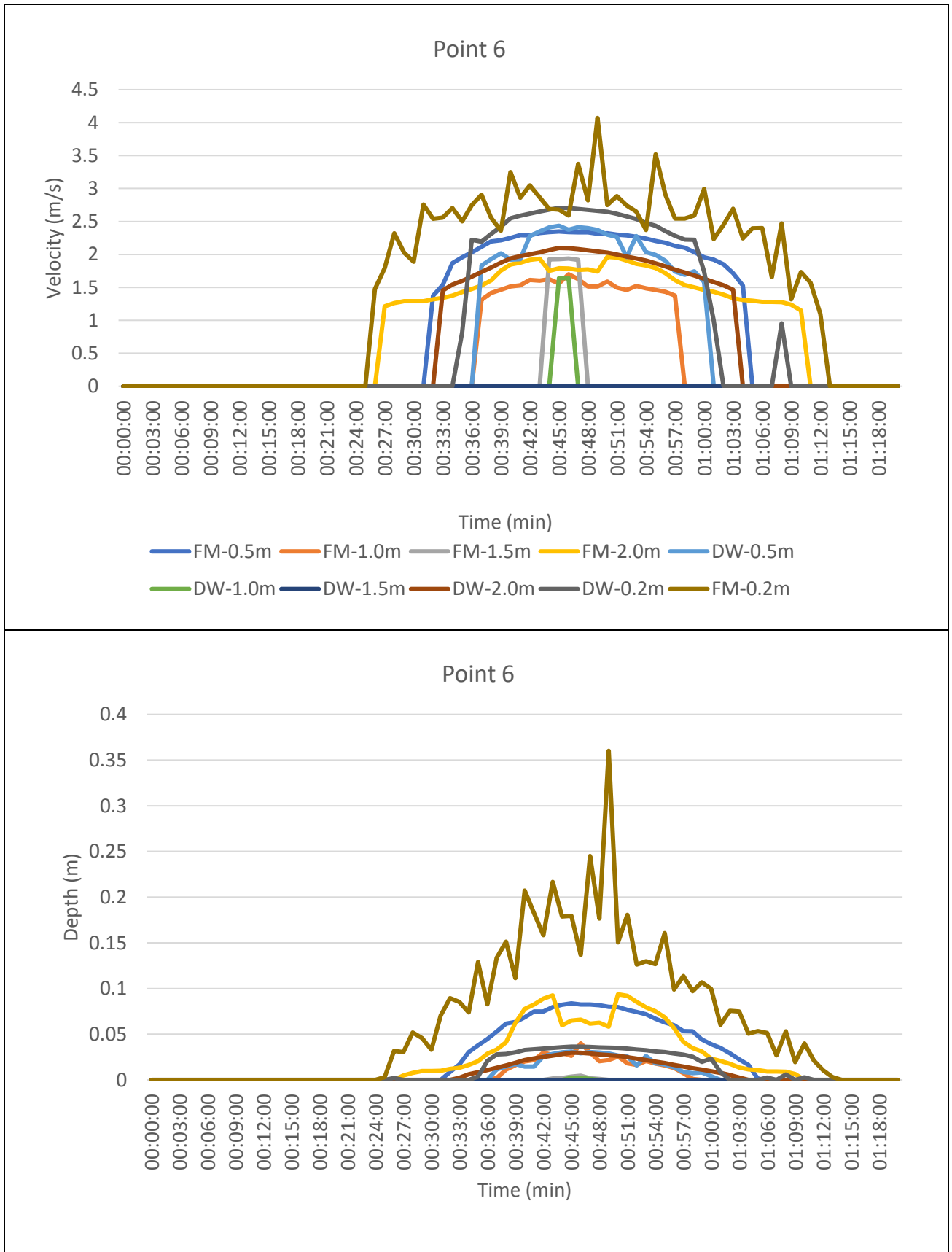
Appendix K – Control point 4



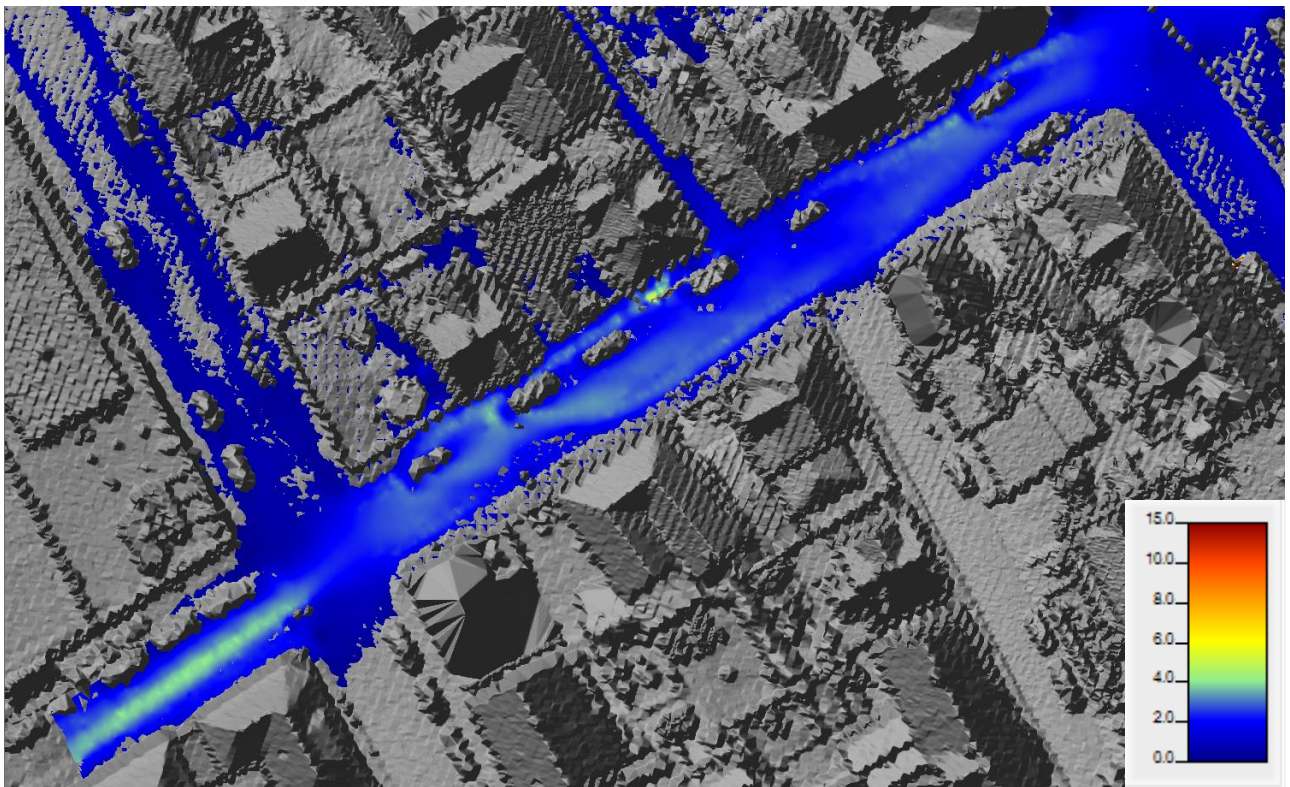
Appendix L – Control point 5



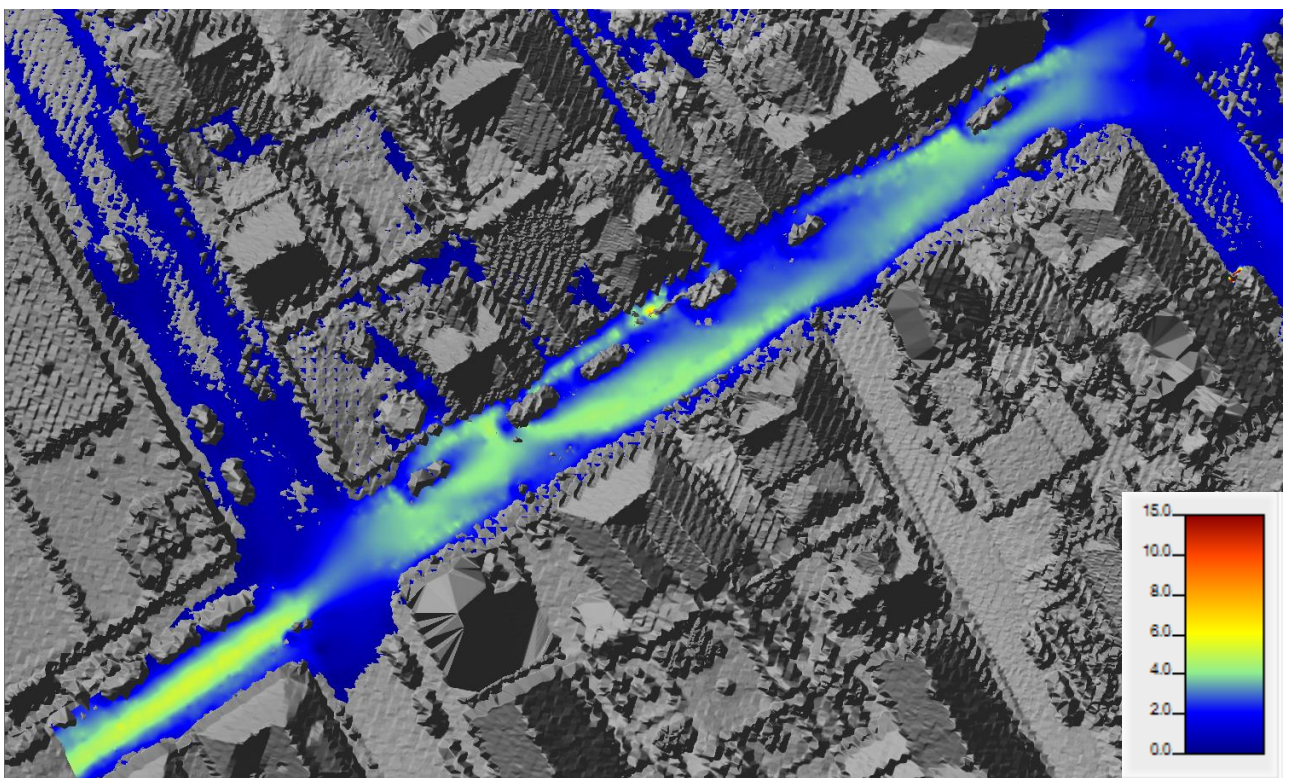
Appendix M- Control point 6



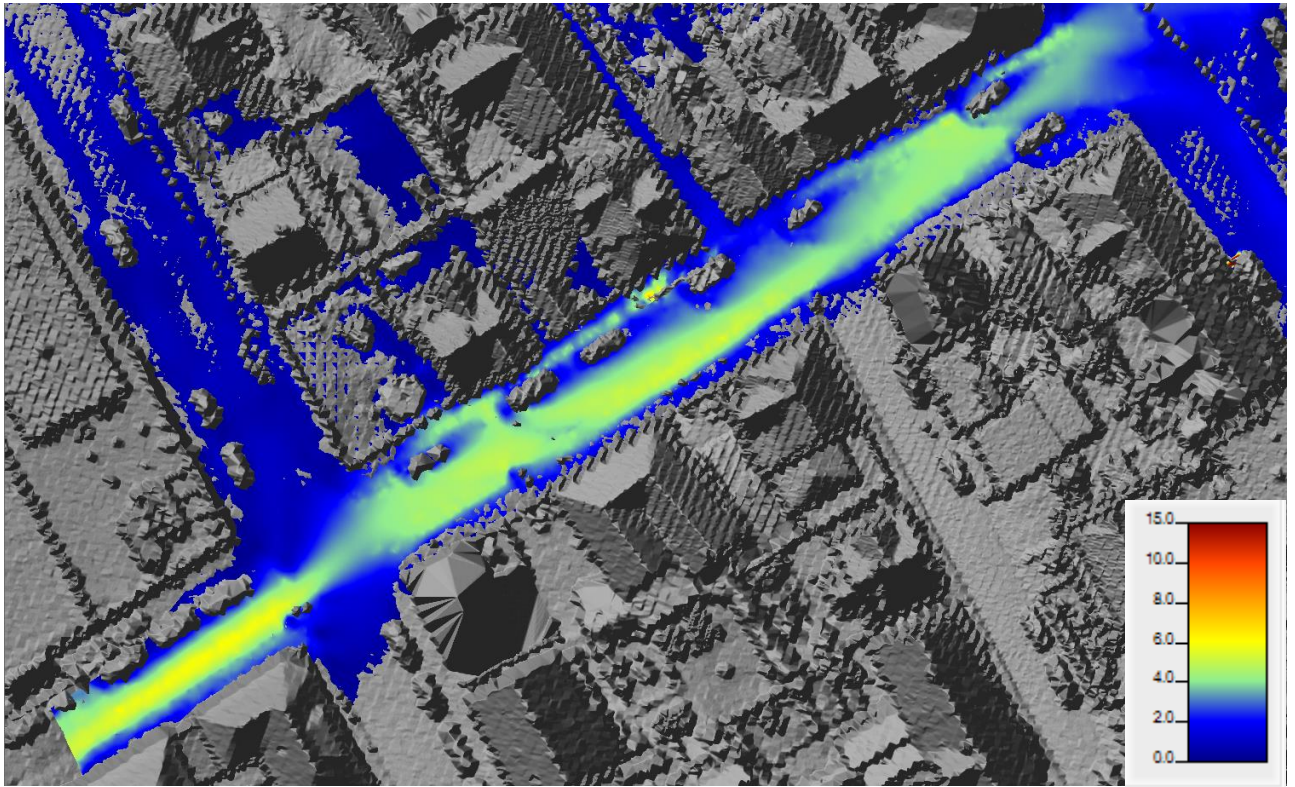
Appendix N- Result from modelling



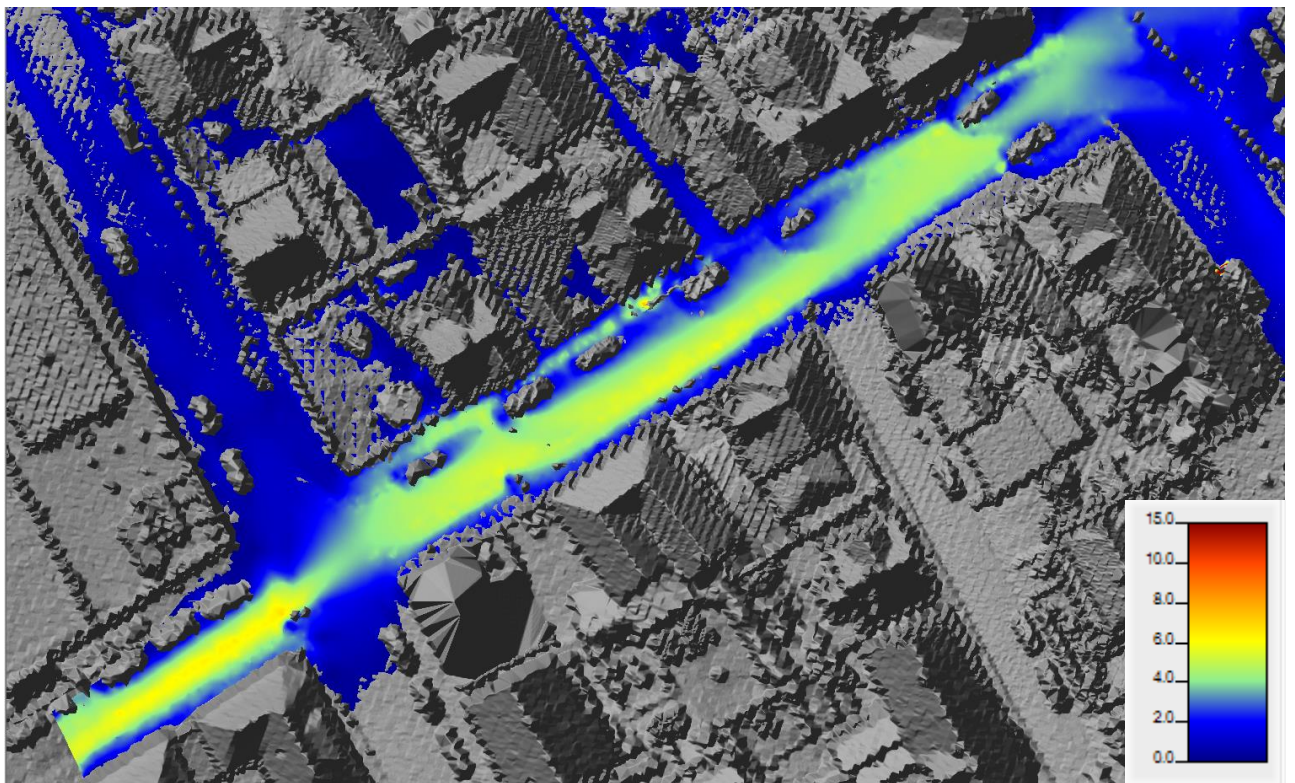
Maximum velocity (m/s) for watershed A25



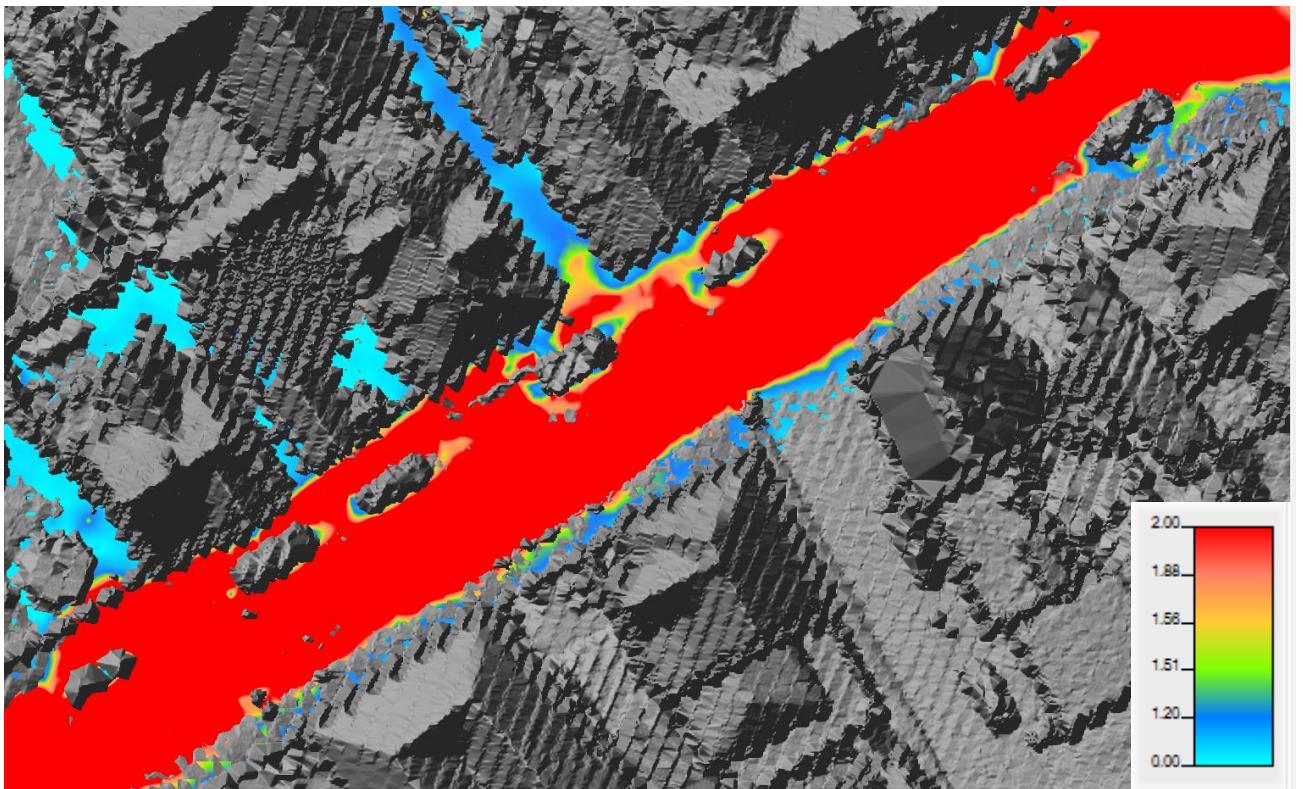
Maximum velocity (m/s) for watershed A100



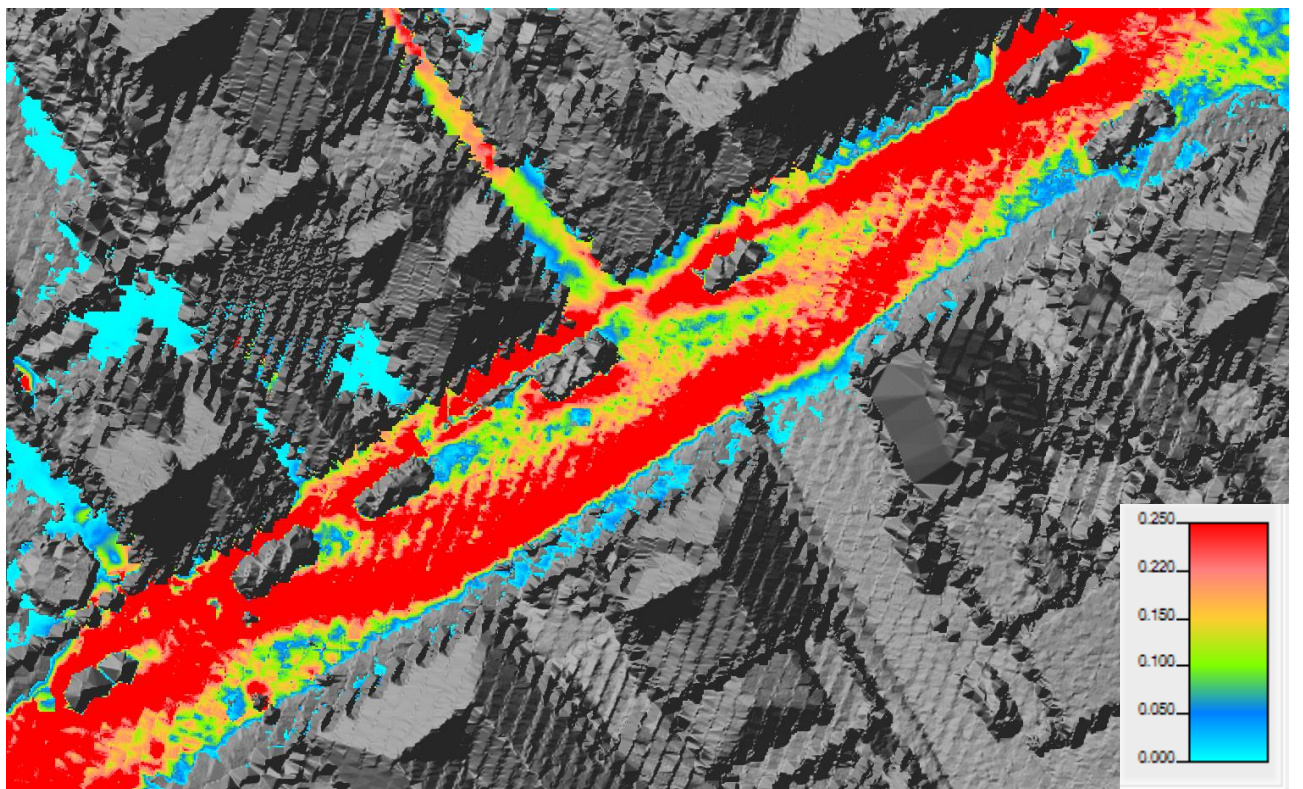
Maximum velocity (m/s) for watershed B25



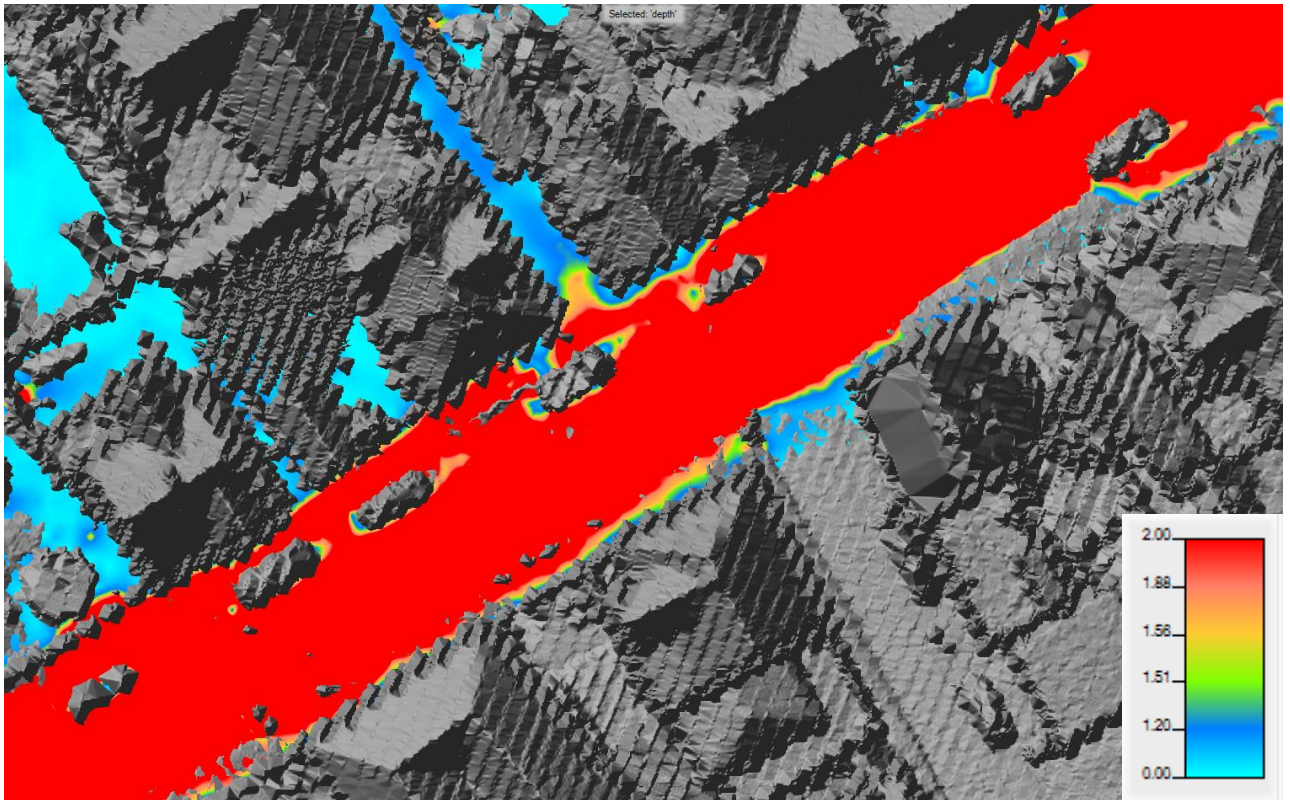
Maximum velocity (m/s) for watershed B100



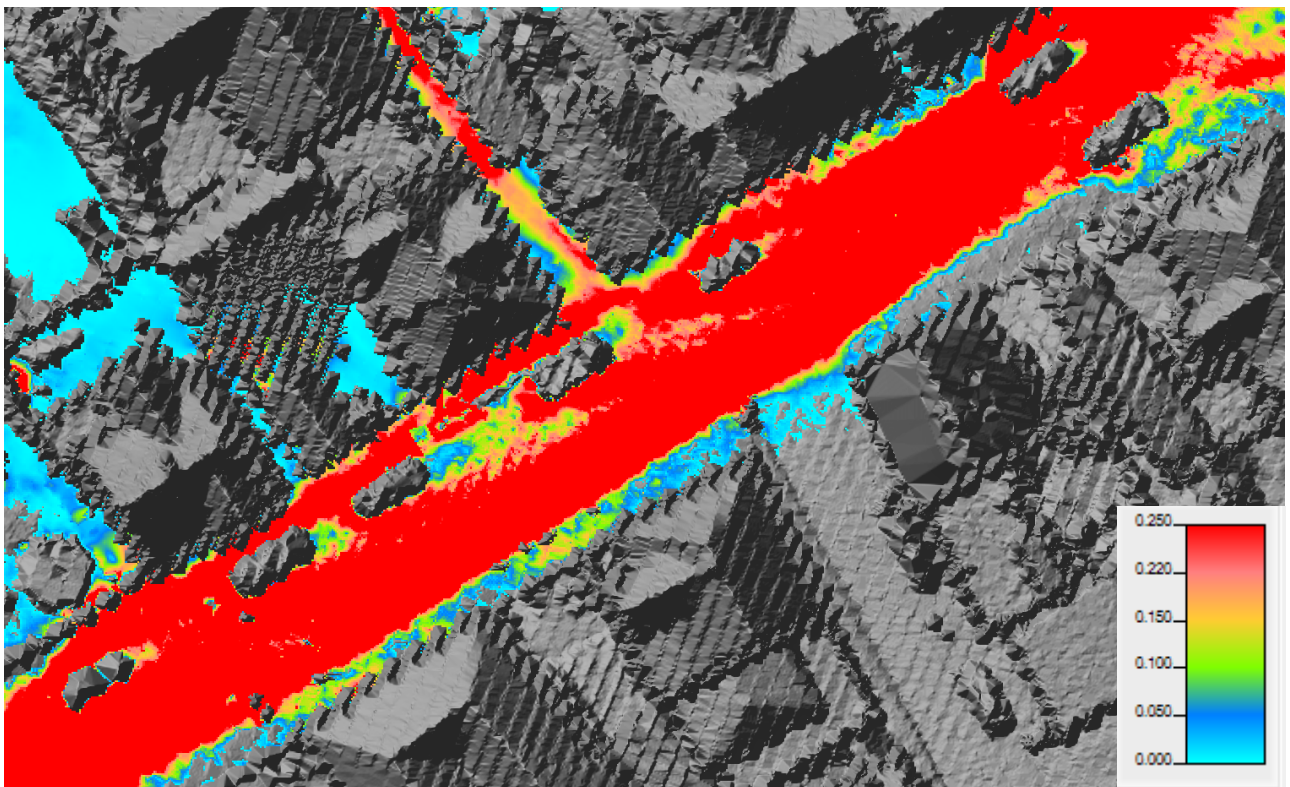
Maximum hazard potential around obstacles for watershed A100- with levels from Table 1 (m/s)



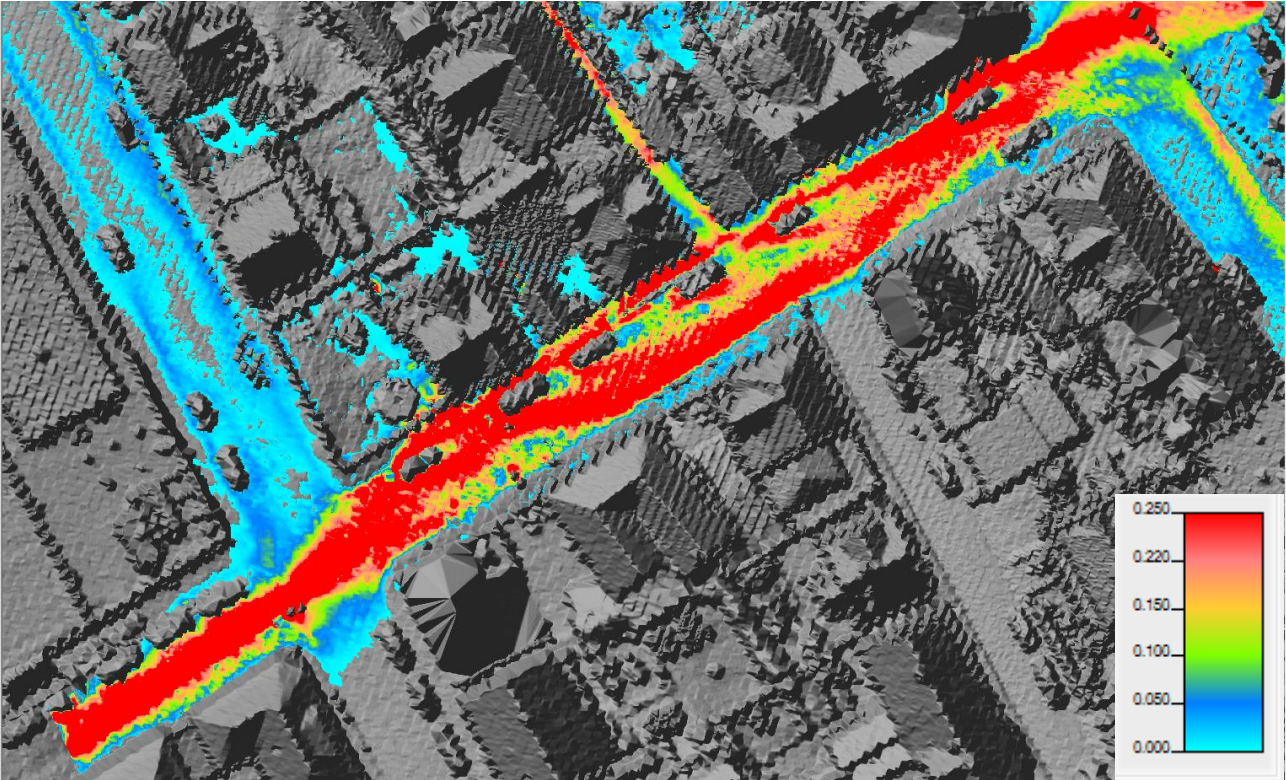
Maximum depth-velocity product around obstacles for watershed A100- (m2/s)



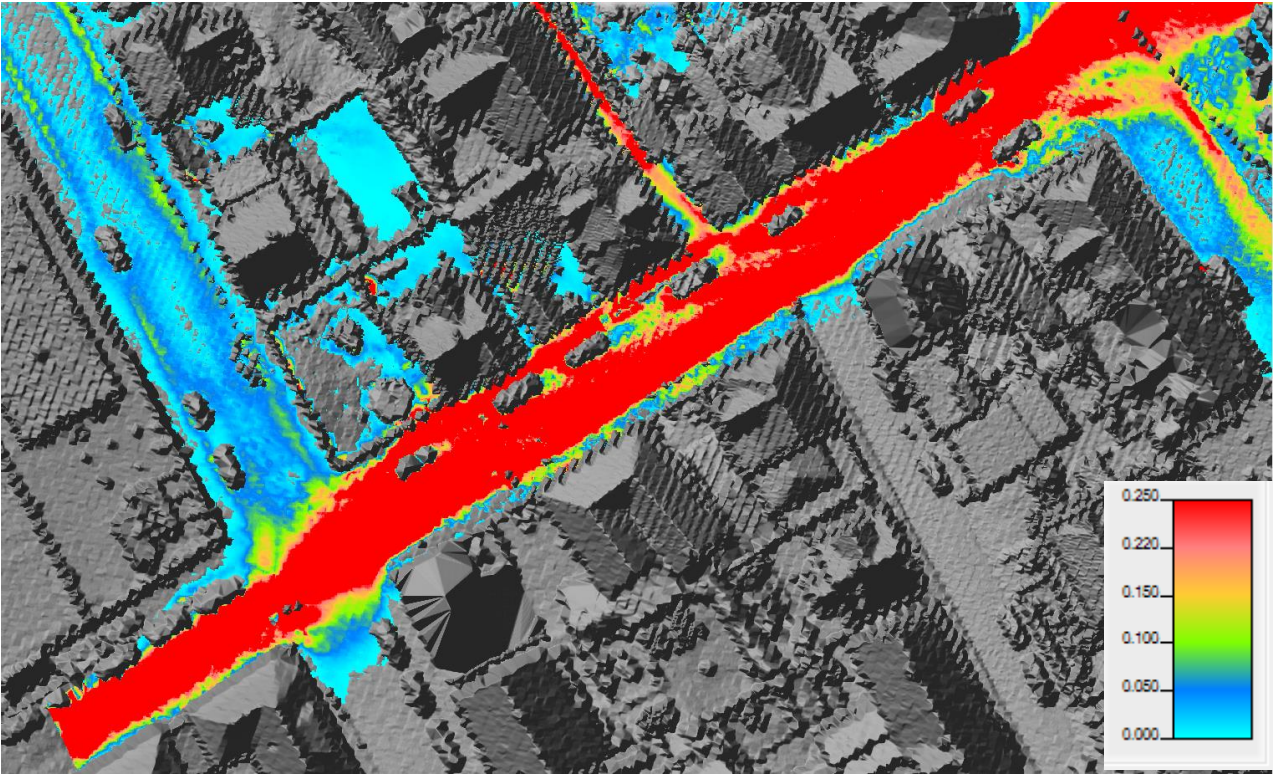
Maximum hazard potential around obstacles for watershed B100- with levels from Table 1 (m/s)



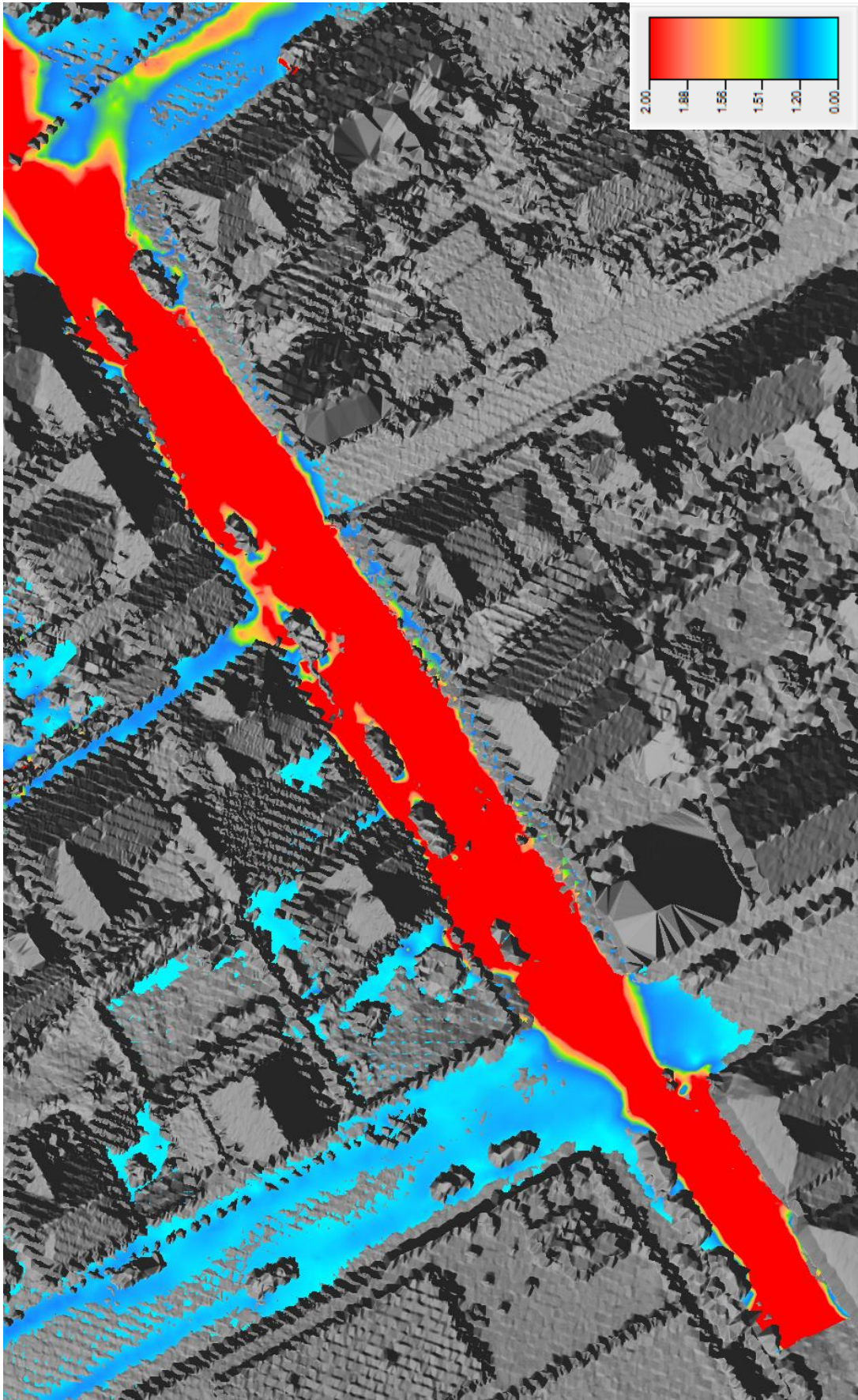
Maximum depth-velocity product around obstacles for watershed B100 (m²/s)



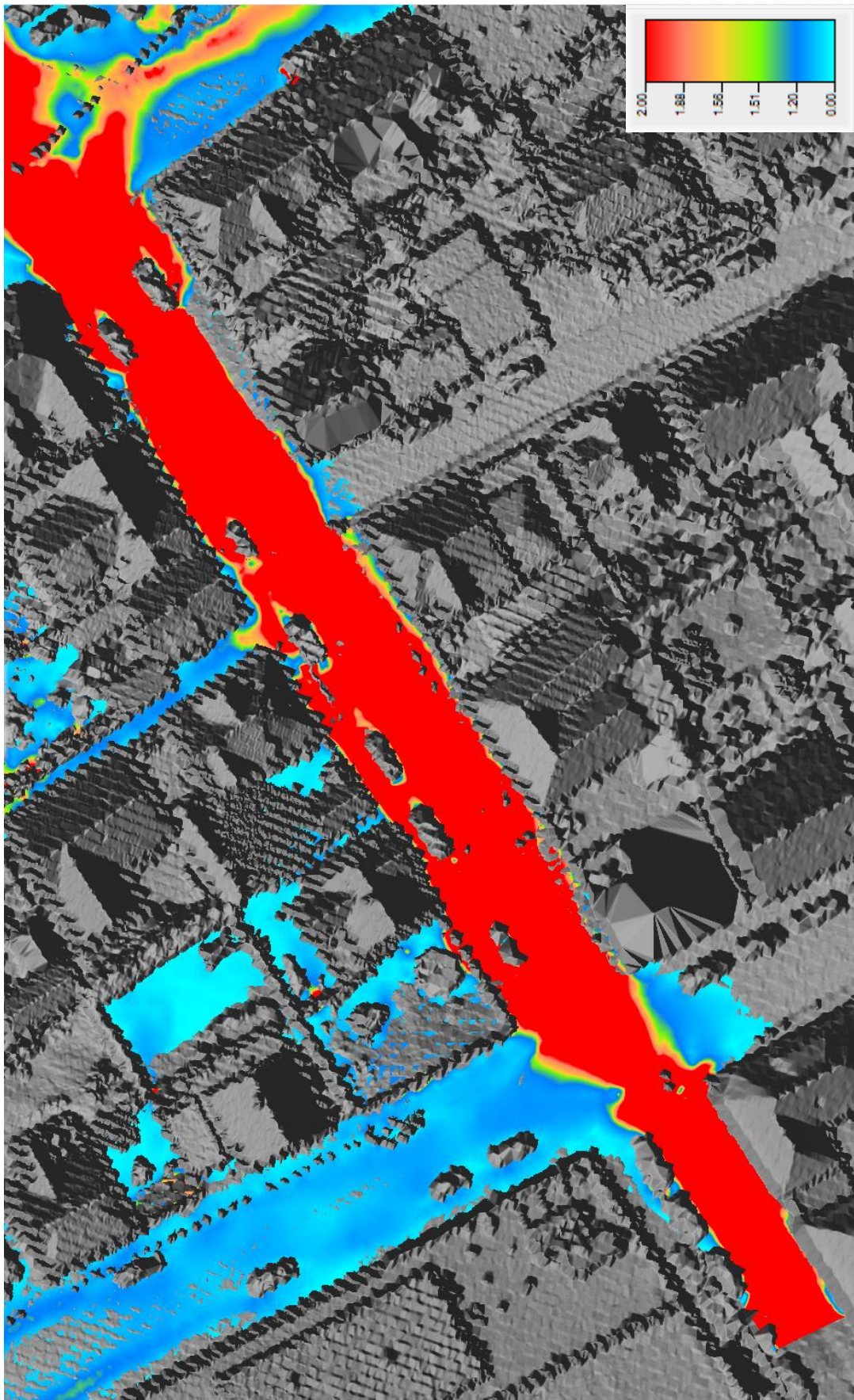
Maximum depth- velocity product (m2/s) over the whole street watershed A100



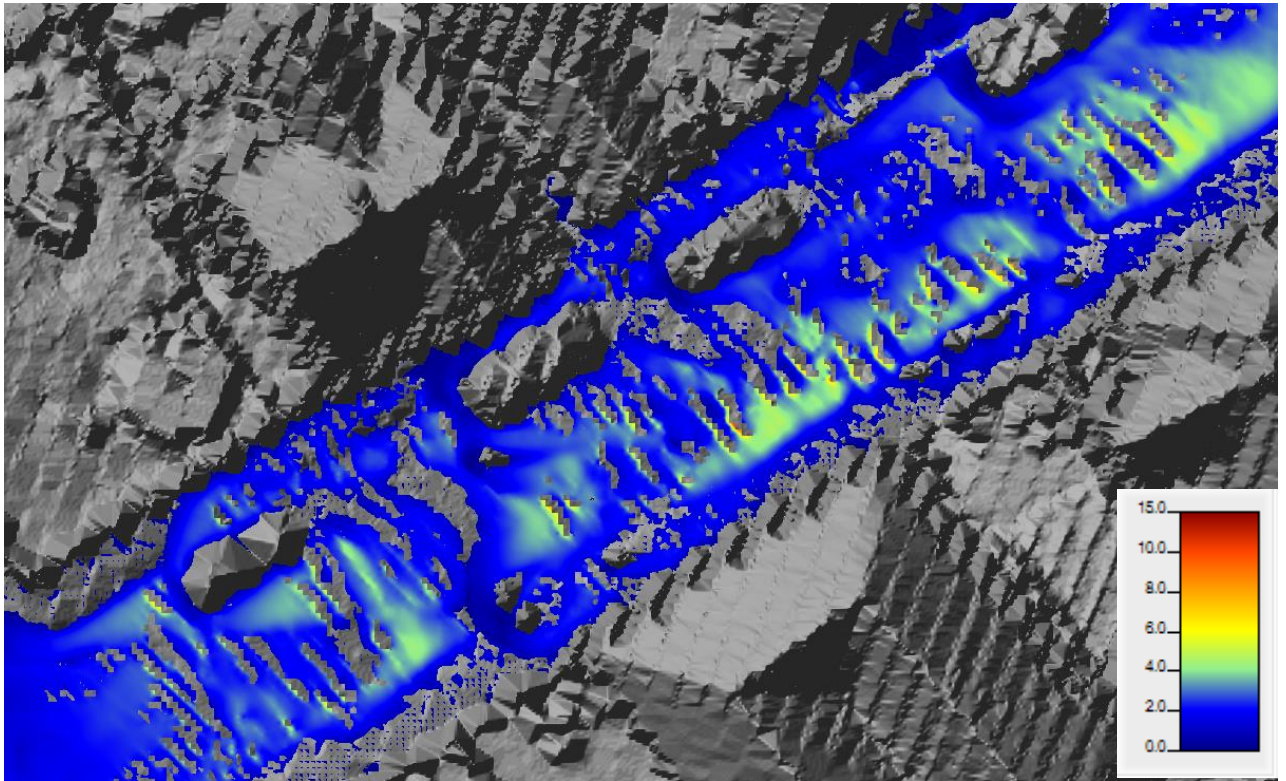
Maximum depth- velocity product (m2/s) over the whole street watershed A100



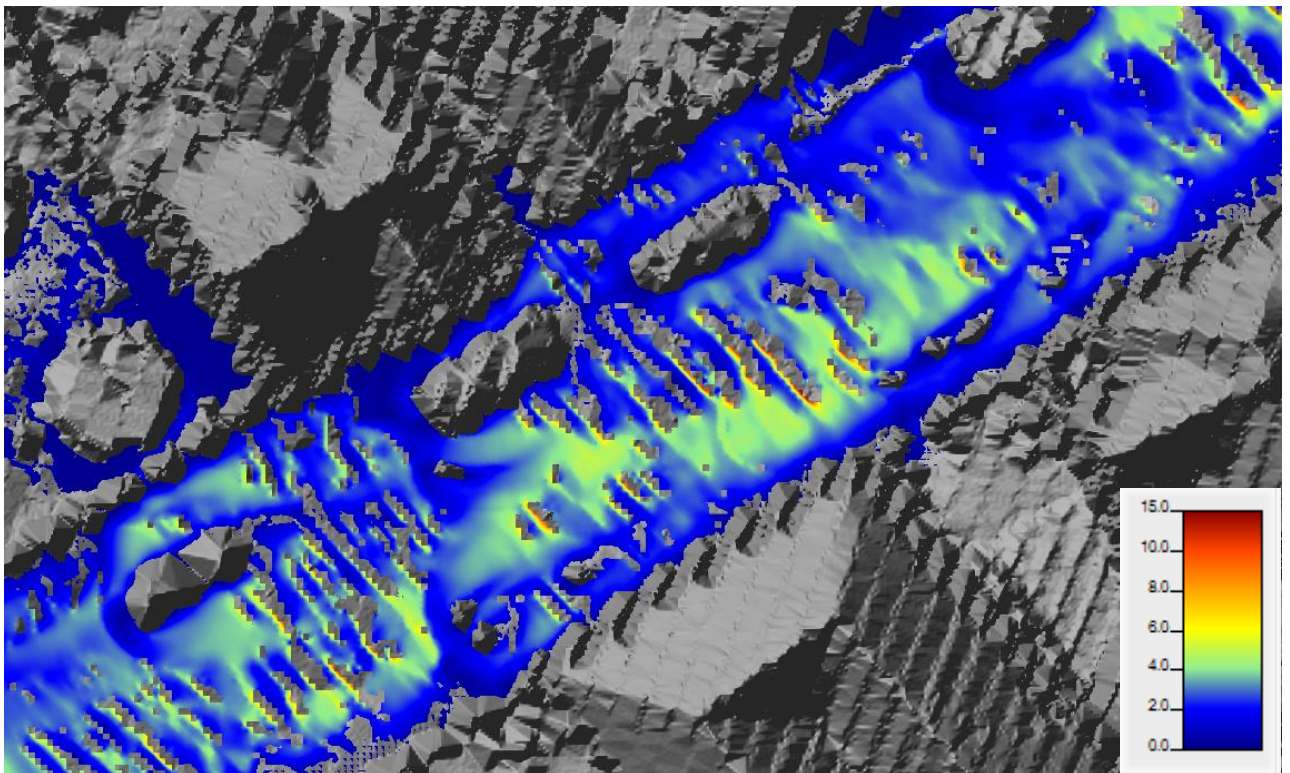
Maximum hazard potential over the whole street A100- with levels from Table 1 (velocity)



Maximum hazard potential over the whole street B100- with levels from Table 1 (velocity)



Sign of instability with Full momentum 0.2 m for watershed B100- Velocity at time 28 min



Sign of instability with Full momentum 0.2 m for watershed B100- Velocity at time 36 min